INVESTIGATING THE ROLE OF NICOTINIC ACID PHOSPHORIBOSYL TRANSFERASE IN CANCER

by

Cathleen Dai

Submitted in partial fulfilment of the requirements
for the degree of Master of Science

at

Dalhousie University
Halifax, Nova Scotia
July 2018

TABLE OF CONTENTS

LIST OF TABLES

LIST OF FIGURES

ABSTRACT

Currently, there is interest in targeting cancer stem cells (CSCs) for cancer therapy. CSCs are characterized by self-renewal and the potential to differentiate into various tumor cell types. One therapeutic strategy is to modulate cancer metabolism, in which NAD^+ is a central molecule. Nicotinic acid phosphoribosyl transferase (NAPRT) is one of the major NAD^+-synthesizing enzymes, and we studied its role in three models of cancer stem-like cells (CSLCs). We show that CSLCs highly express NAPRT. Knockdown of NAPRT in CSLCs inhibits cell proliferation and stemness features, and promotes differentiation, senescence, or cell death. We observed that NAD^+-dependent SIRT7 was consistently downregulated in cancer cells with shNAPRT, a significant correlation between NAPRT and SIRT7 expression is evident in cancer patient datasets, and knockdown of SIRT7 induces a proteomic profile similar to that of shNAPRT cells. We therefore propose that SIRT7 is involved in shNAPRT antitumor effects. Together, these findings put forward novel therapeutic implications for NAPRT-SIRT7 axis in cancer therapy.

LIST OF ABBREVIATIONS AND SYMBOLS USED

ACMS	α-amino-β-carboxymuconate-ε-semialdehyde
ACMSD	ACMS decarboxylase
ADP	adenosine diphosphate
AML	acute myeloid leukemia
AMS	α-amino-β-muconate-ε-semialdehyde
APS	ammonium persulfate
ATG	autophagy-related gene
ATP	adenosine triphosphate
B-H	Benjamini-Hochberg
1,3-BPG	1,3-biphosphoglycerate
BSA	bovine serum albumin
BTIC	brain tumor-initiating cell
˚C	degrees Celsius
Ca^{2+}	calcium ions
cADPR	cyclic-ADP-ribose
CFDA, SE	carboxyfluorescein diacetate succinimidyl ester
CFSE	carboxyfluorescein succinimidyl ester
ChIP	chromatin immunoprecipitation
CQ	chloroquine
CSC	cancer stem cell
CSLC	cancer stem-like cell
DAVID	Database for Annotation, Visualization and Integrated Discovery
DMEM	Dulbecco's Modified Eagle's Medium
ECC	embryonal carcinoma cell

ECL	electrochemiluminescence
ECSLC	embryonic carcinoma stem-like cell
EGF	epidermal growth factor
EMEM	Eagle's Minimum Essential Medium
EMT	epithelial-mesenchymal transition
ER	endoplasmic reticulum
ESC	embryonic stem cell
ETC	electron transport chain
FBS	fetal bovine serum
G3P	glyceraldehyde-3-phosphate
G6PD	glucose-6-phosphate dehydrogenase
GAPDH	glyceraldehydes-3-phosphate dehydrogenase
h	hour
H3K18Ac	histone H3 acetyl Lys 18
HIF1	hypoxia-inducible factor
HK2	hexokinase 2
HMEC	human mammary epithelial cell
hTERT	human telomerase reverse transcriptase
IDH	isocitrate dehydrogenase
IDO	indoleamine 2,3-dioxygenase
KGDH	α-ketoglutarate dehydrogenase
LC3	microtubule-associated protein light chain 3
LDH	lactate dehydrogenase
M	molar
MDH	malate dehydrogenase

MEV	multiple experiment viewer
MFI	mean fluorescent intensity
min	minute
ml	milliliter
mTOR	mammalian target of rapamycin
mTORC1	mTOR complex I
NA	nicotinic acid
NAAD	nicotinic acid adenine dinucleotide
NAD^+	nicotinamide adenine dinucleotide
NADS	NAD^+ synthetase
NAM	nicotinamide
NAMN	nicotinic acid mononucleotide
NAMPT	nicotinamide phosphoribosyltransferase
NAPRT	nicotinic acid phosphoribosyltransferase
NAR	nicotinic acid riboside
NMN	nicotinamide mononucleotide
NMNAT	nicotinamide mononucleotide adenylyl transferase
NR	nicotinamide riboside
NRK	NR kinases
NS	non-silencing
OXPHOS	oxidative phosphorylation
PARP	poly-ADP-ribose polymerase
PBS	phosphate buffered saline
PDH	pyruvate dehydrogenase
PDK1	pyruvate dehydrogenase kinase 1

PE	phosphatidylethanolamine
PI3K	phosphoinositide 3-kinase
PKM2	pyruvate kinase M2
PS	phosphatidylserine
QA	quinolinic acid
QAPRT	quinolinic acid phosphoribosyltransferase
qRT-PCR	quantitative real-time polymerase chain reaction
SD	standard deviation
SDS	sodium dodecyl sulfate
SDS-PAGE	SDS polyacrylamide gel electrophoresis
sec	second
SIRT	sirtuin
TCA	tricarboxylic acid
TCGA	the cancer genome atlas
TDO	tryptophan dioxygenase
TPM	transcripts per million
Trp	tryptophan
UPR	unfolded protein response

ACKNOWLEDGEMENTS

First, I would like to acknowledge my supervisor, Dr. Shashi Gujar, who has always been supportive of my Master's study and related research, in addition to my career aspirations. I am also fortunate to have had Dr. Paola Marcato, Dr. David Waisman, and Dr. Christopher Richardson as members of my thesis advisory committee, to whom I would like to express my thanks for their various help in the completion of this thesis.

I am grateful to the organizations that have funded my work over the years: the Beatrice Hunter Cancer Research Institute, the Canadian Institutes of Health Research, the Nova Scotia Health Research Foundation, and the Nova Scotia Government (along with the Dalhousie University Department of Microbiology & Immunology for their nomination for this award).

I would like to thank all the members of the Gujar lab and past members of the Lee lab, including Dr. Patrick Lee whose teachings have been instrumental. Specifically, thank you to Dr. Patrick Murphy for conducting the proteomics mass spectrometry for this project, and to Dr. Barry Kennedy for helping me analyze my samples by flow cytometry.

My most sincere thanks go to Dr. Tanveer Sharif, who has acted as an amazing mentor and supervisor since I began research in this lab. I am also incredibly thankful to the wonderful team that I am proud to have worked on numerous projects with: Emma Martell, Saleh Ghassemi-Rad, and Mark Hanes.

Finally, thank you to my family and friends who have ceaselessly supported and encouraged me in my endeavors and aspirations.

CHAPTER 1: INTRODUCTION

1.1 CANCER

Cancer is a disease of continual and uncontrolled cell division. Through a multistep process, normal cells acquire genetic alterations that progressively transform them into malignancy. The mutations in the cancer cell of origin drive its abnormal proliferation, generating a population of mutant cells that initiate the formation of the tumor. As the tumor develops, clonal expansion continues, and the daughter cells also acquire additional mutations themselves. This genetic instability leads to a population of cancer cells with diverse profiles, some of which have mutations that confer them a competitive advantage for growth. Thus, clonal selection also occurs as tumor progression advances, ultimately leading to the development of cancer.[1] The most common types of cancer in Canada are lung, breast, colorectal, and prostate cancer.[2] Despite over 100 types of cancers, it is accepted that all forms of cancer have many common physiological alterations. These hallmarks of the disease include dysregulation of growth signals, resistance to apoptosis, extensive replicative potential, angiogenesis, metastasis, evading immune destruction, and reprogramming of energy metabolism.[3,4]

1.2 CANCER STEM CELLS

Tumors are composed of diverse cell types with distinct molecular signatures. These different cancer cells respond with various degrees of sensitivity to certain therapeutic treatments, and such, tumor heterogeneity poses a challenge for effective cancer therapies.[5] The cancer stem cell (CSC) theory proposes that the heterogeneity of tumors arises in part from a small subpopulation of cells known as CSCs, which are an important driver of tumor growth. Existing in an undifferentiated state, CSCs possess multipotent capacity to differentiate into the heterogeneous cancer cell types that comprise the bulk of the tumor (Figure 1.1).[6–8] CSCs are also characterized by self-renewal, a cell division process that gives rise to the same type of cells as the original stem cell, maintaining the undifferentiated state. During self-renewal, daughter cells retain the same ability as the parental cell to replicate and thus have the capacity for long-term proliferation, preserving the CSC population.

CSCs are functionally defined by their ability to self-renew and potential to differentiate into all the cancer cell types of a tumor. The golden standard assay that determines CSCs from bulk tumor cells is transplantation into immunocompromised hosts. Transplantation of CSCs, also referred to as tumor-initiating cells, result in the formation of a heterogeneous tumor. Moreover, serial transplantation of CSCs will also develop *in vivo* tumors that reconstitute to the original tumor composition.[6,8,9] The properties of CSCs, which make them highly tumorigenic, explains their participation in tumor initiation, maintenance, progression, and metastasis.[10]

The emergence of a CSC concept came about in the 1960s, when it was recognized that teratocarcinomas originate from malignant embryonic cells. These germ cell tumors were composed of many types of differentiated cells of all three germ layers, but also contained some undifferentiated cells. The frequency of undifferentiated cells in a transplanted tumor correlated with the yield of tumors generated.[11,12] The first proof of CSCs, involving functional characterization of distinct tumor cell subpopulations, was demonstrated in human acute myeloid leukemia (AML).[13] Since then, the existence of CSCs has been identified in many solid tumors including brain,[14] breast,[15] colon,[16] and ovarian cancers.[17] These assays isolated CSC populations based on cell surface marker expression and then tested their tumorigenicity in immunocompromised mice. Only the putative CSCs formed tumors that were phenotypically diverse and reproduced the composition of the original tumor.

There are two main hypotheses regarding the origin of CSCs. CSCs may develop from adult stem cells that have accumulated oncogenic mutations as a result of their prolonged survival in the organism.[18] Appearance of malignant mutations were observed during long-term culture of mesenchymal stem cells, which became tumorigenic.[19] Alternatively, CSCs may arise from the dedifferentiation of mature cells that reacquire stem cell properties through transforming mutations.[9,20] In glioma, heptoma, and lung cancer, conditions of hypoxia or temozolomide treatment induced conversion of non-cancer stem-like cells (CSLCs) into CSLCs.[21,22]

CSCs share many traits with ESCs and can be identified by their high expression of stem cell markers.[23] In ESCs, pluripotency is maintained by core transcription factors

that include Oct4, Nanog, and Sox2.[24] Two of these are part of the Yamanaka factors (Oct4, Sox2, Klf4, c-Myc), which are a set of proteins capable of reprogramming somatic cells into a pluripotent state, highlighting their role in the ESC phenotype.[25] Oct4, encoded by the *POU5F1* gene, is a member of the POU family and has been established as a master pluripotency factor. Exogenous expression of Oct4 alone is sufficient to confer pluripotency to adult mouse neural stem cells.[26] The pluripotency transcription factors Oct4, Nanog, and Sox2 regulate early development and orchestrate the cell fate of ESCs into one of the three germ layers by repressing differentiation towards specific lineages.[27] In CSCs, these transcription factors not only regulate self-renewal, but also function in inhibiting apoptosis to promote proliferation.[27] Indeed, inhibition of Oct4 in CSLCs reduces tumor growth and induces apoptosis.[28] An Oct4/Akt regulatory axis facilitates the interaction of Oct4 with Sox2 to promote the transcription of stemness genes (*POU5F1* and *NANOG*) and survival gene *AKT1*.[29] Mouse 4T1 cells sorted by Oct4 expression demonstrate that the $Oct4^{high}$ populations have enhanced stemness features such as high expression of stem cell markers (CD133, ALDH1) and increased tumorigenicity *in vivo*.[30] Likewise, Nanog overexpression has been shown to increase the expression of stemness markers (most notably CD133 and ALDH1) in cancer cells, and also plays a role in their tumorigenicity.[31] Lastly, Sox2 promotes cell cycle progression in prostate cancer cells, and inhibits apoptosis through a plausible Ca^{2+}-regulating mechanism.[32] Given the oncogenic potential of these pluripotency factors, it is unsurprising that their overexpression is commonly observed in poorly differentiated tumors, and that higher expression of Oct4, Nanog, and Sox2 is associated with poorer clinical outcomes in breast, bladder, and lung cancers.[23,33–35]

CSCs are of particular interest because of the challenge they pose in therapy. They contribute to chemoresistance, as CSCs are often more resistant to therapeutic assault than their differentiated counterparts. Conventional cancer treatments target rapidly proliferating differentiated cancer cells, but CSCs have slower proliferation rates and are therefore less affected by such methods. Additionally, CSCs are equipped with other resistance mechanisms such as efflux pumps (which can remove harmful chemotherapeutics from the cell), increased DNA damage repair (which neutralizes the genotoxic effects of therapeutic agents) and antiapoptotic proteins (which prevent the

induction of apoptosis by cytotoxic drugs).[11] For example, CD133 positive glioblastoma CLSCs were found to be less sensitive to various drugs than CD133 negative cells. Their resistance was associated with increased expression of the multidrug transporter *BCRP1*, DNA repair protein *MGMT*, and anti-apoptotic genes such as *Bcl-2* and *XIAP*.[36] Another multidrug transporter, ABCB5, was found to be specifically coexpressed with the stem cell marker CD133 in melanoma cells and associated with doxorubicin efflux transport. Inhibition of ABCB5 significantly reversed the doxorubicin-resistant phenotype and promoted cell death, demonstrating its role in chemoresistance.[37] In pancreatic cancer, it was shown that CSLCs have increased expression of the DNA repair gene *BRCA1*, translating to an increased ability to repair DNA upon gemcitabine treatment. Moreover, treating the CSLCs with higher doses of gemcitabine induced further upregulation of *BRCA1* levels, highlighting the role of DNA repair activity in chemoresistance.[38] Overall, the increased likelihood of CSCs surviving therapy allows for tumor regeneration and leads to cancer relapse. Thus, the clinical significance of CSCs in cancer therapy has prompted much interest into the development of strategies that target CSCs (Figure 1.2).

While the study of CSCs is clearly important to our understanding of cancer treatment, the field of CSCs is not expanding without some controversy. A deficiency in the research is lack of standardized functional assays to identify CSCs.[11] Depending on transplantation conditions, there can be a large range in the frequency of cells deemed able to initiate tumors.[39] Additionally, CSC also have diverse phenotypes, and thus the reliance on cell surface markers to isolate CSCs has encountered problems in reproducibility.[12,39,40] Moreover, the cellular properties of individual CSCs may not stay consistent due to the possibility that they may transition between other tumor cell types, known as plasticity. This implies that the CSC population is dynamic and the characterization of CSCs in a tumor therefore remains difficult.[39,40] Despite these challenges, the study of CSCs is nonetheless important in advancing therapeutic strategies in cancer. Stemness properties are arguably the features that distinguish more malignant tumor cells and it is therefore useful to understand the mechanisms that regulate cancer pathways related to stemness.[40] Such studies have already guided the discovery of novel therapeutic targets.[41] Through ongoing investigations on the role of

CSCs in cancer, we can clarify the therapeutic value of targeting CSCs and develop improved strategies for better clinical outcomes.[40]

1.3 Cancer Metabolism

Under normal homeostatic conditions, several metabolic pathways regulate cell growth. Depending on the availability of nutrients, these metabolic pathways coordinate to control the conversion and incorporation of nutrients into forms of molecules that support cell growth and proliferation.[42] Additionally, cells also require energy, commonly in the form of adenosine triphosphate (ATP), in order to proceed with the necessary metabolic reactions for survival. One of the distinguishing characteristics of cancer is dysregulated cellular energetics. Because cancer cells proliferate quickly, they require more than the basic needs for normal biological processes. In fact, cancer cells require rapid generation of ATP and increased synthesis of macromolecules to sustain their growth. In adaptation of these high metabolic demands, multiple molecular mechanisms in cancer cells are modified to meet their altered needs.[43]

Various molecules such as lipids and proteins can be used to supply energy, but glucose and its intermediates are the central molecules in energy metabolism. Glucose is processed through cellular respiration, which is composed of two energy-harvesting stages: glycolysis and mitochondrial oxidative phosphorylation (OXPHOS). Of the two, OXPHOS is an oxygen-dependent process that is more efficient in producing ATP. Thus, normal differentiated tissues primarily rely on OXPHOS. However, glycolysis remains an important pathway as it is closely linked to OXPHOS and can occur without oxygen, enabling the continuance of energy production under anaerobic conditions. When oxygen is scarce, cells are limited to glycolysis for ATP production, known as anaerobic cellular respiration.[44] In the 1920s, it was interestingly noted by Otto Warburg that cancer cells preferentially generate their energy via the more inefficient glycolytic pathway irrespective of oxygen availability. This aerobic glycolysis is thought to have several beneficial functions for cancer cells, including rapid ATP synthesis to compete for limited glucose, and diversion of glycolytic intermediates into biosynthesis pathways such as the serine biosynthetic pathway and the pentose phosphate pathway, which generate molecules required for proliferation.[45] While the proliferation of normal cells is

controlled by growth factors that regulate nutrient uptake from the environment, cancer cells have mutations that constitutively upregulate pathways involved in growth, allowing for aberrant metabolic processes to support their uncontrolled proliferation.[46]

A key pathway regulating both glucose metabolism and growth is the phosphoinositide 3-kinase (PI3K) signaling pathway. PI3K and its downstream molecules, Akt and mammalian target of rapamycin (mTOR), must be activated by growth factors in normal cells but are aberrantly activated in cancer cells.[43,46] In fact, Akt is frequently overexpressed in cancers, and different aspects of its signaling pathway have been targeted for therapy.[47] Akt is activated by phosphorylation and stimulates glucose uptake and glycolysis through mTOR signaling. mTOR stimulates hypoxia-inducible factor 1 (HIF1) which shifts the cell towards glycolysis by regulating the expression of many glycolytic enzymes and glucose transporters (GLUT1 and GLUT3).[43,46] Additionally, HIF1 increases the expression of c-Myc, which is another master transcription factor capable of affecting glycolysis via the regulation of hexokinase 2 (HK2) and pyruvate dehydrogenase kinase 1 (PDK1).[43,46] HK2 converts glucose to glucose-6-phosphate in the irreversible step of glycolysis and is a key enzyme for the Warburg effect,[43,48] while PDK1 inhibits pyruvate dehydrogenase (PDH), which is the rate-limiting enzyme that controls the entry of pyruvate into the TCA cycle for oxidative metabolism.[49] PDK1 thus promotes glycolytic metabolism in cancer cells. The final step in glycolysis is catalyzed by pyruvate kinase, and its M2 isoform (PKM2) has tumorigenic functions that promote Oct4, HIF1, c-Myc, and mTOR, contributing to the Warburg effect.[50] Aside from metabolism, Akt is a central molecule in pathways for several other processes. Akt plays a role in survival by suppressing proapoptotic factors and downregulating p53.[47] It promotes cell cycle progression by antagonizing cell cycle inhibitors and increasing the expression of cyclins.[47] Through mTOR, the PI3K signaling pathway regulates macromolecular biosynthesis for cell growth and proliferation; mTOR promotes ribosomal biogenesis and protein translation when amino acids are available.[51]

Under nutrient-rich conditions, mTOR favors the synthesis of proteins by suppressing autophagy. Autophagy is an evolutionarily conserved process that degrades and recycles cytoplasmic material to supply the cell with metabolic intermediates. When

growth conditions lack nutrients, mTOR will be downregulated to allow for the autophagy machinery to activate.[51] Autophagy is upregulated during times of nutrient stress but it is also responsible in maintaining housekeeping duties to eliminate protein aggregates and damaged organelles. The multistep process of autophagy begins with the formation of a double membrane, called the phagophore, which engulfs cellular constituents to be degraded. Formation of the phagophore is mediated by autophagy-related gene (ATG) complexes which are conjugated in an ubiquitin-like system. Microtubule-associated protein light chain 3 (LC3) plays a role in capturing the targets for degradation, and is also processed before it is inserted into the phagophore membrane. Full length LC3 is cleaved into LC3-I and then conjugated to phosphatidylethanolamine (PE) to generate LC3-II. The ATG complexes recruit LC3-II to the phagophore before they dissociate from the completed autophagosome (Figure 1.3). LC3-II can selectively interact with degradation targets bound to an adaptor molecule such as p62/SQSTM1. The autophagosome and its cargo finally fuse with the lysosome to form the autolysosome, leading to proteolytic degradation of the constituents (Figure 1.4).[52]

In cancer, the role of autophagy has been controversial. Autophagy can serve as a mechanism to sustain the survival of cancer cells during times of metabolic stress, and can provide the necessary materials for anabolic reactions in the metabolically active cancer cells.[53] It was reported that breast CSLCs express higher levels of the autophagy protein Beclin-1, and exhibit increased autophagy flux than non-stem-like cancer cells. Silencing of Beclin-1 reduced the self-renewal ability and tumorigenicity of CSLCs, supporting the role of autophagy as a tumor survival mechanism.[54] Along similar lines, autophagy inhibition in glioblastoma CSLCs impaired migration and invasion, highlighting its role in mediating a more aggressive phenotype.[55] Another report showed that in colorectal CSLCs, oxaliplatin-induced autophagy helped protect stemness and prevent apoptosis.[56] On the other hand, autophagy can also result in cell death by sensitizing cells to apoptosis or act as an alternative to apoptosis due to excessive self-degradation.[53,57] It was reported that treatment with rottlerin in pancreatic CSLCs induces autophagy and leads to cell death.[58] Interestingly, Beclin-1 was shown to play a dual role as it inhibits the tumorigenesis of non-stem-like cancer cells.[54,59] On yet another note, it appears that a critical balance of autophagy activity may be required to maintain the

stemness of embryonic carcinoma CSLCs.[60] Overall, it is evident that more research on autophagy in cancer needs to be performed to clarify its role, which is likely to be context-dependent.

1.4 Nicotinamide Adenine Dinucleotide (NAD^+)

Nicotinamide adenine dinucleotide (NAD^+) is classically known as a coenzyme for oxidoreductases, where it is used for hydride transfers during biochemical reactions. Along with its reduced form, NADH, NAD^+ performs important redox functions that are required in essential metabolic activities, such as the generation of ATP. During glycolysis, NAD^+ is reduced by glyceraldehydes-3-phosphate dehydrogenase (GAPDH) to convert glyceraldehyde-3-phosphate (G3P) to 1-3-biphosphoglycerate (1,3-BPG). Additional NAD^+ molecules are also reduced through the tricarboxylic acid (TCA) cycle to form certain TCA cycle intermediates. The NADH produced from these reactions is then oxidized by Complex I in the electron transport chain (ETC) to generate a proton motive force across the inner mitochondrial membrane (Figure 1.5). ATP synthase then harnesses the chemiosmotic gradient and produces ATP via oxidative phosphorylation.[61]

The participation of NAD^+ in redox reactions involves conversions between its oxidized and reduced form, whereby total levels of the coenzyme remain unchanged. However, it was discovered that a turnover of NAD^+ indeed occurs in cells, detected by a gradual decline in NAD^+ levels.[62] The breakdown of NAD^+ suggested that the molecule had additional roles beyond that of a coenzyme. In later years, NAD^+ was identified to act as a substrate for different classes of enzymes: poly-ADP-ribose polymerases (PARPs), cyclic-ADP-ribose (cADPR) synthases, and sirtuins (SIRTs).[63,64] NAD^+ is composed of two mononucleotides, nicotinamide mononucleotide (NMN) and adenosine monophosphate (AMP).[65] PARPs PARylate target proteins by cleaving and transferring the ADP-ribose moiety of NAD^+, leaving nicotinamide (NAM) as a by-product. They mediate DNA repair, chromatin remodeling, DNA replication, cell death, and metabolism. cADPR synthases use NAD^+ to produce cADPR, a secondary messenger involved in Ca^{2+} mobilization, cell cycle, and insulin signaling. SIRTs are lysine deacetylases that have a broad scope of physiological roles, including the regulation of metabolism and longevity.[61] Through the activity of these enzymes which depend on the consumption of

NAD^+, NAD^+ itself plays a crucial role in a wide range of signaling pathways and cellular activities.

Since NAD^+ is such a central molecule in regulating cellular processes and maintaining homeostasis, NAD^+ is also implicated in several diseases such as diabetes, obesity, and cancer. In particular, much of the original interest in NAD^+ biology stemmed from its link to aging.[61] The hallmarks of aging include depletion of the stem cell population, genomic instability, and senescence. Senescence is a cell cycle arrest process where cells lose their proliferative potential.[66] The decline of cellular function that occurs during aging increases the vulnerability of cells to pathologies including diabetes and cancer.[67] Research in various species have shown that NAD^+ levels decline with age, whereas NAD^+ levels rise during health-benefiting activities such as exercise. Additionally, enhancement of NAD^+ levels via supplementation with precursors prolongs the lifespan of multiple species,[61,68] and improves the phenotypes of aging in mouse stem cell models.[69] These effects occur in a SIRT1-dependent manner, and it is worth noting that of the NAD^+-dependent enzymes, only SIRTs have been consistently linked with cell survival and longevity, where they regulate many NAD^+-mediated control of aging.[63] As such, SIRTs have also been the interest of much research and their roles in cellular processes are described in the following section.

1.4.1 NAD^+ Synthesis Pathways

Since NAD^+ is continuously consumed by enzymes during regulation of various cellular processes, the regeneration of NAD^+ levels via biosynthetic pathways is crucial for the maintenance of cellular homeostasis (Figure 1.6).

***De novo* pathway**: Biosynthesis of NAD^+ is accomplished through multiple routes in mammals. These routes of NAD^+ synthesis can be classified as either *de novo* or salvage pathways. *De novo* synthesis of NAD^+ starts with the essential amino acid L-tryptophan and proceeds through the kynurenine pathway. In fact, 90% of the cell's free tryptophan is metabolized through the kynurenine pathway which leads to production of NAD^+, along with intermediates such as kynurenine, 3-hydroxyanthranilic acid, quinolinic acid (QA), kynurenic acid, and picolinic acid.[70,71] In the first and rate-limiting

step of the pathway, tryptophan is converted to N-formylkynurenine by the action of indoleamine 2,3-dioxygenase (IDO) or tryptophan dioxygenase (TDO), localized in the cytoplasm.[72,73] After a series of subsequent enzymatic conversions, α-amino-β-carboxymuconate-ε-semialdehyde (ACMS) is formed at a branch point in the pathway. At this point, ACMS may be diverted from NAD^+ synthesis by ACMS decarboxylase (ACMSD). The decarboxylation of ACMS to α-amino-β-muconate-ε-semialdehyde (AMS) can route it towards a spontaneous reaction to produce picolinic acid, or can lead to its complete oxidation via the glutarate pathway and TCA cycle. Alternatively, ACMS can be directed towards the NAD^+ synthesis pathway, where it spontaneously undergoes cyclization to form QA (Figure 1.7). Therefore, the formation of QA is inversely correlated with ACMSD activity, which exerts a major regulatory mechanism on the *de novo* pathway.[61] Once QA has been committed to the NAD^+ synthesis pathway, it is converted by quinolinic acid phosphoribosyltransferase (QAPRT) to nicotinic acid mononucleotide (NAMN). QAPRT is the second rate-limiting enzyme of the *de novo* pathway and is most highly expressed in the liver and kidney.[74] NAMN is then adenylated to nicotinic acid adenine dinucleotide (NAAD) by one of the three nicotinamide mononucleotide adenylyl transferase isoforms (NMNAT1-3). NMNAT1 is localized in the nucleus, NMNAT2 in the cytoplasm and Golgi, and NMNAT3 in the mitochondria. Finally, the last step in the *de novo* pathway involves amidation of NAAD to NAD^+ by NAD^+ synthetase (NADS).[61,75]

Salvage pathways: Although most cells can synthesize NAD^+ *de novo* from tryptophan, the main source of NAD^+ is supplied by salvage pathways that synthesize NAD^+ from dietary vitamin B3, or niacin, as precursors. The NAD^+ salvage pathway has several possible starting metabolites: NAM, nicotinic acid (NA), and their nucleoside derivatives, nicotinamide riboside (NR) and nicotinic acid riboside (NAR). Each of these precursors is converted to either NMN or NAMN as intermediates in the NAD^+ pathway.[74,76,77] Fittingly, NAM is also the by-product of NAD^+-consuming reactions and is therefore more readily available to be used as a NAD^+ precursor. The recycling of NAM to synthesize NAD^+ makes the salvage pathway more direct and more economical than other pathways. In the classical salvage pathway, NAM is catalyzed by the rate-limiting enzyme nicotinamide phosphoribosyltransferase (NAMPT) to NMN, which is

then adenylated to NAD^+ by NMNATs. NAMPT is localized in the cytosol and nucleus.[75] In the Preiss-Handler salvage pathway, the precursor NA is first converted to NAMN by nicotinic acid phosphoribosyltransferase (NAPRT) in the cytosol or nucleus. NAMN can then converge with the *de novo* pathway, where it is converted to NAAD and then to NAD^+.[78,79] Synthesis of NAD^+ from NR or NAR is catalyzed by the rate-limiting NR kinases (NRK1 and NRK2) in the cytosol, which phosphorylate the precursor to NMN or NAMN, respectively. These intermediates are then metabolized via the salvage pathways as described above.[61,76,77]

1.5 Therapeutic Potential of NAD^+ Modulation

From the diverse applications of NAD^+ as an intervention against diseases, several therapeutic strategies emerged and have undergone or are undergoing clinical trials. Two precursors of NAD^+, NR and NMN, are currently being tested for the augmentation of NAD^+ levels to treat or prevent various age-related conditions such as diabetes and cardiovascular disease.[80] For cancer treatments, targeting NAD^+ has been an attractive strategy given that many aberrant cellular processes in cancer rely on NAD^+. Therapies have been developed on the basis of targeting NAD^+ synthesis directly, or modulating cellular activities surrounding NAD^+, such as NAD^+-dependent enzymes.

1.5.1 Targeting NAD^+ Synthesis for Cancer Therapy

There is accumulating interest in therapeutics targeting NAD^+ for the treatment of cancer. This strategy emerged from the rationale that the increased metabolic activities of cancer cells should make them susceptible to modulations interfering with metabolism. Early NAD^+-interfering compounds such as tiazofurin and selenazofurin acted as NAD^+ analogues, which directly affected energy metabolism and caused general cytotoxicity.[81] Later, inhibitors of NAD^+ synthesis were identified, such as the specific and potent first-generation inhibitors of NAMPT, FK866 and GMX1778 (CHS828). GMX1778 decreased NAD^+ levels in HeLa cells and caused cell death, while exogenous addition of either NMN or NA, to restore NAD^+ levels, rescued GMX1778-mediated effects.[82] Because NAMPT inhibitors affects the production of NAD^+, the time course of their action consists of a gradual depletion of cellular NAD^+ content as the existing supply is

exhausted in NAD^+-hydrolyzing reactions. Since cancer cells have, in addition to higher energy demands, increased activity of SIRTs or PARP, their depletion of NAD^+ would occur at a faster rate upon inhibition of NAMPT.[81] Indeed, reduction in NAD^+ levels caused by NAMPT silencing decreased the growth rate of colon cancer cells, an effect which could be reversed by the addition of extracellular NMN, and which was mediated by SIRT1 and PARP1.[83] In prostate cancer cells too, SIRT1 function seemed to be involved in the downstream effects of NAMPT knockdown.[84] In another study using pancreatic cancer cells, it was reported that reduction of NAD^+ levels by FK866 resulted in cell death. Here, the detrimental effects of reduced NAD^+ levels were caused by disruption of redox status in glycolysis and a collapse in energy. Meanwhile, SIRT1 and PARP1 did not play significant roles in mediating the effects of FK866.[85] Regardless of the mechanisms behind the effects of NAD^+ inhibition, it is recognized that NAD^+ is a crucial molecule in multiple physiological pathways that are important for carcinogenesis.

To modulate NAD^+ levels, targeting the NAD^+-synthesizing enzymes is necessary. While inhibition of the enzymes in the *de novo* NAD^+ synthesis pathway has been studied as a therapeutic strategy, they are targeted primarily as an immunotherapy and not for the purpose of limiting NAD^+ production. The expression of IDO and other *de novo* enzymes has been reported to vary across cancers, but more interestingly, the endogenous IDO pathway is often hijacked by tumors to induce immune tolerance.[86–88] Instead of the *de novo* pathway, cancers depend heavily on the salvage pathways. Since the predominant precursor for NAD^+ synthesis is NAM, inhibitors of the enzyme NAMPT have been extensively studied as anticancer drugs that decrease NAD^+ levels. NAMPT is found in most tissues and is commonly overexpressed in cancers, including colorectal, ovarian, breast, gastric, and prostate.[89,90] In some malignancies, expression of NAMPT further correlates with tumor aggressiveness, chemoresistance, and poor prognosis.[83] The oncogenic role of NAMPT has also been associated with CSC properties, whereby NAMPT promoted CSC-like phenotypes including expression of CSC markers, pluripotency, and the ability of cells to form tumorspheres.[60,83] Unfortunately, the promising results that NAMPT inhibitors displayed in preclinical trials were not matched in clinical trials. Phase I clinical trials reported that administrations of APO866 (FK866) or GMX1778 (CHS828) were relatively well-tolerated, with common adverse events of

gastrointestinal symptoms and a dose-limiting toxicity of thrombocytopenia. However, no objective tumor regression was observed, although some patients showed stable disease after therapy.[91,92] APO866 continued to be tested in Phase II clinical trials for treatment against lymphomas, but similarly showed lack of efficacy.[93]

1.5.1.1 NAPRT in Cancer

NAPRT is a homodimer protein that localizes to both the cytoplasm and nucleus.[78,94] Until recently, studies surrounding NAPRT have focused on the absence of NAPRT in certain cancer cells in order to exploit their susceptibility to NAMPT inhibitors. In efforts to increase the therapeutic index of NAMPT inhibitors, researchers proposed the use of NA, an alternative NAD^+ precursor. It was hypothesized that supplementing exogenous NA during NAMPT inhibition allows cells to bypass the classical salvage pathway blockade and synthesize necessary NAD^+ via NAPRT, the enzyme of the Preiss-Handler pathway. This rescue is only possible in cells that express NAPRT and could help to protect normal tissues from the cytotoxicity of NAMPT inhibition. Opportunely, a significant number of cancers were identified to be deficient in NAPRT, including some lymphomas and neuroblastomas.[82,95,96] Thus, co-administration of NA during NAMPT inhibition in cancers lacking NAPRT can increase the tolerability of the drug without diminishing its antitumor effects. It was shown in certain NAPRT-deficient cancer cell lines that supplementation of NA did not protect against GMX1778 or APO866 cytotoxic effects. Moreover, xenograft mice treated with a lethal dose of NAMPT inhibitor also showed reduced mortality in the presence of NA, thus implicating that higher clinically effective doses of NAMPT inhibitors can be more safely administered.[82,97] However, the rescue strategy still requires further investigation as there seems to be differences in the efficacy of co-dosing between *in vitro* and *in vivo* models. One study found that co-treatment with NA did not protect NAPRT-deficient A2780 ovarian cancer cells from APO866-induced death *in vitro*; however, co-treatment in A2780 xenografts reduced the antitumor effects of APO866 *in vivo*.[97] Similarly, another study compared the *in vitro* and *in vivo* efficacy of the co-treatment strategy in multiple NAPRT-deficient cell lines and patient-derived cell lines. The NAMPT inhibitors, GNE-617 and GNE-618, remained effective in inhibiting the proliferation of cancer cells

during NA supplementation *in vitro*, but significantly or completely lost their anti-proliferative effects in all xenograft models *in vivo*.[98] Therefore, it appears that while toxicity can be ameliorated by NA supplementation, the beneficial effect is not exclusive to normal cells and can compromise the antitumor effects of NAMPT inhibition.

Despite the considerable number of studies in the context of NAPRT-deficient cancers, one recent paper from Piacente et al. has emerged which focuses on the role of NAPRT itself in cancer. Importantly, although NAM is the by-product of NAD^+-consuming reactions and is therefore more readily available to be used by NAMPT for NAD^+ synthesis, NA is more efficiently used by NAPRT to increase NAD^+ levels. This could be due to the fact that unlike NAMPT, NAPRT is not subject to feedback inhibition by NAD^+ and can thus continuously contribute to rising NAD^+ levels when supplemented with NA.[94] The NAPRT enzyme is therefore a crucial provider of cellular NAD^+, especially in tissues that highly express NAPRT, such as the liver, kidney, heart, and small intestine.[94]

In contrast to the studies that noted the lack of NAPRT in cancers, Piacente et al.[99] showed that a significant number of cancers actually have amplified *NAPRT* transcripts and increased NAPRT expression. These included ovarian, pancreatic, prostate, and breast cancers. They focused on endogenous NAPRT-overexpressing ovarian and pancreatic cancer cells. While NAPRT knockdown or FK866 treatment alone depleted NAD^+ levels, cell viability only decreased when NAPRT knockdown was combined with FK866. This was likely due to the varying extents of NAD^+ depletion in the single treatments, which were insufficient to affect cell viability. The survival of xenograft mice bearing tumors with silenced NAPRT was significantly increased when they were treated with FK866, and despite the *in vitro* results, mice injected with NAPRT knockdown cells exhibited a trend in increased survival compared to those injected with control cells. NAPRT knockdown in BRCA-deficient cancer cells decreased their ability to form colonies after MMS-induced DNA damage, suggesting that NAPRT plays a role in PARP-mediated DNA repair mechanisms through provision of NAD^+.[99] Furthermore, the role of NAPRT in promoting OXPHOS and ATP production was also examined.[99]

Concluding from the results of the investigation, the authors proposed that NAPRT is an attractive target to sensitize cells to NAMPT inhibitors or DNA damaging agents.[99]

1.5.2 Targeting NAD^+-Dependent Enzymes for Cancer Therapy

Related to NAD^+, other therapies have focused on directly targeting NAD^+-utilizing enzymes due to their links to cancer. PARP has been an attractive target for cancer therapy, given its role in DNA repair. Spontaneous mutations that occur during cellular replication are normally resolved by genome maintenance systems. If mutation rates are increased by mutagenic agents or as a result of defective DNA repair machinery, cells will acquire successive genome mutations and eventually become cancerous.[3] While genetic instability enables the transformation of cancer cells, it has also been shown that patient samples of hepatocellular carcinoma tissues have increased expression of PARP, likely as a survival mechanism.[100] The viability of $PARP^{-/-}$ mice show that PARP can be dispensable for normal activity, but PARP is crucial for cell survival upon DNA damage.[101] Similarly, BRCA-deficient cancer cells are defective in the homologous recombination pathway of DNA repair and are highly dependent on PARP for maintaining genome stability. Thus, treating BRCA-deficient cancer cells with PARP inhibitors increases genome instability and causes apoptosis.[102] Moreover, tumor cells that are resistant to DNA-damaging chemotherapies, such as cisplatin, often display increased DNA repair activity as a response.[101] For this reason, PARP inhibition has been a focus in cancer treatment strategies, and several inhibitors have been developed. These inhibitors are currently in clinical trials for use as both monotherapy and combination therapy.[102]

1.5.2.1 Sirtuins

Another reason that targeting NAD^+ in cancer is of interest is because such modulation will inevitably affect SIRTs. SIRTs have many implications in cancer and although a few pharmaceuticals have been developed, there remains some uncertainty regarding the oncogenic or tumor suppressor nature of SIRTs due to their complex roles.[103]

Sirtuins are class III deacetylases that remove acetyl groups from lysine residues on histones and non-histone proteins. They have an evolutionarily conserved catalytic site and differ from other deacetylases due to their dependence on NAD^+ for activity.[104] Meanwhile, other classes of histone deacetylases (class I, II, and IV) require a zinc ion to function and are categorized according to their sequence similarities.[105] In a two-step deacetylation reaction, SIRTs first hydrolyze NAD^+ before transferring the acetyl group onto ADP-ribose to form O-acetyl-ADP-ribose and release NAM.[104] There are seven mammalian SIRTs (SIRT1-7), some of which possess additional catalytic activities. SIRT4 and SIRT6 have ADP-ribosyltransferase activity, while SIRT5 has desuccinylase, demalonylase, and deglutarylase activity. As such, SIRTs participate in a wide range of post-translational modifications and are prominent regulators of cellular processes. SIRTs are distributed throughout the cell, with SIRT3-5 located in the mitochondria, SIRT2 in the cytoplasm, and SIRT6-7 in the nucleus. SIRT1 is predominantly found in the nucleus, where it regulates many known gene targets, but it can also shuttle to the cytoplasm. Even in extranuclear locations, SIRTs are able to regulate gene expression via the modification of transcription factors.[61]

SIRT1: SIRT1 was the first SIRT discovered in yeast, where its longevity-promoting effects garnered a lot of interest.[106] The link of SIRT1 to aging is still unclear but it seems that SIRT1 influences lifespan by mediating the effects of NAD^+. Thus, its reduced activity in aging cells is likely due to the concomitant decrease in NAD^+.[106,107] SIRT1 is the most well-characterized SIRT and extensive studies have demonstrated its role in cancers, where it regulates processes such as proliferation, differentiation, cell survival, metabolism, and DNA repair.[104,106] Targets of SIRT1 modification include proteins involved in tumorigenesis such as the signaling molecule c-Myc and transcription factors p53 and p73. SIRT1 is notably known for deacetylating and deactivating the tumor suppressor p53, the effects of which are inhibition of p53-dependent apoptosis. SIRT1 overexpression is observed in lung, colon, and liver cancers, where it stabilizes and increases the level of c-Myc to promote cell proliferation. Expression of SIRT1 in breast cancer specimens is also associated with poor prognosis. Accordingly, SIRT1 was considered as a tumor promoter, but its role in cancer has since revealed itself to be more controversial.[108] Expression or induction of SIRT1 in mouse

models reduces the incidence and progression of tumor formation in various studies, while reduced SIRT1 expression increases metastasis of HMLER breast cancer cells in nude mice. SIRT1 negatively regulates survivin, an apoptosis inhibitor that promotes growth in BRCA1-associated breast cancers which have lower SIRT1 levels. More recent studies showed that SIRT1 level is decreased in some human cancers, and another study showed that SIRT1 level in breast cancer patients is associated with better prognosis. Hence, the role of SIRT1 remains complex, in part because many of its substrates are also its regulators; SIRT1 is repressed by p53 under normal conditions, and consumption of NAD^+ generates the bi-product NAM, which exerts end product inhibition on SIRT1.[61]

SIRT2: SIRT2 is mainly a cytoplasmic deacetylase with many substrates. It regulates enzymes involved in cell cycle and activates glucose-6-phosphatase dehydrogenase (G6PD) from the pentose phosphate pathway. Similar to SIRT1, there is evidence to suggest it serves as both a tumor suppressor and promoter. Mice that are SIRT2-deficient develop HCC or mammary tumors. Conversely, the upregulation of SIRT2 in neuroblastoma cells and pancreatic cancer cells stabilizes the Myc oncoprotein, and SIRT2 downregulation results in apoptosis of cervical carcinoma HeLa cells.[106,109] Pharmacological inhibition of SIRT2 by AK-1 leads to cell cycle arrest and degradation of epithelial-mesenchymal transition (EMT) marker Snail.[110]

SIRT3-5: SIRT3 is present in the mitochondrial matrix and is thus in the ideal location to regulate cellular energy metabolism through the deacetylation of major mitochondrial enzymes involved in cellular respiration ATP production. SIRT3 inhibits the generation of reactive oxygen species, which protects against cancer, as seen by SIRT3-null mice that develop tumors. SIRT4 is also located in mitochondria, and is involved in similar functions as SIRT3, regulating fatty acid oxidation and NAD^+ levels. Its expression is observed to be reduced in several types of cancers, proposing it as a tumor suppressor. SIRT5 can additionally regulate metabolic pathways through its demalonylase and desuccinylase activity to positively regulate glycolysis, and is involved in the urea cycle. While SIRT5 has not been extensively studied in cancer, its overexpression in lung cancer and association with poor outcomes suggest that it may act as an oncogene.[106]

SIRT6: SIRT6 resides in the nucleus where it has been linked to promote lifespan as SIRT6-deficient mice die prematurely of age-related conditions. Its downregulation in colon cancers correlates with poor prognosis, but it increases tumor aggressiveness in breast and pancreatic cancers. Nevertheless, SIRT6 is commonly regarded as a tumor suppressor as it exhibits aerobic glycolysis-inhibiting effects via repression of HIF1α.[109]

SIRT7: SIRT7, one of the lesser studied SIRTs, is a nuclear deacetylase that is enriched in the nucleolus, where it regulates ribosomal RNA expression and is implicated in supporting protein synthesis for proliferating cells.[111] Under normal circumstances, SIRT7 promotes ribosome biogenesis and activity, which can fuel cancer cell growth. However, during endoplasmic reticulum (ER) stress in cancer cells, SIRT7 helps in the unfolded protein response (UPR) by repressing the transcription of ribosomal proteins and thereby preventing stress-induced apoptosis.[111] In U2OS cells and gastric cancer cells, SIRT7 is required for survival as knockdown of SIRT7 induces apoptosis.[106,112] Other stress-adapting pathways in which SIRT7 is involved include the regulation of HIF1. SIRT7 is overexpressed in colon, kidney, ovarian, breast, and prostate cancers, correlating with the expression of other oncogenes.[106,109] In colorectal cancer, SIRT7 knockdown decreased cell proliferation, while SIRT7 overexpression induced EMT and invasion *in vivo*.[113] Similarly, xenografts of SIRT7-depleted U251 and Hep3B cells are dramatically less tumorigenic *in vivo*, positioning SIRT7 as an oncogene.[111] However, the potential for SIRT7 to pose as a therapeutic target remains unclear as SIRT7 also executes beneficial health effects. SIRT7 deficiency is associated with aging phenotypes and SIRT7 can prevent fatty liver pathology via alleviation of ER stress.[111]

1.6 Research Rationale

Given the altered metabolic properties of tumor cells which support their high energy demands for rapid cell proliferation, the modulation of cancer metabolism is an attractive anticancer therapeutic strategy. Moreover, recent studies showed that the metabolic profiles of CSCs and non-CSCs also differ, whereby CSCs rely even more heavily on glycolysis than other tumor cells.[114] Glycolysis requires the redox molecule NAD^+ which is synthesized via three main pathways: the *de novo* pathway, salvage pathway, and Preiss-Handler pathway. Much research has been conducted on the rate-

limiting enzyme of the classical salvage pathway, NAMPT, to target NAD^+ synthesis in cancer cells. Unfortunately, inhibitors of NAMPT have shown disappointing efficacy in clinical trials, possibly due to the continued availability of NAD^+ supplied via other pathways. To improve the strategic treatment of NAD^+ modulation, researchers are beginning to expand their investigations on better understanding the other NAD^+-synthesizing enzymes. NAPRT is the rate-limiting enzyme of the Preiss-Handler pathway and has scarcely been studied as a target for cancer therapy.

Moreover, the role of NAPRT in the context of CSLCs has never been studied, and my involvement in two separate works conducted during my Master's degree has highlighted that CSLCs and bulk tumor cell responses can vary drastically, with important clinical implications. In our recently accepted *Autophagy* paper, we uncovered that HDAC6 has a differential role in regulating autophagy in CSLCs and differentiated cells. Additionally, knockdown of HDAC6 promoted cell death in differentiated cancer cells but not in CSLCs. In a second paper, which is currently undergoing revisions for *Clinical Cancer Research*, we demonstrate an unexpected role of TAp73 in CSLCs. TAp73 is a tumor suppressor that belongs in the well-known p53 family, but in CSLCs, TAp73 contributes to the maintenance of stemness properties. Thus, cancer treatments aiming to modulate TAp73 are not likely to affect the CSLC population significantly and can lead to chemoresistance. With these distinctions between CSLCs and bulk tumor cells in mind, it is warranted that research on NAPRT does not neglect to study its role in the context of CSLCs. I hypothesized that NAPRT has important functions in cancer cells and CSLCs, which could be exploited for therapeutic modulation. The purpose of my research was to explore the role of NAPRT in CSLCs and examine its mechanisms of action.

This research was undertaken with three models of CSLCs: the NT2/D1 embryonal carcinoma cells (ECCs), the HMLE-based breast cancer progression model (Figure 1.8), and $CD133^+$ patient-derived brain tumor-initiating cells. In investigating the effects of NAPRT in multiple CSLC models, my research anticipates the purposing of NAPRT as a novel target in cancer therapy. As well as the use of these CSLCs, other heterogeneous cancer cell lines were also used to serve as a basis for comparison.

1.6.1 Characterization of Models

1. Poorly differentiated tumors have an ESC-like signature that make ECCs a good model to study CSCs at the embryonic stage.[11,115–118] ECCs are the malignant stem cells of teratocarcinomas, which are germ cell tumors that contain undifferentiated stem cells and their differentiated derivatives. Teratocarcinomas are distinct from benign teratomas which do not contain ECCs and are composed of only somatic tissues.[119] The stemness of ECCs has been demonstrated *in vivo*, where the undifferentiated core of teratocarcinomas can be successfully serially transplanted to generate tumors.[11,120,121] In addition to their tumor-initiating ability, ECCs can also differentiate into somatic cells of all three germ layers.[122,123] The NT2/D1 cell line is one of the most studied ECC line and is commonly used as a embryonal carcinoma stem-like cell (ECSLC) model.[29,124–127] NT2/D1 is a subclone derived from a nude mouse xenograft of the TERA2 line, which was isolated from a metastasized testicular teratocarcinoma.[126] They harbor high levels of pluripotency stem cell markers such as Oct4, Nanog, and Sox2, resembling the ESC pluripotency gene signature which is linked to poorly differentiated tumors and poor prognosis. Also, they have been shown to differentiate into all three germ layers.[128–130]

2. The human mammary epithelial (HMLE)-based CSLC model includes a transition of cells from normal-to-transformed-to-stem-like cancer cells through the acquisition of specific genes. Primary human mammary epithelial cells (HMECs) were immortalized by ectopic expression of SV40 large T-antigen and the catalytic subunit of human telomerase reverse transcriptase (hTERT). The non-tumorigenic immortalized mammary cell line is termed HMLE and represents a normal cell line with epithelial characteristics.[131] HMLE cells were transformed to tumorigenic cancer cells through ectopic expression of oncogenic H-RAS^{G12V}, termed HMLER. Further silencing of E-cadherin in HMLER cells was shown to induce EMT and generate stem-like cells with significantly increased tumorigenicity. These HMLER-shEcad cells acquired a CD44^{high}/CD24^{low}

expression pattern that is associated with breast CSCs and were proficient at metastatic dissemination, whereas HMLER cells were nonmetastatic.[132–135]

3. Patient-derived brain tumor-initiating cells (BTICs) are identified based on their expression of neural stem cell surface marker CD133.[14] The $CD133^+$ cells exhibited stem cell phenotypes such as a lack of neural differentiation markers and *in vivo* self-renewal capacity. Xenograft assays injecting as few as 100 BTICs developed differentiated tumors that resembled the original patient tumor.[14,136] For *in vitro* growth, the culturing of BTICs in serum-free conditions has been established to retain their genotypic and stem cell properties after isolation from the patient's primary tumor.[137]

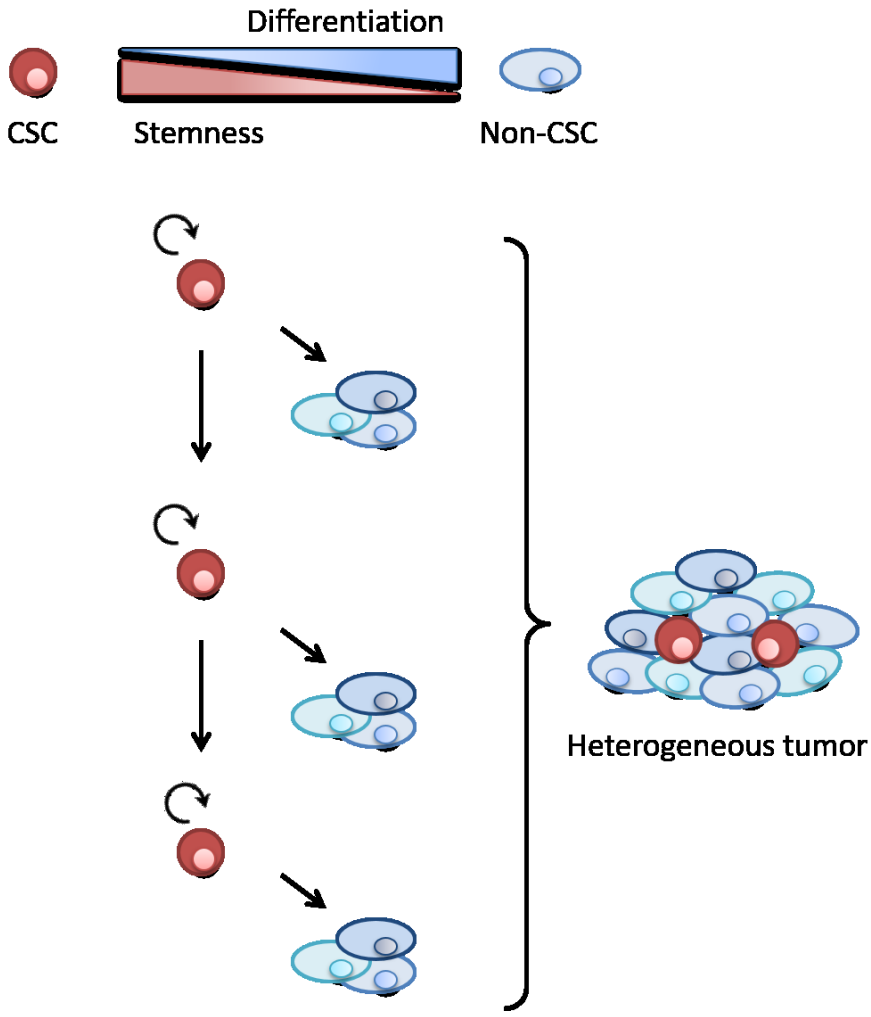

Figure 1.1 Cancer stem cell model of tumor development.

In the CSC model, a subpopulation of tumor cells possesses stemness characteristics of self-renewal and the ability to differentiate into various cell types. These CSCs, also known as tumor-initiating cells, are highly tumorigenic and are important in sustaining tumor growth. Through self-renewal divisions, the CSC pool is maintained, and the differentiation of CSCs into various cell types gives rise to a heterogeneous tumor.

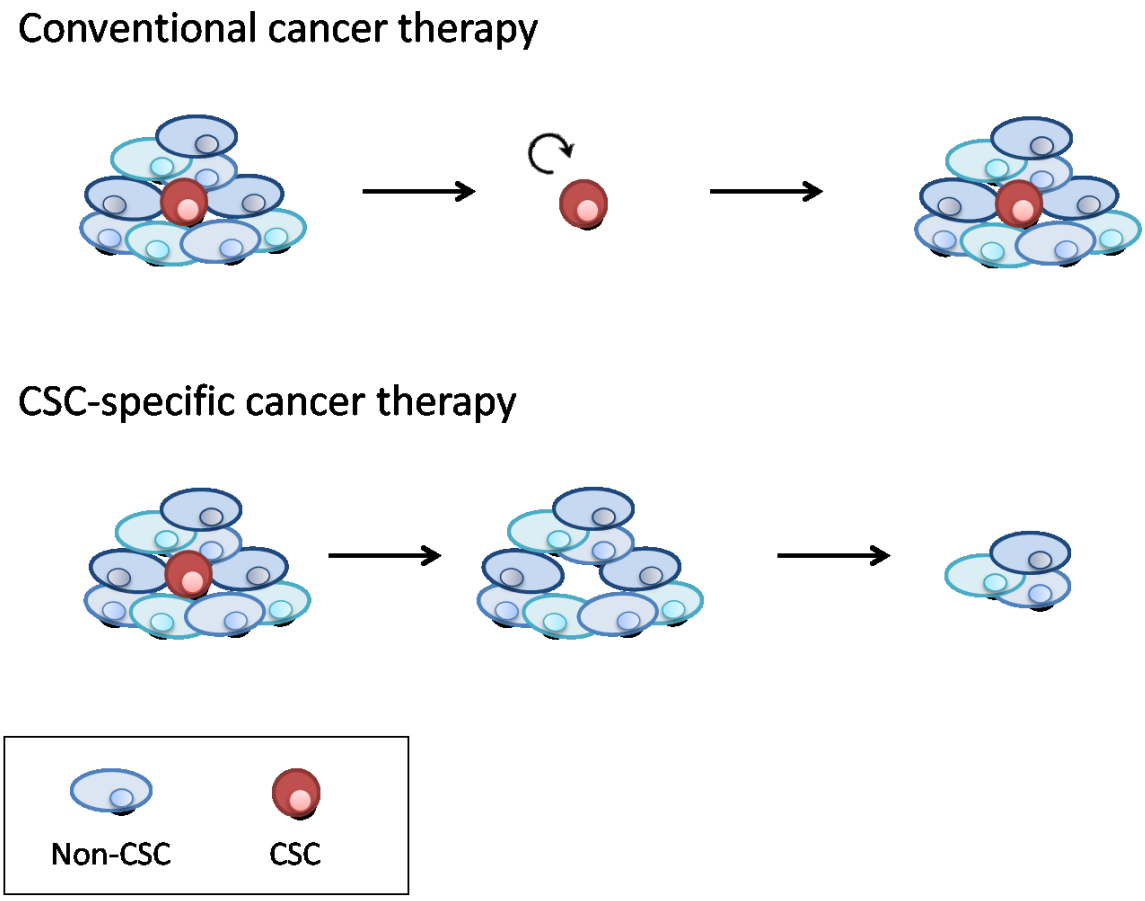

Figure 1.2. Targeting CSCs to suppress chemotherapy resistance and cancer relapse. Conventional cancer therapies are designed to target rapidly proliferating bulk tumor cells. However, CSCs have properties that make them generally more resistant to the therapeutic treatments that are effective against differentiated cancer cells. The survival of CSCs after treatment enables regeneration of tumors. Hence, many therapies are ultimately unsuccessful and result in the recurrence of cancer. For this reason, there is currently a focus in developing CSC-specific therapies to eradicate the source of tumor initiation for successful tumor regression.

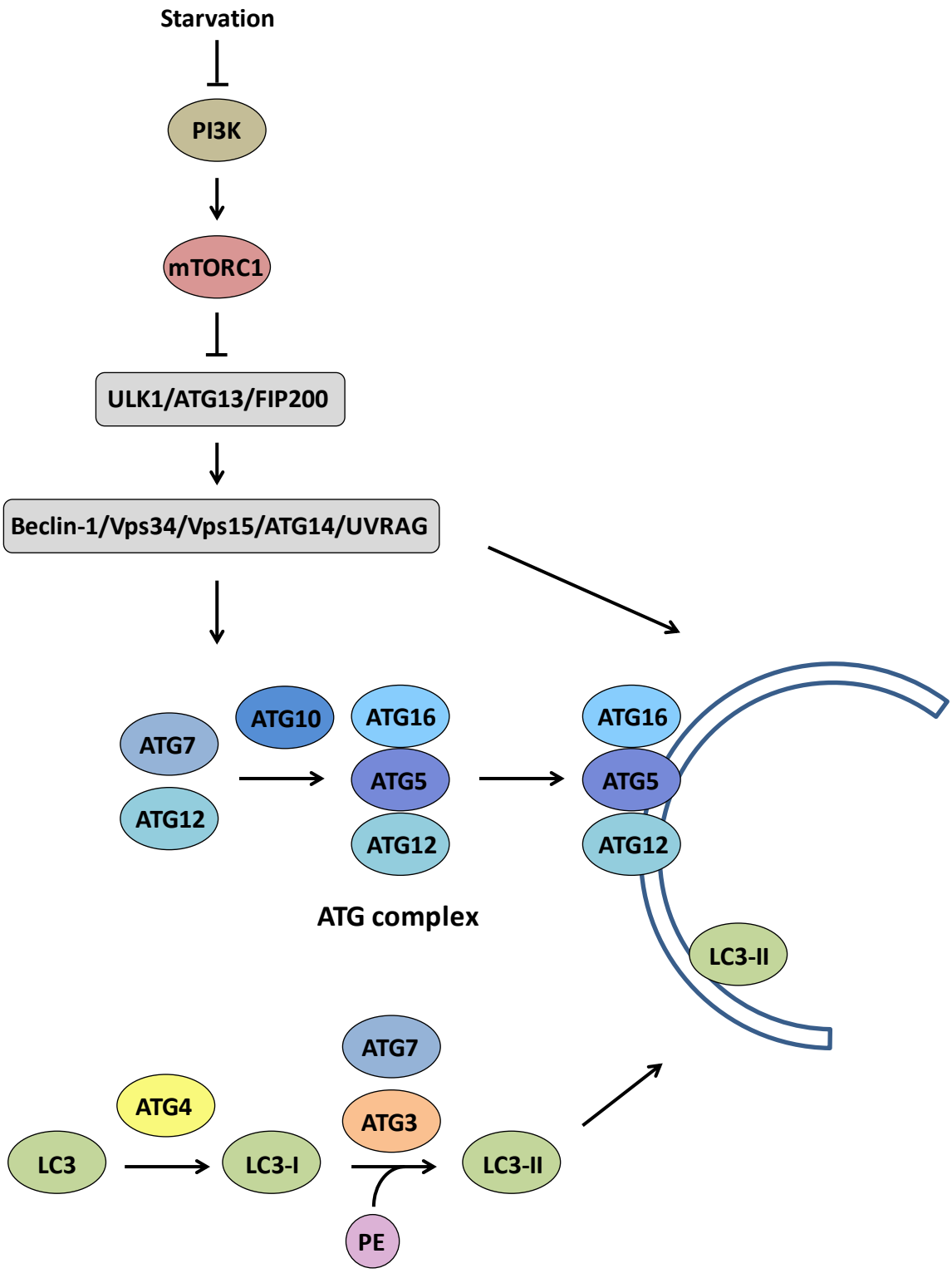
Starvation
PI3K
mTORC1
ULK1/ATG13/FIP200
Beclin-1/Vps34/Vps15/ATG14/UVRAG
ATG7
ATG12
ATG10
ATG16
ATG5
ATG12
ATG16
ATG5
ATG12
ATG complex
LC3-II
ATG4
LC3
LC3-I
ATG7
ATG3
LC3-II
PE

Figure 1.3

Figure 1.3. Autophagy induction and autophagosome formation.

During nutrient starvation, the PI3K pathway responds by inactivating mTOR complex 1 (mTORC1).[138] This releases the inhibition of ULK1, which forms a complex with ATG13 and FIP200.[139] The ULK complex then activates Beclin-1, which forms a complex with Vsp34, Vps15, ATG14, and UVRAG. This complex functions in initiating autophagosome formation, and also activates the ATG proteins.[139,140] The ATG proteins are processed in a ubiquitin-like system, where ATG7 activates ATG12 and transfers it to ATG10, which links ATG12 to ATG5 and ATG16. The ATG complex associates with the phagophore and is responsible for its maturation. In another ubiquitin-like system, LC3 is cleaved by ATG4 to LC3-I, which is transferred by ATG7 and ATG3 to PE, forming LC3-II. The ATG complex recruits LC3-II to the phagophore before dissociating from the mature autophagosome.[139]

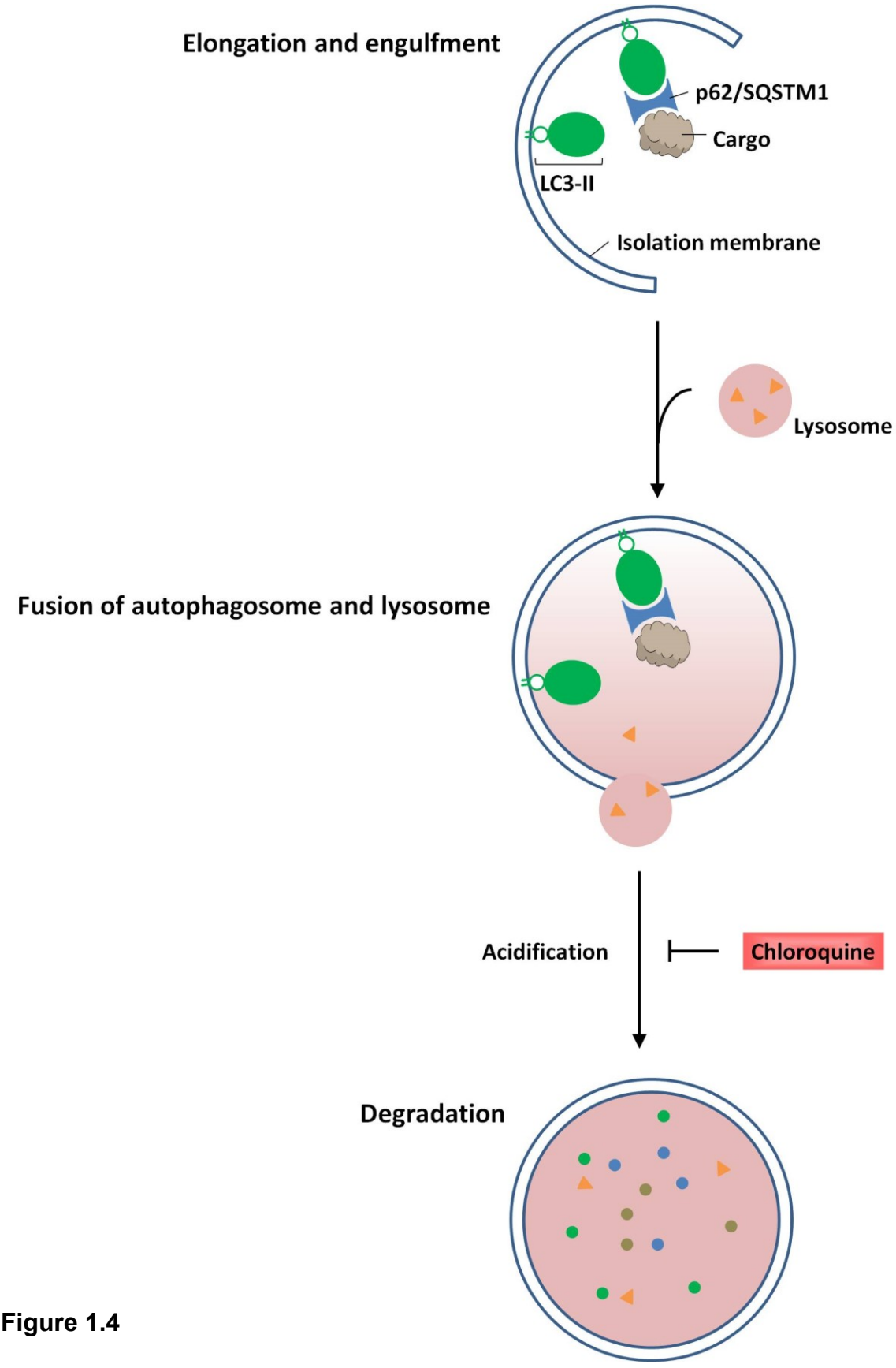
Elongation and engulfment
p62/SQSTM1
Cargo
LC3-II
Isolation membrane
Lysosome
Fusion of autophagosome and lysosome
Acidification
Chloroquine
Degradation

Figure 1.4

Figure 1.4 Schematic of autolysosome formation and degradation during autophagy. Isolation membrane begins to form for the engulfment of cargo. Processed LC3A/B-II associates with the autophagosome membrane to mediate its curvature. Adaptor protein p62/SQSTM1 links the cargo to the autophagic machinery. Autophagosomes fuse with lysosomes and are degraded by lysosomal hydrolases, resulting in turnover of LC3A/B-II and p62/SQSTM1. Chloroquine inhibits autophagic degradation of autophagosome contents, thus resulting in increased accumulation of autophagy proteins to assess for autophagy flux.

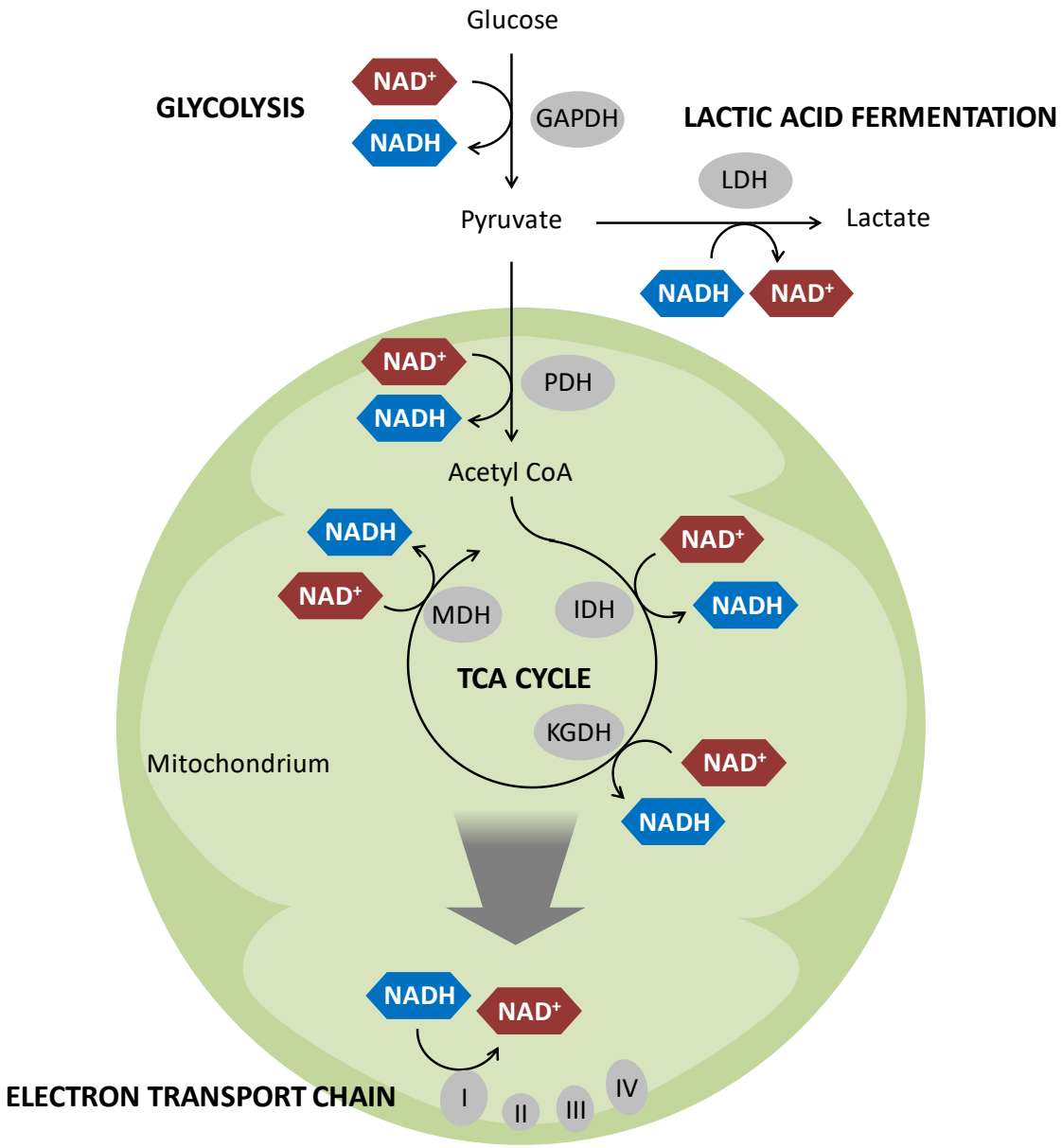
Glucose
GLYCOLYSIS
NAD+
NADH
GAPDH
LACTIC ACID FERMENTATION
LDH
Pyruvate
Lactate
NADH
NAD+
NAD+
NADH
PDH
Acetyl CoA
NADH
NAD+
MDH
IDH
NAD+
NADH
TCA CYCLE
KGDH
NAD+
NADH
Mitochondrium
NADH
NAD+
ELECTRON TRANSPORT CHAIN
I
II
III
IV

Figure 1.5

Figure 1.5. Role of NAD^+ in metabolism.

NAD^+ is used in glycolysis by GAPDH, to convert G3P to 1,3-BPG. NAD^+ can be regenerated by lactate dehydrogenase (LDH) during lactic acid fermentation, which converts pyruvate to lactate. Pyruvate which is shuttled to the mitochondrial matrix is converted to acetyl CoA by PDH, using NAD^+. Acetyl CoA enters the TCA cycle, which is used by isocitrate dehydrogenase (IDH), α-ketoglutarate dehydrogenase (KGDH), and malate dehydrogenase (MDH) to produce NADH from NAD^+. NADH is then used in the ETC by Complex I to generate a proton motive force for the production of ATP.

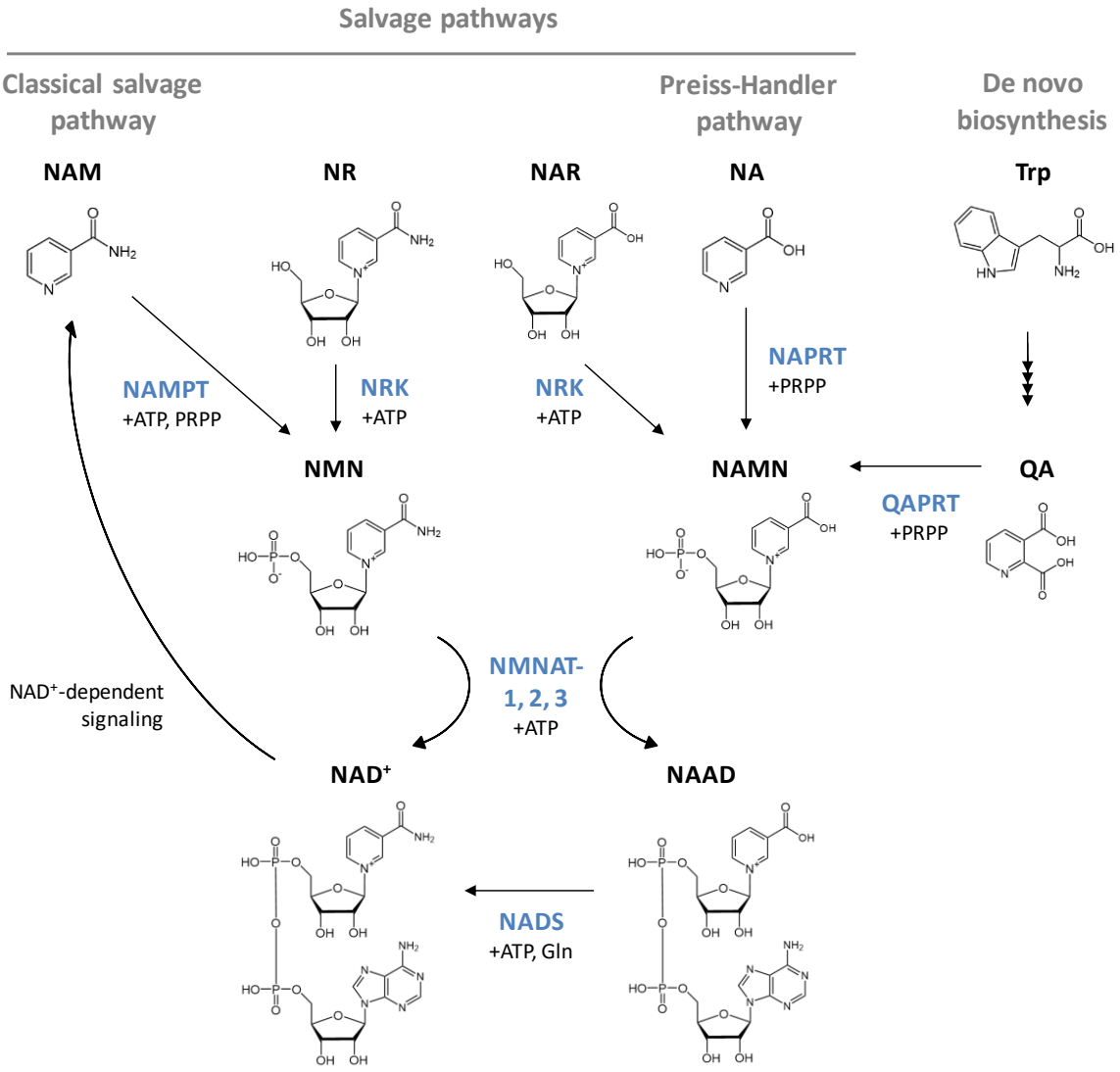
Salvage pathways
Classical salvage pathway
Preiss-Handler pathway
De novo biosynthesis
NAM
NR
NAR
NA
Trp
NAMPT
+ATP, PRPP
NRK
+ATP
NRK
+ATP
NAPRT
+PRPP
NMN
NAMN
QA
QAPRT
+PRPP
NMNAT-1, 2, 3
+ATP
NAD+-dependent signaling
NAD+
NAAD
NADS
+ATP, Gln

Figure 1.6

Figure 1.6. NAD^+ biosynthesis pathways.

NAM is converted to NMN by the action of NAMPT. NR or NAR is converted to NMN or NAMN respectively by the action of NRK. In the Preiss-Handler pathway NA is converted to NAMN by the action of NAPRT. NAD^+ is synthesized *de novo* by converting Trp to QA which is then converted to NAMN by the action of by QAPRT. NMN and NAMN are converted to NAD^+ and NAAD respectively by the action of NMNATs. NAAD can then be converted to NAD^+ by NADS.[141] Image reproduced with permission (Appendix A).

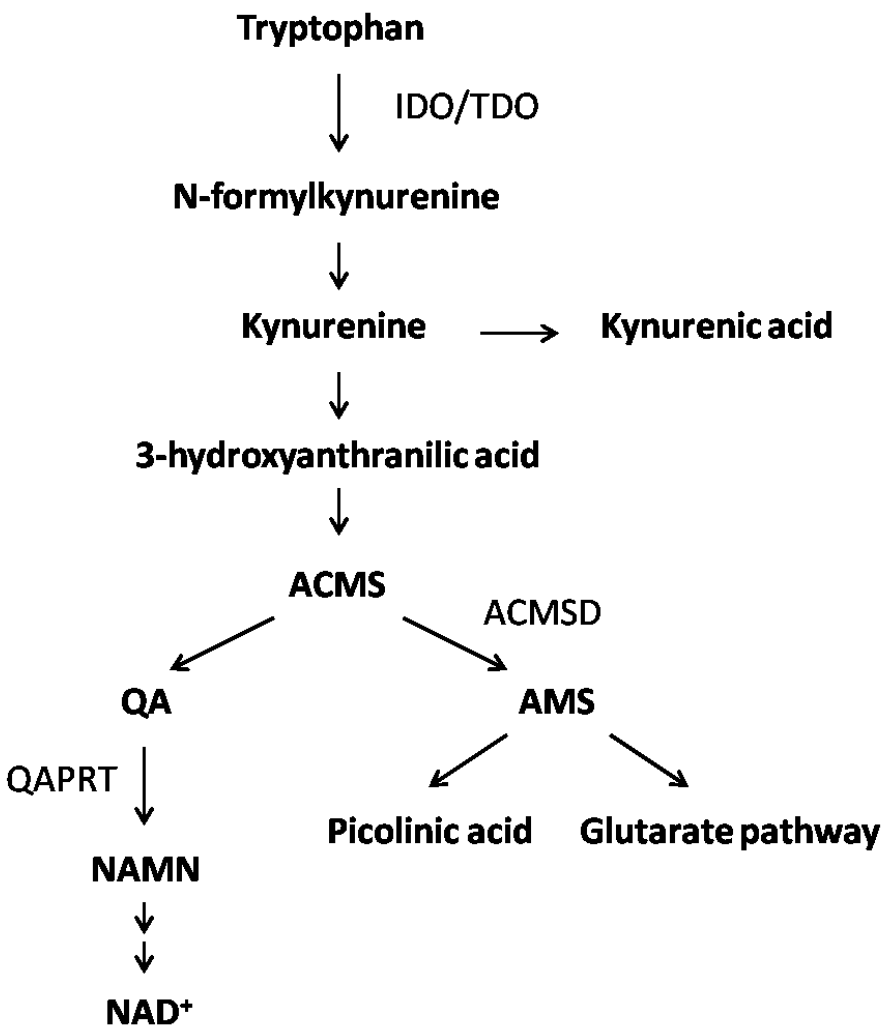

Figure 1.7. *De novo* NAD^+ synthesis pathway.

Tryptophan is converted to N-formylkynurenine in the rate-limiting step, catalyzed by IDO or TDO. After a series of reactions, ACMS is produced at a branch point in the pathway. Spontaneous conversion of ACMS into QA results in the production of NAD^+. Alternatively, ACMS is decarboxylated by ACMSD to AMS, to produce picolinic acid or to be used in the glutarate pathway.

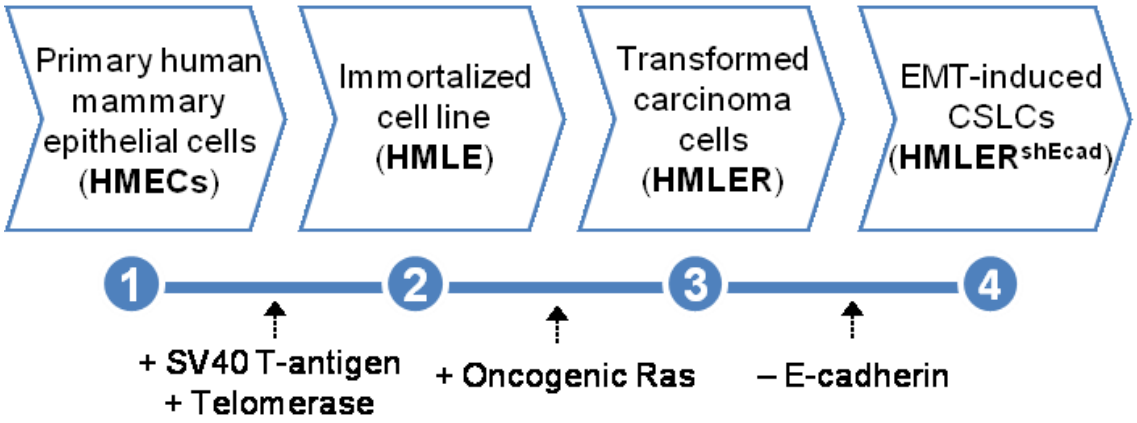

Figure 1.8. HMLE-based cancer progression model.

The HMLE-based model consists of cell lines that represent a transition from normal-to-transformed-to-stem-like cancer cells. Primary HMECs were immortalized by ectopic expression of SV40 large T-antigen and the catalytic subunit of hTERT. Non-tumorigenic normal cells, termed HMLE, were transformed by ectopic expression of oncogenic Ras. Transformed carcinoma cells, termed HMLER, were induced to undergo EMT by silencing of E-cadherin, generating HMLER-shEcad cells that had stem-like characteristics.[131,132,134,135]

CHAPTER 2: MATERIALS & METHODS

2.1 CELL CULTURE

Cell lines were obtained from ATCC, with the exception of HMLE-based cells and BT698. NT2/D1 cells were maintained in Dulbecco's Modified Eagle's Medium (DMEM) supplemented with 10% heat-inactivated fetal bovine serum (FBS) and 5% non-essential amino acid. IMR90 and WI38 were cultured in Eagle's Minimum Essential Medium (EMEM) supplemented with 10% FBS. MDA-MB-231, MDA-MB-468, MCF7, H1299, and A549 cells were cultured in DMEM supplemented with 10% FBS. HCT116 (p53 -/-) cells were cultured in McCoy's 5A Medium supplemented with 10% FBS. MCF10A were cultured in DMEM/F12 as described below.

The human mammary epithelial cell lines, HMLE, HMLER, and HMLER-shEcad, were generously provided by Dr. Robert Weinberg (Whitehead Institute, MIT).[132,134,135] HMLE and HMLER cells were maintained in DMEM/F12 supplemented with 5% FBS, 0.5 μg/ml of hydrocortisone, 20 ng/ml of epidermal growth factor (EGF), and 10 μg/ml of insulin. HMLER-shEcad cells were maintained in HuMEC serum-free medium containing supplements from the supplier (Thermo Fischer Scientific) that included EGF, hydrocortisone, isoproterenol, transferrin, insulin, and 50 μg/ml of bovine pituitary extract.

The patient-derived brain tumor-initiating cells (BTICs) enriched in CSCs were kindly provided by Dr. Sheila Singh (McMaster University).[14,136] These BTICs were derived from glioblastoma tumor tissues of consenting patients. Upon surgical removal, tissue samples were dissociated into single cells and sorted by magnetic beads using the Miltenyi Biotec CD133 cell isolation kit. BT698 cells contain a high population of $CD133^{+}$ BTICs and are thus considered $CD133^{high}$ BTICs. BT698 were cultured in NeuroCult™ NS-A Proliferation Medium (STEMcell Technologies), supplemented with 20 ng/ml of EGF, 10 ng/ml of basic fibroblast growth factor, and 2μg/ml of Heparin. This serum-free media allows the cells to be propagated as tumorspheres.

All cell culture media were supplemented with 5% Antibiotic-Antimycotic (Thermo Fisher Scientific), and cells were maintained at 37˚C in a humidified incubator

containing 5% CO_2. Excluding BT698, cells were grown in 10 cm tissue culture plates and were passaged at 80% confluency using 0.05% trypsin-EDTA (Thermo Fischer Scientific). BT698 were grown in 6 cm tissue culture plates and were passaged by titurating to single cells depending on size of tumorsphere.

2.2 TREATMENTS

Cells were seeded 24 h prior to treatment with 100 μM of NAMN (Sigma Aldrich) or 12 μM of chloroquine (Sigma Aldrich). Treatment period was 24 h before cells were collected for protein.

2.3 LENTIVIRUS PRODUCTION AND TRANSDUCTION

Knockdowns were generated using lentiviral plasmids expressing shRNA against NAPRT , SIRT7, or NAMPT. Non-silencing (NS) lentiviral shRNA controls were also used to ensure specificity of the knockdowns. shRNA bacterial glycerol stocks were purchased from Dharmacon and the *E. coli* cultures were grown in LB media with 100 μg/ml carbenicillin at 37˚C for 16 h. Plasmid DNA was extracted from bacteria using HiPure Plasmid Midiprep Kit (Thermo Fischer Scientific). HEK293T cells were seeded for a confluency of 70% on the day of transfection. HEK293T cells were co-transfected with the shRNA plasmid and packaging vectors *pMD2.G* and *psPAX2* (Addgene). The supernatant containing lentiviral particles was collected and filtered 24 h post-transfection. For transduction, cells were seeded in 6-well plates to be 70% confluent. Cells were transduced to yield 30-60% infection efficiency by incubating with high titer lentivirus and 8 μg/ml of polybrene (Sigma Aldrich) for 2 h. Transduced cells were selected with 2 μg/ml puromycin for 24 h. When single shNAPRT clones are presented, shRNA clone #1 is used.

2.4 TRYPAN BLUE EXCLUSION CELL COUNTING

To monitor cell proliferation, the trypan blue exclusion assay was used to determine the viability of cells in a suspension.[142] Trypan blue is a dye that does not penetrate the membrane of live cells, and thus live cells appear clear under examination by light microscopy. Meanwhile, non-viable cells have breached membrane integrity and

will be permeable to the dye, thus appearing blue and distinguishing them from viable cells.[142] 2 x 10^4 cells were seeded in triplicates in 2 ml of medium in 6-well plates. Cells were treated with specified chemical 24 h after seeding, at the indicated concentrations. Adherent cells were dissociated at the indicated times with 0.05% trypsin-EDTA and then centrifuged into a pellet. The pellet was then re-suspended in trypan blue solution (Thermo Fischer Scientific). 10 µl of mixed cell suspension was loaded on a hemacytometer and viewed under a light microscope. The number of viable cells within the grids of the hemacytometer was counted to calculate the number of viable cells per volume of cell suspension, as per the formula average cells/quadrant x 10^4.

2.5 Tumorsphere Formation Assay

Formation of tumorspheres depends on the self-renewal ability of stem cells in the population and thus a tumorsphere assay can be used to assess the presence of stem cells.[143] Adherent NT2/D1 and HMLER-shEcad cells were dissociated with trypsin-EDTA and then titurated to generate single cell suspensions. The number of cells was counted as previously described, and then NT2/D1 cells were seeded at a density of 10,000 cells/ml while HMLER-shEcad cells were seeded at a density of 20,000 cells/ml. Cells were plated in ultralow-attachment 6-well plates in serum-free HuMEC Ready Media and left in the incubator to form tumorspheres. Microscopic images of tumorspheres were taken 5 days after initial seeding from multiple microscopic fields of view. Using ImageJ for quantification, spheres with a diameter equal to or larger than 50 µm were deemed tumorspheres and the average area of tumorspheres was determined from 3 independent experiments.

2.6 Protein Extraction

Cells were scraped in cold 1x phosphate buffered saline (PBS) at pH 7.4 and centrifuged at 2500 rpm for 5 min at 4˚C. Pellets were lysed in 70 µl of RIPA lysis buffer (25 mM Tris pH 7.6, 150 mM NaCl, 1% NP-40, 1% sodium deoxycholate, 1% sodium dodecyl sulfate [SDS]) containing 1% protease and phosphatase inhibitors. Whole cell lysates were incubated on ice for 45 min, and then sonicated for 1 min. The samples were

centrifuged at 14,000 rpm for 15 min at 4˚C and the supernatants containing the proteins were collected.

2.7 Protein Quantification

Protein concentrations were determined using the colorimetric Micro BCA assay kit (Thermo Fisher Scientific) in a 96-well flat bottom plate. Protein samples were diluted 1:5 in ddH_2O, and 5 µl of diluted protein sample was loaded in duplicates to 150 µl of Micro BCA solution. Protein standards from 0.2 to 2.0 µg/ml were prepared using bovine serum albumin (BSA) to generate a protein standard curve. The plate was covered and incubated with shaking for 45 min before measuring the absorbance at 570 nm using the SpectraMax Microplate Reader. Protein concentrations were calculated using the protein standard curve.

2.8 Western Immunoblotting

SDS-polyacrylamide gels were prepared (8-12% acrylamide, 0.1% SDS, 375 mM Tris-HCl at pH 8.8, 0.1% ammonium persulfate [APS], TEMED), along with stacking gels (acrylamide, 375 mM Tris-HCl at pH 6.8, 0.1% SDS, 0.1% APS, TEMED). Equivalent quantities of whole cell lysate samples (5-15 µg) were prepared in 5 µl of loading buffer (95% BioRad 2x Laemmli sample buffer, 5% β-mercaptoethanol) and heated at 90˚C for 5 min. Protein samples were loaded and resolved by SDS polyacrylamide gel electrophoresis (SDS-PAGE) in SDS running buffer (0.1% SDS, 200 mM glycine, 20 mM Tris-HCl) at 120 V for 1 h. Proteins were transferred from the gel to a nitrocellulose membrane (BioRad) by electrotransfer in transfer buffer (glycine, Tris-HCl, methanol) at 120 V for 1 h. Membranes were blocked in 5% nonfat milk in PBST (PBS, 0.05% Tween 20) for 45 min, then washed in PBST and incubated with the appropriate primary antibody overnight at 4°C. The following day, membranes were washed in PBST before incubating in horseradish peroxidase-labeled secondary antibodies (Jackson ImmunnoResearch) against the primary antibodies. Secondary antibody was prepared 1:10,000 in 5% milk in PBST and added to the membranes for 1.5 h at room temperature. Membranes were washed in PBST before they were visualized with electrochemiluminescence (ECL) detection reagent (BioRad) using the ChemiDoc

Touch imaging system (BioRad). To verify that equal amounts of protein were loaded for each sample, membranes were probed for Actin, β-tubulin, or stained with Ponceau to detect total protein. The intensity of the visualized protein bands was quantified by densitometry using ImageJ software (National Institutes of Health). Protein bands were first normalized by their respective loading controls and then relative fold changes of samples compared to the first sample were calculated.

Membranes were probed with primary antibodies (diluted 1:1000 in 1% BSA) against the following proteins: NAPRT (Santa Cruz Biotechnology), SIRT1-7 (Cell Signaling), Oct4 (Santa Cruz Biotechnology), Nanog (Cell Signaling), Sox2 (Cell Signaling), β3-tubulin (Santa Cruz Biotechnology), β-casein (Santa Cruz Biotechnology), SQSTM1 (Cell Signaling), LC3A (Cell Signaling), LC3B (Cell Signaling), Caspase-3 (Cell Signaling), E-cadherin (Cell Signaling), Bmi1 (Cell Signaling), NAMPT (Novus Biologicals), β-tubulin (Developmental Studies Hybridoma Bank), and Actin (Santa Cruz Biotechnology).

2.9 Quantitative Real-Time PCR Analysis

RNA was extracted from cultured cells using Trizol and isolated using the Invitrogen PureLink RNA Mini Kit. cDNA was synthesized using Superscript II enzyme (Thermo Fischer Scientific) and Eppendorf Mastercycler ep Gradient S thermal cycler. Primers were purchased from Invitrogen and sequences are described in Table 2.1. Samples of cDNA were quantified using the NanoVue Plus Spectrophotometer (General Electric) and diluted to 10 ng/ml. Quantitative real-time PCR (qRT-PCR) was completed on the BioRad CFX96 PCR machine using BioRad SYBR Green Supermix. Actin was used for normalization of the genes of interest. The results were analyzed using $2^{-\Delta\Delta CT}$ method and expressed as fold change relative to NS controls.

2.10 CFSE Analysis

Carboxyfluorescein succinimidyl ester (CFSE) is an intracellular fluorescent stain that is used to measure cell proliferation. Cells are labeled with the membrane permeable dye, carboxyfluorescein diacetate succinimidyl ester (CFDA, SE). Cellular esterases then cleave CFDA, SE into CFSE, which is less permeable and therefore remains inside the

cell. As cell division occurs, the concentration of CFSE inside individual cells decreases, as measured by cell fluorescence.[144] NS and shNAPRT cells were pelleted and resuspended in 1 ml of PBS-EDTA. Equal numbers of cells were labeled with 5 μM of CFDA, SE (eBioscience) and incubated at 37 ˚C for 10 min. Cells were washed with 5% FBS in PBS-EDTA and then washed again with PBS-EDTA. Equal numbers of cells were then seeded in 6-well plates and cultured for 4 days. To measure cell fluorescence, cells were pelleted and resuspended in FACS buffer (PBS with 1% FBS), then analyzed using the BD FACSCanto II flow cytometry system. Mean fluorescent intensity (MFI) was measured using the Flowing software.

2.11 β-Galactosidase Staining Assay

Senescent cells which are characterized by increased β-galactosidase activity were detected using the senescence β-Galactosidase staining kit from Cell Signaling, following the manufacturer's protocol.[145] Cells were seeded in triplicates in 2 ml of media in 6-well plates, 24 h prior to staining. The growth media was removed and the cells were washed once with PBS (Thermo Fisher Scientific). Cells were fixed with 1x Fixative solution and incubated for 15 minutes at room temperature. After the incubation, the cells were rinsed two times with PBS and then 1 ml of the β-Galactosidase Staining Solution was added to each well. The plate was sealed with parafilm to prevent evaporation and incubated at 37 °C in a dry incubator. Representative images of the samples were captured using a light microscope, 24 h after staining.

2.12 Annexin V Staining

When cells undergo apoptosis, phosphatidylserine (PS), which is normally present within the plasma membrane, is externalized to the outer leaflet. Annexin V is a protein that is able to bind exposed PS, thus detecting apoptotic cells.[146] Annexin V that is conjugated to PE fluorochrome was used to stain and detect apoptotic cells by flow cytometry. $1.5x10^5$ cells were seeded in 6-well plates in triplicates. In addition, no stain and annexin positive stain controls were included. Apoptosis was induced by adding 30% ethanol for 15 minutes prior to staining for analysis.[147] Media was collected and cells were trypsonized then centrifuged into pellet. Cells were washed with FACS buffer (PBS

with 1% FBS). Each sample was stained with 5 µl of annexin V-PE in 500 µl of annexin V binding buffer (10 mM HEPES, 150 mM NaCl, 2.5 mM $CaCl_2$ in PSB), vortexed, and then analyzed using the BD FACSCanto II flow cytometry system. Data was analyzed using the Flowing software.

2.13 BIOINFORMATICS ANALYSIS

To correlate the expression of *SIRT7* with *NAPRT* and *NAMPT* in cancer patient tumors, datasets from The Cancer Genome Atlas (TCGA) were downloaded using cBio Cancer Genomics Portal. A logarithmic transformation was applied to the mRNA expression levels of *SIRT7*, *NAPRT*, and *NAMPT*. Correlations were performed between *SIRT7* and *NAPRT* or *NAMPT* and statistics (correlation index, R, and p-value) were calculated using the Pearson correlation method. Correlation plots were generated using R software.

2.14 TMT LABELLING AND 2D-LC-SPS-MS3 ANALYSIS

NT2/D1 cells at 80% confluency in 15 cm tissue culture plates were scraped into ice cold PBS and centrifuged. Protein from pelleted cells was extracted using 2% SDS, 150 mM NaCl, 50 mM Tris pH 8.5 containing complete mini protease inhibitor cocktail (Roche). Lysates were sonicated on ice for 12 sec and then centrifuged at 13000 g for 5 min to clear cell debris. Cysteine residues were reduced using 5 mM dithiothreitol for 40 min at room temperature, then alkylated using 14 mM iodoacetamide for 40 min in the dark. Proteins were precipitated by methanol chloroform and resuspended in 8 M urea, 50 mM Tris. Protein concentrations were determined using BCA assay (Thermo Fischer Scientific) as previously described. Volumes containing 100 µg of protein were diluted to 1 M urea, 50 mM HEPES pH 8.5, and digested overnight with trypsin at a ratio of 1:100 trypsin/protein. Peptides were then again digested at a ratio of 1:100 trypsin/protein for 4 h. Digested peptides were desalted using 60 mg solid-phase C18 extraction cartridges (Waters) and lyophilized. Dried peptides were re-suspended in 200 mM HEPES pH 8.5, 30% acetonitrile. Peptides were labeled using 10 µl of TMT10 (10-plex) reagents (Thermo Fisher Scientific) for 1 h at room temperature, then quenched with

hydroxylamine at a final concentration of 0.5%. Samples were desalted using solid-phase C18 extraction cartridges (Waters) and lyophilized.[148]

TMT10-labeled samples were fractionated using high-pH reversed phase chromatography using an Onyx monolithic 100 x 4.6 mm C18 column (Phenomenex). The flow rate was 800 µl/min and a gradient of 5% to 40% acetonitrile (10 mM ammonium formate, pH 8) was applied over 60 min using an Agilent 1100 pump (Agilent) from which 12 fractions were collected. Individual fractions were desalted using Stage Tips[149] and lyophilized, then analyzed using an Orbitrap Velos Pro mass spectrometer (Thermo Fischer Scientific) using an MS3 method.[150] Proteins were identified using the Sequest algorithm for the database search against a human proteome database (downloaded from UniprotKB in September 2014) concatenated to a database of common proteomic contaminants.[148]

Using t-tests to compare relative protein expressions from NAPRT or SIRT7 knockdown with NS samples, proteins that were significantly (p-value<0.10) upregulated or downregulated in either condition were identified. Of those, an integrated signature was obtained, consisting of proteins that were commonly regulated between knockdowns. Database for Annotation, Visualization and Integrated Discovery (DAVID) was used for pathway enrichment analysis of these proteins. The integrated signature protein list was run against all the measured proteins as background, using the database UP_KEYWORD. Benjamini-Hochberg (B-H) adjusted p-values were generated by DAVID. For heatmaps of proteins from enriched pathways, mean relative protein expression values of NS, NAPRT, and SIRT7 knockdown were used. The heatmaps were generated using Multiple Experiment Viewer (MeV) software.

2.15 Statistical Analysis

Analyses were completed using Microsoft Office Excel and GraphPad Prism software. Error bars represent mean ± standard deviation (SD) or standard error of the mean (SEM). Two-tailed unpaired Student's t-tests were used to evaluate statistical significance, or two-way ANOVA with a Tukey posttest were used for multiple comparisons. $P < 0.05$ was considered significant.

Table 2.1. qRT-PCR primer sequences

Gene	Forward 5'→3'	Reverse 5'→3'
Oct4	GGAAGGTATTCAGCCAAACGACCA	GGAAGGTATTCAGCCAAACGACCA
Nanog	TGAACCTCAGCTACAAACAG	TGGTGGTAGGAAGAGTAAAG
Sox2	GGGAAATGGAGGGGTGCAAAAGAGG	TTGCGTGAGTGTGGATGGGATTGGTG
SIRT7	TGTGGACACTGCTTCAGAAAGGGA	CACAGTTCTGAGACACCACATGCT
Actin	GAGCACAGAGCCTCGCCTTT	AGAGGCGTACAGGGATAGCA

CHAPTER 3: RESULTS

3.1 ENDOGENOUS EXPRESSION OF NAPRT IS ELEVATED IN CANCER CELLS

Previous studies[82,95,97] have focused on the absence of NAPRT in certain cancers and limited research has investigated the role of NAPRT in cancers that do express the protein.[99] Therefore, before moving towards a study of NAPRT in CSLCs, a preliminary experiment was conducted to gauge the possible importance of NAPRT in cancer. Here, the endogenous expression of NAPRT in a small panel of normal cells and cancer cell lines of lung or breast origins were determined by western immunoblotting. IMR90 and WI38 are human lung fibroblasts and were used for the comparison of NAPRT expression in normal cells. Immunoblots of whole cell lysates showed that NAPRT was weakly expressed in IMR90 and WI38 (Figure 3.1). This weak expression in normal cells was in contrast to the NAPRT expression levels detected in breast cancer cells (MDA-MB-231 and MDA-MB-468) and lung cancer cells (H1299 and A549). As can be seen in Figure 3.1, these four cancer cell lines expressed relatively higher levels of NAPRT compared to the normal cells. This result not only exhibits the presence of NAPRT in some cancers but suggests that these cancer cells may prefer to maintain high levels of NAPRT to perform important functions that support malignant growth.

3.2 THE ROLE OF NAPRT IN NT2/D1 EMBRYONAL CARCINOMA CELLS

To date, only one publication[99] has studied the role of NAPRT in cancer and showed that it contributes to cancer metabolism, but NAPRT has never yet been studied in the context of CSLCs. For this investigation, three models of CSLCs were used to elucidate and generalize the functions of NAPRT in CSCs. First, the human ECSLC line NT2/D1 was chosen because it possesses an ESC-like gene expression profile which also characterizes CSCs. NT2/D1 cells originate from a metastasized testicular cancer and are poorly differentiated cells that have the capacity to differentiate towards all three germ layers: endoderm, mesoderm, and ectoderm. Their undifferentiated state is preserved by self-renewal and is controlled through the abundant expression of pluripotency-maintaining factors such as Oct4, Nanog, and Sox2.[128–130] These features that NT2/D1

cells share with CSCs make them a useful model to study changes in the CSLC gene signature at an embryonic stage.

3.2.1 NAPRT knockdown inhibits NT2/D1 cell proliferation

Given the hypothesis that NAPRT is important for cancer cells, and specifically, CSLCs, NAPRT was knocked down in NT2/D1 CSLCs using two different shRNA constructs. Western immunoblotting was used to determine that NT2/D1 cells indeed express NAPRT and that the knockdown was successful (Figure 3.2A). The effects of NAPRT deficiency on the malignant phenotype of NT2/D1 cells was then assessed. A trypan blue exclusion assay was used twice, first to study the effect of NAPRT knockdown on overall cell proliferation, and then to measure changes in cell viability. Trypan blue is a dye that is excluded from viable cells, thus identifying them from non-viable cells. To obtain a 72-hour time course proliferation curve, equal numbers of cells were seeded and then the number of viable cells was counted every 24 hours using trypan blue. As seen in Figure 3.2B, both clones of NAPRT knockdown had lower numbers of viable cells compared to the non-silencing (NS) controls at each respective time point, suggesting that NAPRT knockdown reduces the proliferation rate of NT2/D1 cells. This difference in the number of NAPRT knockdown and control cells could be partly explained by a decrease in cell viability, as shown in Figure 3.2C. Here, trypan blue was used to count both the number of viable and non-viable cells. Indeed, the results showed that percentage cell viability was decreased in the NAPRT knockdown cells compared to control cells (Figure 3.2C), representing one factor that contributes to the decreased proliferation of shNAPRT cells.

Since the effect on cell proliferation seemed more pronounced than the results on cell viability, it was also possible that the difference in cell number between the NAPRT knockdown and control cells was due to cells that remained viable but stopped proliferating. To clarify whether shNAPRT cells were proliferating slower, cells were stained with CFSE, an intracellular dye that decreases in concentration as cellular division occurs.[144] After culturing the labeled cells for 4 days, flow cytometry analysis showed that the MFI of shNAPRT cells was greater than NS cells, indicating a slower proliferation rate (Figure 3.2D). We further examined whether the decreased proliferation

was a result of cells becoming senescent. Cells proliferate by progressing through the cell cycle, but those that have ceased to divide enter a state of replicative senescence which is marked by increased β-galactosidase activity.[145] During a senescence assay, β-galactosidase positive cells cleave a chromogenic substrate that produces a blue color which can be viewed under light microscopy.[151] The results in Figure 3.3 illustrate that more than half of the viable shNAPRT cells stained blue, indicative of their senescent state. Thus, it can be deduced that following NAPRT knockdown, a large majority of cells are induced towards senescence, while another subset of cells undergo cell death. In effect, NAPRT knockdown suppresses the proliferation of NT2/D1 cells and this finding strengthens the hypothesis that NAPRT deficiency disturbs CSLC functions.

3.2.2 NAPRT knockdown decreases stemness features of NT2/D1 cells

Since the decrease in proliferation observed following NAPRT knockdown in NT2/D1 cells signifies a disturbance in their cancer cell physiology, the effect of NAPRT knockdown on stemness features was investigated next. NT2/D1 control cells express high levels of embryonal stem cell markers such as Oct4, Nanog, and Sox2, as detected by immunoblotting. Upon NAPRT knockdown, the protein levels of these pluripotency factors were observed to be reduced in both shRNA clones (Figure 3.4A). Downregulation of the pluripotency factors appeared to occur at a transcriptional level, as quantitative reverse transcription polymerase chain reaction (qRT-PCR) revealed that the mRNA levels of Oct4, Nanog, and Sox2 in shNAPRT cells were decreased compared to the NS control cells (Figure 3.4B). These results exhibit a shift from the ECSLC gene expression signature that accompanies NAPRT deficiency, suggesting that NAPRT plays a role in maintaining this transcriptional profile.

As an additional method to evaluate the decrease in stemness character of NAPRT knockdown cells, a tumorsphere formation assay was performed.[152] The assay cultures cells *in vitro* and tests for their ability to grow as nonadherent spheres in serum-free culture conditions. This specialized serum-free media supports the growth of cells with stem-like characteristics, and tumorspheres formed are enriched with cells that possess the functional characteristics of stem cells.[153,154] As demonstrated in Figure 3.5, NAPRT knockdown impaired tumorsphere formation and cells formed significantly smaller

tumorspheres than control cells. Moreover, to elucidate whether the NAD^+-synthesizing function of NAPRT is implicated in stemness, NAMN was supplemented to NAPRT knockdown cells. Supplying NAPRT-deficient cells with the downstream product of NAPRT increased their tumorsphere formation ability, producing tumorspheres with more comparable sizes to those of NS controls (Figure 3.5). Taken together, these results are consistent with the role of NAPRT in supporting a stemness phenotype in CSLCs.

Given that stemness is maintained by a lack of differentiation, loss of stemness is often accompanied by induction of differentiation.[60] NT2/D1 cells have been shown to form tumors composed of derivatives from all three germ layers,[129,130] but they are most notably known for their differentiation along the neural ectodermal pathway.[130] Upon differentiation into post-mitotic neurons, NT2/D1 cells alter their morphology and form dendrite-like outgrowths termed neurites.[129] Visual inspection of NT2/D1 under microscopy showed that control cells grew in clusters in a compact morphology, with well-defined borders. In contrast, NAPRT knockdown cells displayed morphological changes such as cell scattering, flattening of the cells, and neurite outgrowths (Figure 3.6A). To confirm the observed effect of NAPRT knockdown on differentiation, immunoblotting was performed for the neuronal lineage marker β3-tubulin.[155] Indeed, as expected, both clones of shNAPRT promoted increased levels of β3-tubulin (Figure 3.6B), indicating that loss of NAPRT promotes ECSLCs to undergo differentiation.

3.2.3 NAPRT knockdown decreases autophagy and promotes cell death in NT2/D1 cells

Previously, it was reported that NT2/D1 cells could be stimulated to differentiate by a disruption in autophagy.[60] Given the function of NAPRT in NAD^+ synthesis, NAPRT deficiency likely impairs energy homeostasis which could elicit a response in autophagy. For this reason, the autophagy activity of NAPRT knockdown cells was examined using an autophagy flux assay. Cells were treated with or without chloroquine, a late stage inhibitor of autophagy which prevents the acidification of lysosomes and thus results in the accumulation of autophagosomes and associated autophagy proteins.[156] As can be seen in Figure 3.7A, NAPRT knockdown cells appeared to have lower steady-state levels of autophagy markers SQSTM1, LC3A-II, and LC3B-II, compared to control

cells. This can be due to either an increased rate of autophagosome turnover, or due to a blockade of autophagosome sequestration. Basal autophagic flux was observed by comparing the levels of autophagy proteins in the control cells treated without and with chloroquine. Accumulation of the autophagy proteins upon autophagy inhibition indicated that autophagic flux was occurring in control cells.[157] In NAPRT knockdown cells treated without and with chloroquine, autophagic flux was also observed to be occurring as indicated by the accumulated LC3 levels. However, SQSTM1 levels did not accumulate, suggesting that flux for selective autophagy was absent. Overall, the data show that NAPRT knockdown does not increase autophagy flux compared to control cells. Moreover, the amount of cumulative autophagy levels detected in NAPRT knockdown cells was less than the detected levels in control cells, indicating decreased autophagy capacity. These results signal that NAPRT deficiency downregulates autophagy in NT2/D1 cells, and may correspond to an exacerbated metabolic disturbance following NAPRT knockdown.

Since shNAPRT cells did not employ autophagy as a mechanism to respond to cellular stress, the consequence of NAPRT knockdown on cell fate was investigated. Results from the cell viability assay alluded to the event of cell death in NAPRT knockdown cells. Additionally, immunoblotting detected cleaved Caspase-3 in NAPRT knockdown cells (Figure 3.7B). Caspase-3 is an executioner of apoptosis that is frequently activated during programmed cell death. The cleavage of pro-Caspase-3 activates the enzyme's proteolytic functions in cell shrinkage and DNA fragmentation.[158] However, because Caspase-3 also has other functions that are unrelated to death processes,[159] cell death in NAPRT knockdown was further confirmed by annexin V staining. During apoptosis, the PS that is normally present on the inner leaflet of viable cell membranes is externalized to the outer leaflet, where it can be detected and stained by fluorescent-tagged Annexin V.[146] Using flow cytometry, it was determined that a greater percentage of NAPRT knockdown cells stained positive for annexin V than control cells, confirming that NAPRT knockdown promotes cell death in NT2/D1 (Figure 3.7C-D). The results demonstrate that NAPRT deficiency can cause cellular stress that is severe enough to promote apoptosis.

3.3 THE ROLE OF NAPRT IN HMLER-SHECAD BREAST CANCER STEM-LIKE CELLS

Next, to verify the results observed in the NT2/D1 ECSLC model, another CSLC model based on HMLER-shEcad cells, which have previously been reported as a useful model of breast CSLCs in several studies, was employed.[132,134,135] As part of the HMLE-based tumor progression model, these cells can present insights on the differences between normal cells and CSLCs. The earlier data suggesting that NAPRT might be overexpressed in some cancers were examined again in this HMLER-shEcad model. Consistent with the other two normal cell lines tested, HMLE cells also expressed low levels of NAPRT, detected by immunoblotting. The HMLER cancer cells expressed higher levels of NAPRT compared to the normal HMLE cells. Interestingly, stem-like HLMER-shEcad cells exhibited the highest expression of NAPRT among the three cell lines, supporting the notion that CSLCs have an increased dependency on NAPRT (Figure 3.8).

The findings of NAPRT deprivation in NT2/D1 cells were reiterated in HMLER-shEcad cells. HMLE-shEcad NAPRT knockdown cells were generated, as displayed in Figure 3.9A. Equal numbers of control cells and NAPRT knockdown cells were seeded for a time-course assay using trypan blue. The results showed that there were fewer numbers of NAPRT knockdown cells than control cells at respective time points, implying that cell proliferation is decreased (Figure 3.9B). NAPRT knockdown in HMLER-shEcad cells also impaired the cells' ability to form tumorspheres, resulting in tumorspheres that were significantly smaller in size than the tumorspheres formed by control cells (Figure 3.10). However, addition of NAMN was able to bypass the decreased tumorsphere formation ability of shNAPRT cells. As can be seen in Figure 3.10, shNAPRT cells supplemented with NAMN formed larger tumorspheres than shNAPRT cells alone. Overall, the data show that NAPRT deficiency also impacts the cell proliferation of HMLER-shEcad cells and its growth in nonadherent conditions.

The molecular profile of HMLER-shEcad cells was similarly affected by NAPRT knockdown. Since these cells are of breast and not embryonal origin, they do not possess all of the pluripotency factors present in NT2/D1 cells. However, as demonstrated in Figure 3.11A, HMLER-shEcad cells do express Sox2, along with Bmi1, a stem cell

marker which promotes the self-renewal of CSCs and is associated with chemoresistance and metastasis.[160] Knockdown of NAPRT in HMLER-shEcad cells decreased the protein levels of both Sox2 and Bmi1, consistent with the results obtained in NT2/D1 cells. To determine whether NAPRT knockdown in HMLER-shEcad cells promoted their differentiation, an appropriate marker for cells of mammary origin was used. β-casein is a marker for mammary epithelial cell differentiation and its protein levels were found to be drastically upregulated in NAPRT knockdown cells (Figure 3.11B).[161] This confirms that loss of stemness markers from NAPRT knockdown is coupled with increased differentiation in HMLER-shEcad cells.

To determine whether NAPRT similarly affects the stress response in HMLER-shEcad cells, an autophagy flux assay was also performed. Like NT2/D1 cells, the steady-state levels of autophagy proteins SQSTM1, LC3A-II, and LC3B-II appeared to be lower in NAPRT knockdown cells compared to control cells. Using chloroquine to measure flux, Figure 3.12A shows that NAPRT knockdown cells exhibited increased autophagy flux than control cells, although levels of SQSTM1 again did not accumulate upon chloroquine treatment. However, cumulative levels of autophagy proteins in NAPRT knockdown cells were equal to or less than cumulative levels detected in normal cells, indicating that autophagy capacity was not upregulated more than basal levels. Despite the slight activation of autophagy flux, cleaved Caspase-3 was nevertheless detected in HMLER-shEcad NAPRT knockdown cells (Figure 3.12B). To confirm that the presence of Caspase-3 was an indication of cell death, an annexin V staining assay was performed. As depicted in Figure 3.12C-D, there was a significant shift in the percentage of annexin V positive cells in NAPRT knockdown cells, suggesting that cell death was occurring. Overall, the data demonstrate that despite the increased autophagy flux, the levels of autophagic machinery may not be sufficient to cope with shNAPRT-mediated cellular stress, resulting in cell death.

3.4 THERAPEUTIC RELEVANCE OF TARGETING NAPRT IN CANCER

To test the hypotheses made using NT2/D1and HMLER-shEcad cells in a more clinically-relevant CSC model, the effect of NAPRT knockdown was tested in patient-derived brain tumor-initiating cells. The BT698 patient-derived cells harbor a high

population of $CD133^+$ tumor cells, which have been shown to possess CSC functions such as tumor-initiating capacity during serial transplantation.[14,136] In addition to expressing CD133, immunoblotting revealed that BT698 also express stemness markers Sox2 and Bmi1. To examine the effect of NAPRT on stemness, NAPRT was knocked down in BT698 cells. As shown in Figure 3.13, NAPRT knockdown in BT698 decreased the protein levels of the stemness markers Sox2 and Bmi1, further confirming the role of NAPRT in maintaining the stemness of patient-derived CSCs.

3.5 TARGETING NAPRT IN DIFFERENTIATED CANCER CELLS

To evaluate the utility of targeting NAPRT as a therapeutic approach, whether its effects extend to non-CSC cancer cells should also be considered. Therefore, NAPRT knockdowns were generated using shRNA in HMLER cells, which are the non-stem-like cancer counterpart of HMLER-shEcad cells. A trypan blue exclusion time-course assay showed that NAPRT knockdown in HMLER cells effectively decreased cell proliferation (Figure 3.14A). To broaden the possible therapeutic applications of NAPRT, additional cancer cell lines were also included, such as lung cancer cells A549 and H1299, and colorectal cancer cells HCT116 (p53 -/-). NAPRT knockdowns were generated and equal numbers of cells were seeded for trypan blue exclusion assay. Figure 3.14B shows that after 72 hours, there were fewer numbers of viable cells in NAPRT knockdown compared to control cells. Although the efficacy of NAPRT knockdown on proliferation varied among the cell lines, the results suggest that it may be a feasible option to target NAPRT in heterogeneous cancers, affecting both CSLCs and their differentiated derivatives.

3.6 TARGETING NAPRT ONLY MARGINALLY AFFECTS NORMAL NON-TRANSFORMED CELLS

Ideal anticancer treatments have minimal adverse effects on normal cells. Since the immunoblot data of normal cells showed that they do not highly express NAPRT, it is likely that they are not heavily dependent on the protein and that targeting NAPRT would have relatively lesser effects on normal cells. To be sure, NAPRT was knocked down in the non-transformed breast cell lines, HMLE and MCF10A, and a trypan blue exclusion assay was performed. Figure 3.15 shows that NAPRT knockdown had marginal and non-

significant effects on the cell proliferation of HMLE and MCF10A cells. These results support the idea that NAPRT can be a useful therapeutic target for cancer as its modulation is unlikely to have significant adverse effects on normal cells. Normal cells appear to have limited need for this NAD^+-synthesizing enzyme, most likely in the context of their relatively less stringent energy demands compared to cancer cells.

3.7 SIRT7 IS NEGATIVELY REGULATED BY NAPRT KNOCKDOWN IN CANCER CELLS

Moving forward, an investigation on the molecular mechanisms of NAPRT-mediated effects was conducted. Recalling that SIRTs are a class of enzymes which are dependent on NAD^+ and regulate many cellular processes, the effect of NAPRT deficiency on SIRT expression was studied. Immunoblotting for six of the SIRTs in NT2/D1 cells showed that NAPRT knockdown did not significantly affect their protein expression levels, except for SIRT7 which was preferentially decreased (Figure 3.16A). This downregulation of SIRT7 was also found to occur at a transcriptional level, as revealed by qRT-PCR (Figure 3.16B). The data show that deficiency in NAPRT, which is a NAD^+-synthesizing enzyme, regulates the expression of SIRT7, one of the NAD^+-dependent enzymes. Due to the many functions that SIRT7 has, this may unveil a mechanism by which NAPRT exerts its roles in cancer.

To explore whether NAPRT exerts unique regulating functions distinct from NAMPT, the classical NAD^+-synthesizing enzyme, NAMPT knockdowns were also generated in NT2/D1 cells. NAMPT knockdown differentially affected the expression of certain SIRTs compared to knockdown of NAPRT; however, SIRT7 expression remained unchanged (Figure 3.16C), showing the uniqueness of the NAPRT-SIRT7 nexus. The downregulation of SIRT7 in NAPRT but not NAMPT knockdown cells was of interest and a better understanding of their relationship was further pursued.

First, to determine whether the relation between NAPRT and SIRT7 was cell type-dependent and unique to NT2/D1 cells, the results were confirmed in additional CSLC models. SIRT7 expression was blotted for in HMLER-shEcad and BT698 cells, and was found to also be downregulated upon NAPRT knockdown (Figure 3.17). These

results support the hypothesis that SIRT7 is commonly regulated by NAPRT in a variety of CSLC types.

Since NAPRT knockdown was found to affect the proliferation of not only CSLCs but also differentiated cancer cells, SIRT7 expression was probed in NAPRT knockdown of various differentiated cancer cell lines. As Figure 3.18 demonstrates, the downregulation of SIRT7 following NAPRT knockdown was consistent in breast cancer cells (HMLER and MCF7), lung cancer cells (H1299 and A549), and colorectal cancer cells (HCT116 p53 -/-). This extends our hypothesis on the NAPRT-SIRT7 nexus to even more cancer cell types.

To further establish the correlation observed between NAPRT and SIRT7 and determine whether it exists in patient tumors, datasets from The Cancer Genome Atlas (TCGA) were employed. Pearson correlation analysis was performed on mRNA expression levels of *NAPRT* and *SIRT7*. Figure 3.19 displays that a positive ($r > 0.40$) and significant correlation was found in datasets of breast invasive carcinoma, pancreatic adenocarcinoma, lung adenocarcinoma, and prostate adenocarcinoma. These results support the plausible mechanism that SIRT7 is a downstream target of NAPRT. Correlations between SIRT7 and NAMPT were also performed in the same TCGA datasets to confirm whether the lack of association that was found in NT2/D1 cells was also universal. Figure 3.20 shows that SIRT7 had either no correlation or a weak negative correlation with NAMPT, which was the opposite relationship to that of NAPRT. This data unveils an association of NAPRT that seems to differentiate its role from that of NAMPT.

Finally, the association between NAPRT and SIRT7 was tested in the non-transformed cell lines, MCF10A and HMLE. In contrast to the cancer cells, NAPRT knockdown in the non-transformed cells did not noticeably affect SIRT7 levels, highlighting that the relationship between NAPRT and SIRT7 depends on whether it is in the context of transformed or non-transformed cells (Figure 3.21). Moreover, the unaffected SIRT7 levels in non-transformed cells may explain the marginal effects that NAPRT knockdown had on their cell proliferation.

3.8 NAPRT AND SIRT7 KNOCKDOWN INDUCE COMPARABLE PROTEOMIC REMODELLING

Overall, the association of SIRT7 with NAPRT exposes SIRT7 as a protein of interest in cancer. To better understand the role of SIRT7 and whether it is a mediator of NAPRT-related effects, SIRT7 was knocked down using shRNA (Figure 3.22A). In NT2/D1, MDA-MB-468, H1299, and A549 cells, trypan blue exclusion assays performed at 72 hours showed that SIRT7 knockdown cells had decreased proliferation compared to control cells (Figure 3.22B). These results insinuate that SIRT7 acts as an oncogene.

To elucidate the role of SIRT7 in CSLC stemness, SIRT7 knockdowns were generated in the CSLC models, NT2/D1 and BT698. As shown in Figure 3.23, similar to NAPRT knockdown cells, SIRT7 knockdown cells exhibited a decrease in stemness markers Oct4, Nanog, Sox2, and Bmi1. The data indicate that SIRT7 regulates the expression of stemness genes in cancer and is consistent with the hypothesis that SIRT7 mediates NAPRT-related effects.

Having demonstrated that NAPRT and SIRT7 regulate cell proliferation and stemness in similar fashions, it was possible that they also regulated other cellular processes concomitantly. To better understand the related functions of NAPRT and SIRT7, a whole-cell proteome analysis was performed on NAPRT knockdown and SIRT7 knockdown NT2/D1 cells. Out of 3885 measured proteins, the expression of 1232 were significantly changed in either NAPRT or SIRT7 knockdown. Of these, 72% were commonly regulated by NAPRT and SIRT7, with approximately half being upregulated and the other half being downregulated (Figure 3.24A-B). From the list of proteins with significant changes, those that were commonly upregulated or downregulated between NAPRT and SIRT7 knockdown cells were identified, obtaining an integrated signature. Pathway enrichment analysis of this integrated signature was performed with the DAVID software, which suggested that glycoproteins were the most affected, followed by proteins associated with calcium, metal binding, transcription, chromatin regulation, protein synthesis, and the proteasome (Figure 3.24C). Heatmaps of mean protein expression values for transcription and proteasome proteins were generated, which illustrated that transcription was decreased while proteasome proteins were increased in

the integrated signature (Figure 3.24D). Overall, the shared proteomic profile of NAPRT and SIRT7 knockdown cells imply that NAPRT may exert its functions in ECSLCs via SIRT7.

Taken together, the data show that knockdown of NAPRT can target stemness features in ECSLCs, and that NAPRT-related effects may be mediated by the downregulation of SIRT7.

3.9 Future Experiments

The results of this study propose NAPRT as a novel therapeutic target in cancer, specifically against CSLCs. Due to the novelty of NAPRT as a therapeutic strategy, little is known about its mechanism of action, the knowledge of which would help in the design of treatments that can exacerbate the tumor suppressive effects or manage the unwanted effects of NAPRT inhibition. Therefore, to further explore the use of NAPRT in therapy, it would be advantageous to obtain a comprehensive understanding of its mechanisms via the following experiments.

1. Understanding how NAPRT knockdown regulates the expression of stemness markers: NAPRT knockdown resulted in reduced levels of stemness markers such as Oct4, Nanog, and Sox2. This downregulation was observed at mRNA level, but further chromatin immunoprecipitation (ChIP) experiments could clarify whether NAPRT is able to act as a transcription factor and directly regulate the transcription of these genes. Other post-translational regulations can also be investigated; NAPRT knockdown increased the expression of proteins involved in the proteasome pathway. To determine whether the stability of stemness factors also contributes to their lowered protein levels, NAPRT knockdown cells can be treated with a proteasome inhibitor such as MG132 or bortezomib, or treated with a protein synthesis inhibitor such as cycloheximide.
2. Understanding the role of SIRT7 in NAPRT-related effects: There is evidence to suggest that SIRT7 could be a downstream effector of NAPRT, although the mechanisms are unclear. First, this may be confirmed through addback experiments, whereby the levels of SIRT7 are restored in NAPRT knockdown

cells via ectopic expression of SIRT7. This should rescue the phenotypes observed from knockdown of NAPRT, including effects on proliferation and expression of stemness markers. Second, the importance of SIRT7 catalytic activity in maintaining CSLC stemness can be determined by ectopic expression of a SIRT7 mutant that is functionally inactive instead. If NAPRT knockdown cells do not revert back to a wild-type phenotype, the function of SIRT7 deacetylation in regulating target proteins should be investigated. Finally, the finding that NAPRT knockdown reduces SIRT7 expression is of interest, given that the NAD^+ dependence of SIRT7 relates to its activity. Further avenues can be pursued to determine whether SIRT7 acts in a feedback fashion that is particularly sensitive to altered NAD^+ levels, or whether NAPRT has additional functions other than related to NAD^+-synthesis.

3. Exploring combination treatments: Additive or synergistic tumor suppressive effects of NAPRT knockdown with other chemotherapies should be explored for potential combination treatment strategies. The inhibition of NAPRT with NAMPT has been studied in cancer cells by Piacente et al., but disruption of the Preiss-Handler pathway with the *de novo* NAD^+ synthesis pathway can also be considered. An even more effective method to limit NAD^+ levels would involve combining strategies to inhibit NAPRT and NMNATs, which are the enzymes used by all pathways of NAD^+ synthesis. Moving away from the focus of NAD^+ availability, one study showed the synthetic lethality of NAMPT and PARP inhibitors in breast cancer.[162] Therefore, strategies involving NAPRT inhibition with impairment of other NAD^+-dependent pathways can also be explored.
4. Inclusion of more cancer cell lines: To better evaluate the applicability of NAPRT inhibition as a therapeutic target in cancer, the study should be expanded to include a larger panel of cancer cell lines with different molecular phenotypes. More patient-derived cell lines can also be obtained and sorted by their CSLC markers to analyze changes in stem cell features. For example, using flow cytometry or magnetic beads, BTICs can be sorted by their CD133 expression before being subjected to NAPRT knockdown. Comparing the effects in the CD133 negative and CD133 positive populations can give insight on how

NAPRT knockdown affects cancer cell plasticity or whether it elicits any differential responses.

5. *In vivo* experiments: Given the challenges that NAMPT inhibition faced during clinical trials, it is imperative that the prospects of NAPRT inhibition are tested *in vivo*. Limiting dilution tumorigenicity assays of CSLCs with NS control or NAPRT knockdown should be performed to measure the impact on tumorigenicity. The resulting tumors can be analyzed for their molecular profiles to validate the *in vitro* findings. *In vivo* experiments should also be performed to test the efficacy of prospective combination strategies involving NAPRT inhibition, as described above. Mice injected with NAPRT knockdown CSLCs would be treated with other treatments to determine whether NAPRT inhibition, in combination with other NAD^+-related inhibitors, can prevent tumor development. The work would elucidate novel NAPRT-based combination strategies for cancer therapy. Furthermore, one possible factor that prevented pre-clinical tests from accurately predicting the outcome of NAMPT inhibition during clinical trials is that most of the *in vivo* studies were performed in immunocompromised hosts. The immune response during treatment should be accounted for by performing experiments in immunocompetent mice, as recently described.[163,164] Considering the role of the immune system during treatments related to NAPRT could lead to novel immunotherapies.

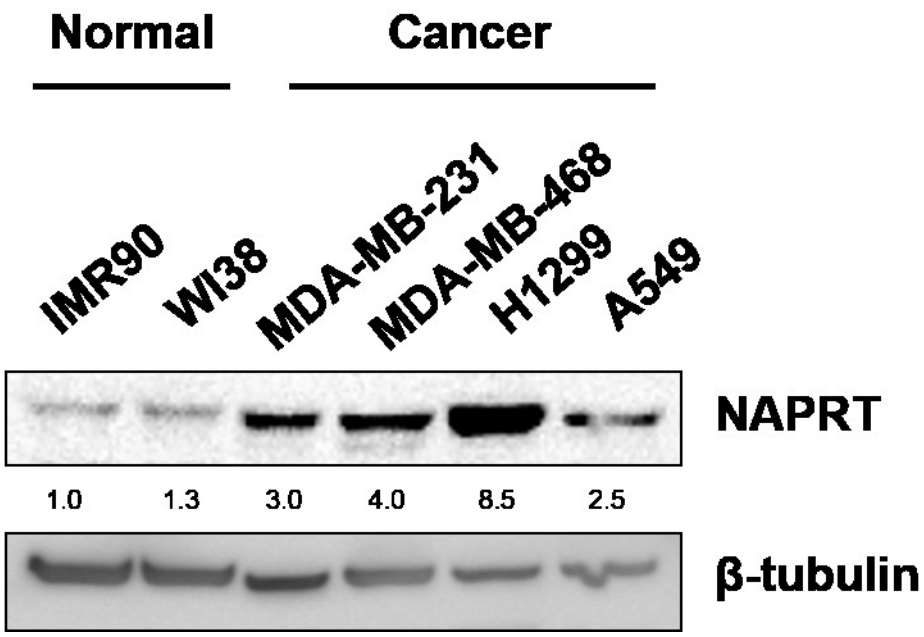

Figure 3.1. Endogeneous expression of NAPRT is elevated in some cancer cells. Normal IMR90 and WI38 cells were used for the comparison of NAPRT expression against cancer cell lines (MDA-MB-231, MDA-MB-468, H1299, and A549). Whole cell lysates were extracted and subjected to SDS-PAGE. Levels of NAPRT were detected by immunoblotting. Quantification of representative blot is shown from n=3.

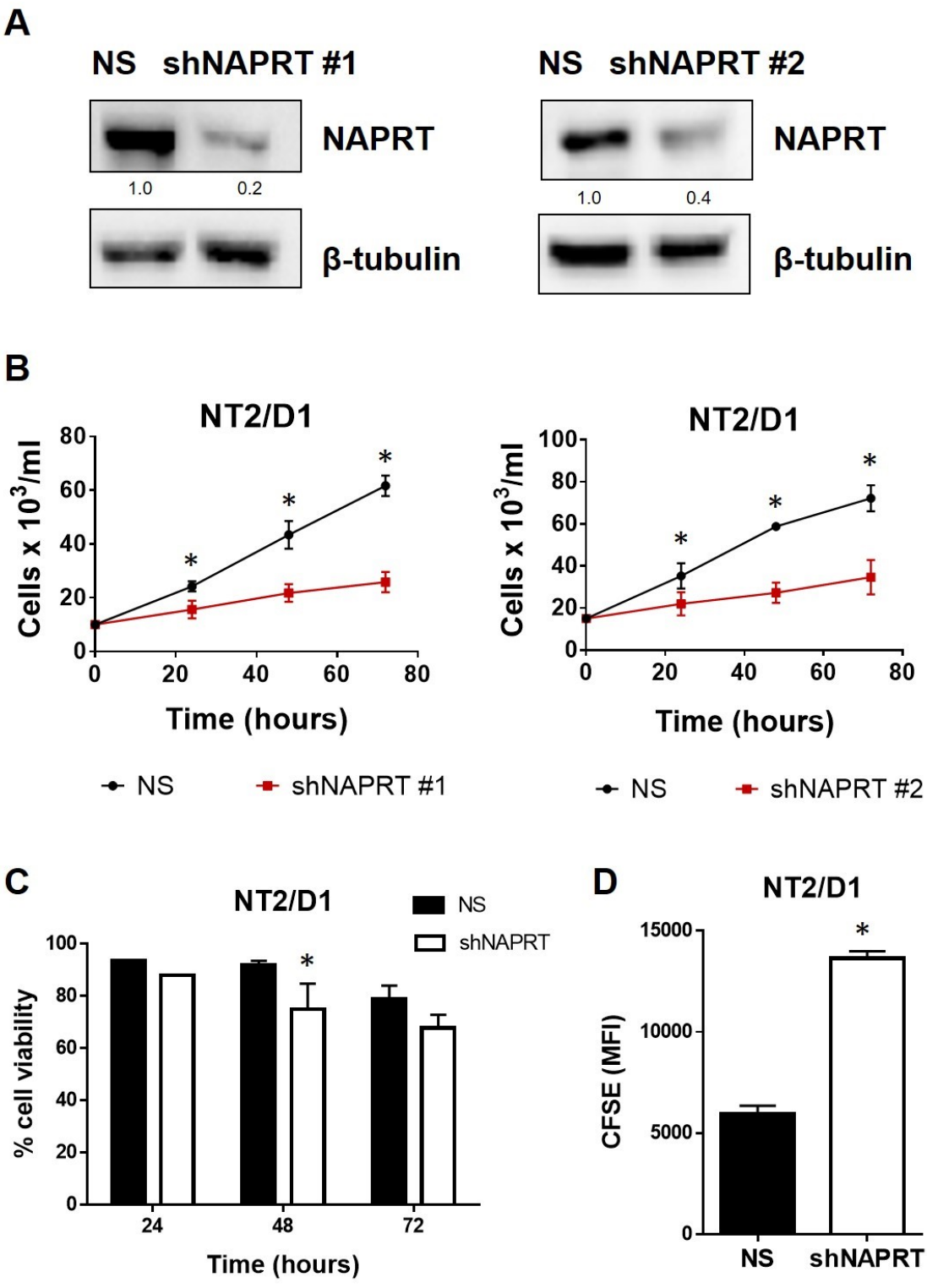
A
NS
shNAPRT #1
NAPRT
1.0
0.2
β-tubulin
NS
shNAPRT #2
NAPRT
1.0
0.4
β-tubulin
B
NT2/D1
Cells x 10^3/ml
Time (hours)
NS
shNAPRT #1
NT2/D1
Cells x 10^3/ml
Time (hours)
NS
shNAPRT #2
C
NT2/D1
NS
shNAPRT
% cell viability
Time (hours)
D
NT2/D1
CFSE (MFI)
NS
shNAPRT

Figure 3.2

Figure 3.2. NAPRT knockdown inhibits the proliferation of NT2/D1 cells.
(A) NT2/D1 cells that were transduced with shNAPRT or control shRNA (NS) were subjected to SDS-PAGE. The levels of NAPRT were detected by immunoblotting. Quantification of representative blot is shown from n=3. (B) The number of viable cells were determined by trypan blue exclusion in a 72-hour time-course assay and presented as a proliferation curve. (C) Cell viability over 72 hours was measured by counting the number of viable and non-viable cells, using trypan blue exclusion. (D) Cells were labelled with CFSE and then analyzed by flow cytometry for CFSE fluorescence after 4 days of culturing. Results shown as mean±SD, *p-value<0.05 obtained by a Student's t-test comparing the knockdown with NS control, n=3.

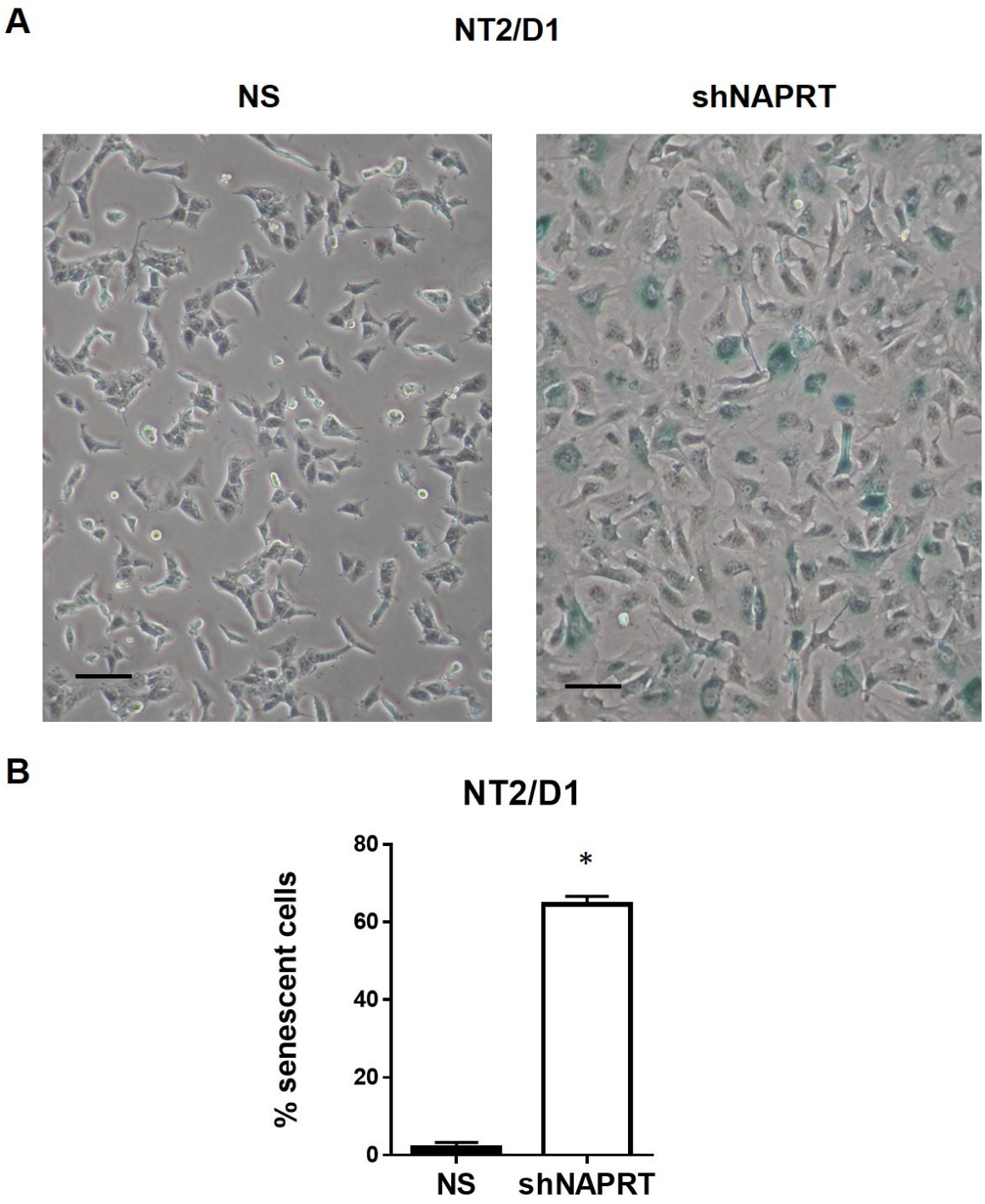
A
NT2/D1
NS
shNAPRT
B
NT2/D1
% senescent cells
80
60
40
20
0
*
NS
shNAPRT

Figure 3.3

Figure 3.3. NAPRT knockdown induces senescence in NT2/D1 cells.
(A) NT2/D1 cells were transduced with shNAPRT or control shRNA (NS). Senescence was detected by a β-galactosidase staining assay, where senescent cells stained blue in color. Photos were taken 24 hours after staining, over multiple fields of view. Representative images are shown from n=3. Scale bars 100 μm. (B) The senescence assay was quantified by determining the percentage of senescent cells in multiple images. Results shown as mean±SD, *p-value<0.05 obtained by a Student's t-test comparing the knockdown with NS control.

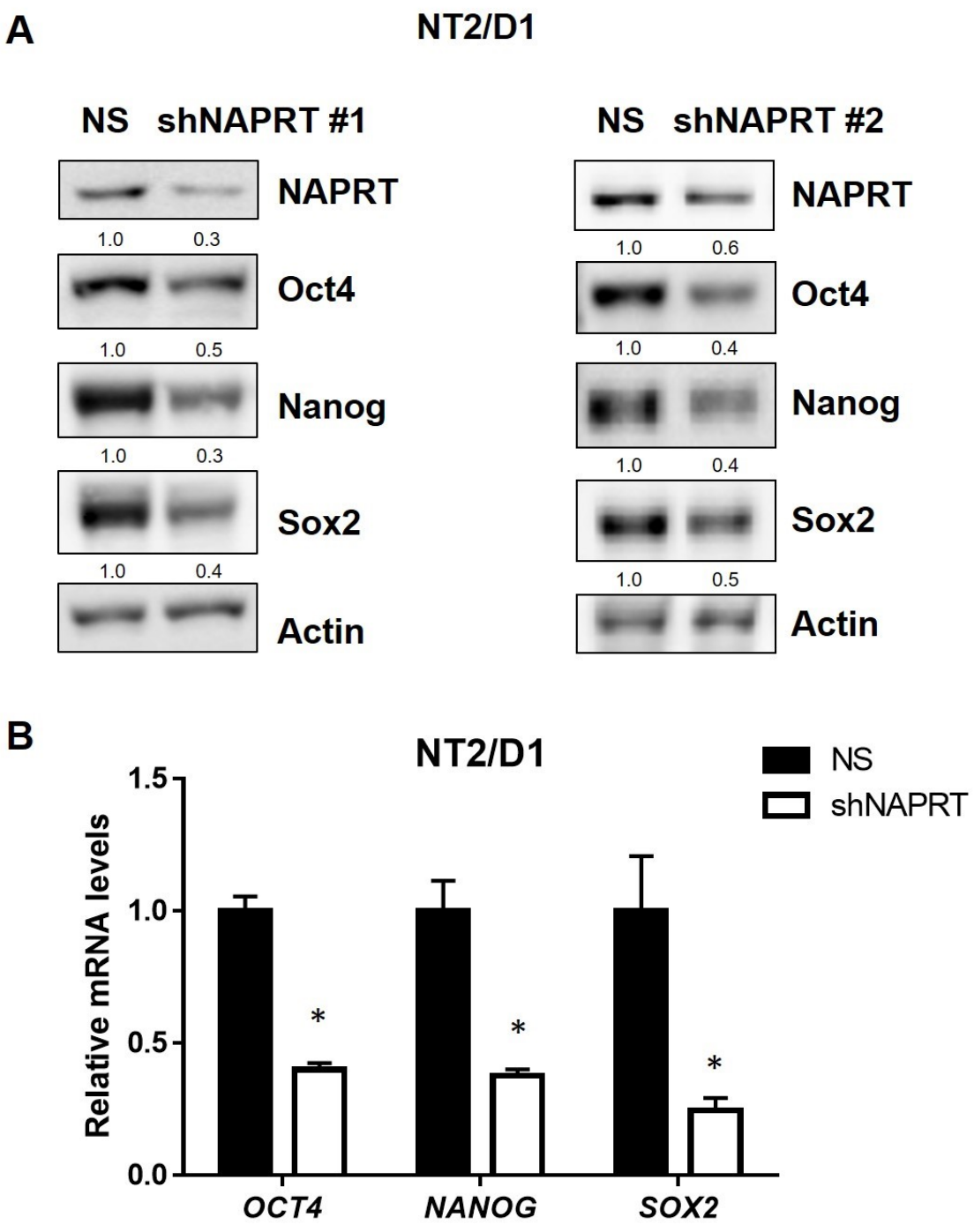
A
NT2/D1
NS
shNAPRT #1
NS
shNAPRT #2
NAPRT
1.0
0.3
NAPRT
1.0
0.6
Oct4
1.0
0.5
Oct4
1.0
0.4
Nanog
1.0
0.3
Nanog
1.0
0.4
Sox2
1.0
0.4
Sox2
1.0
0.5
Actin
Actin
B
NT2/D1
NS
shNAPRT
Relative mRNA levels
1.5
1.0
0.5
0.0
*
*
*
OCT4
NANOG
SOX2

Figure 3.4

Figure 3.4. NAPRT knockdown decreases expression of stemness markers in NT2/D1 cells.

(A) NT2/D1 cells were transduced with shNAPRT or control shRNA (NS). Whole cell lysates were subjected to SDS-PAGE and the levels of stemness markers (Oct4, Nanog, Sox2) were detected by immunoblotting. Quantification of representative blot is shown from n=3. (B) qRT-PCR analysis was performed for stemness-related genes. Results shown as mean±SEM, *p-value<0.05 obtained by a Student's t-test comparing the knockdown with NS control, n=3.

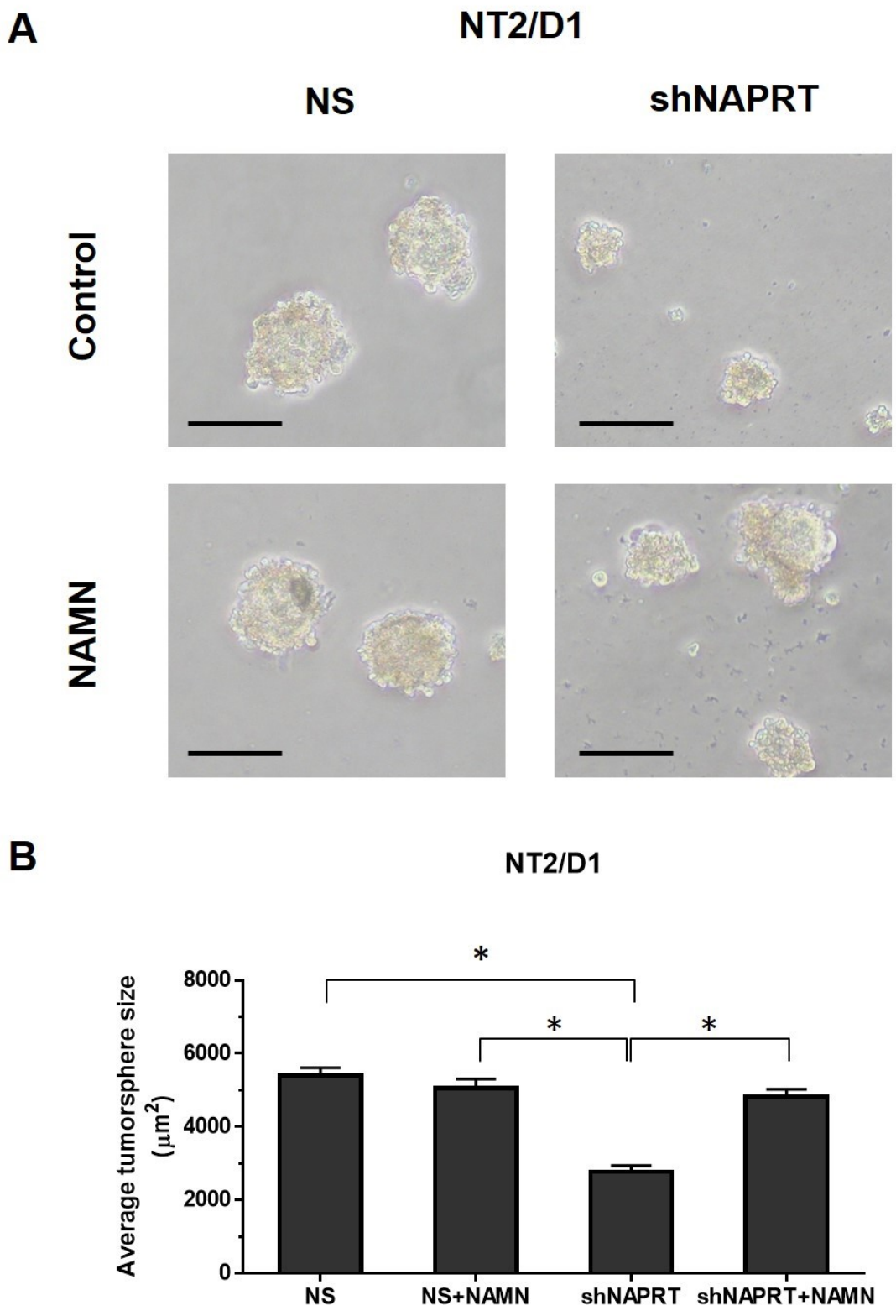
A
NT2/D1
NS
shNAPRT
Control
NAMN
B
NT2/D1
Average tumorsphere size (μm²)
8000
6000
4000
2000
0
*
*
*
NS
NS+NAMN
shNAPRT
shNAPRT+NAMN

Figure 3.5

Figure 3.5. NAPRT knockdown decreases tumorsphere size of NT2/D1 cells.
(A) NT2/D1 cells that were transduced with shNAPRT or control shRNA (NS) were plated in nonadherent conditions and treated or not treated with 100 μM of NAMN. Tumorspheres were allowed to form for 5 days. Photos were taken over multiple fields of view. Representative images are shown from n=3. Scale bars 100 μm. (B) Average area of tumorspheres (μm^2) that were equal or greater than 50 μm were analyzed over multiple images. Results shown as mean±SEM, *p-value<0.05 obtained using two-way ANOVA with a Tukey posttest.

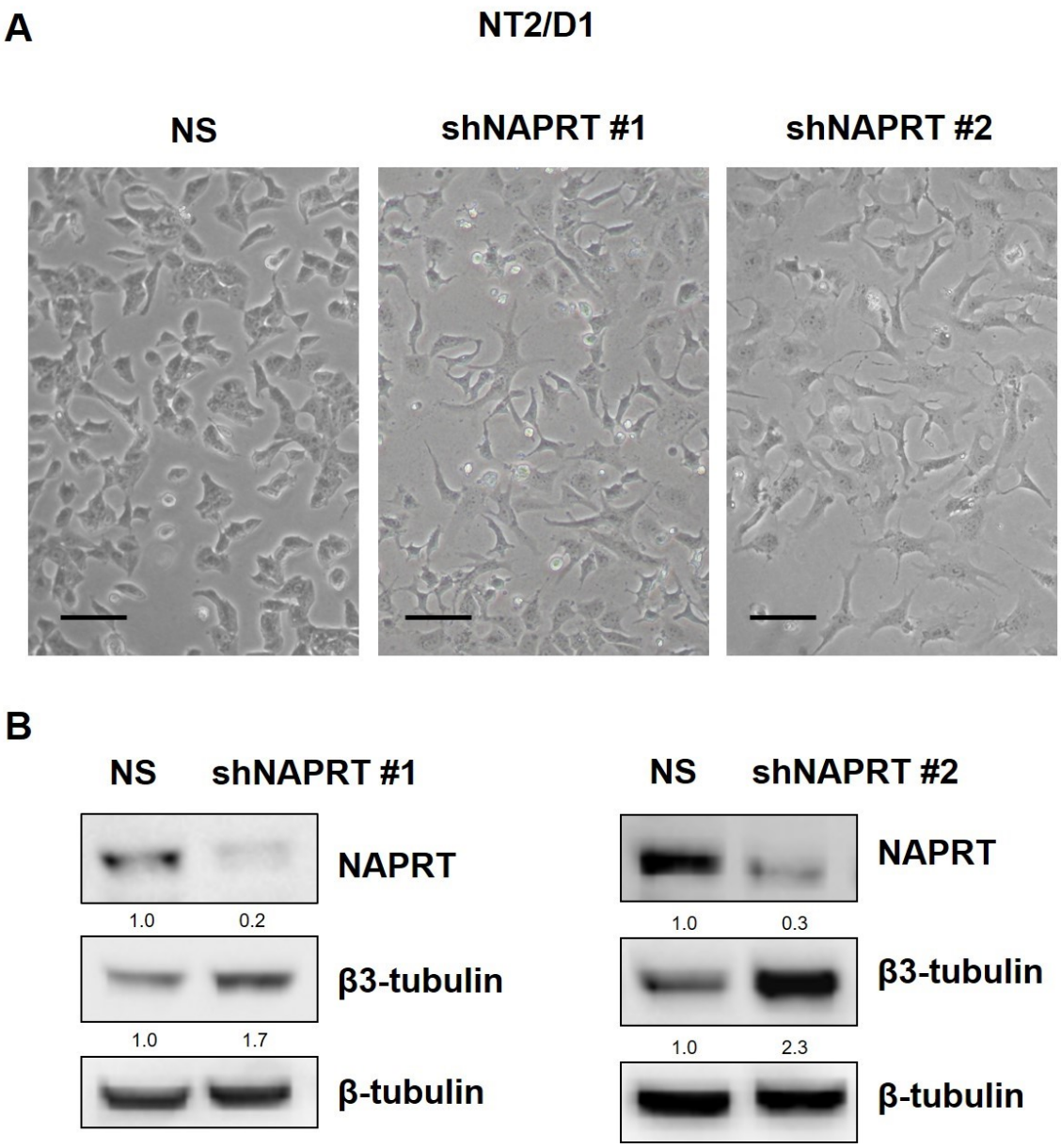

Figure 3.6. NAPRT knockdown promotes differentiation of NT2/D1 cells.
(A) Microscopy photos of NT2/D1 cells that were transduced with shNAPRT or control shRNA (NS) were taken to show cell morphology. Scale bars 100 μm. (B) Whole cell lysates were subjected to SDS-PAGE and the levels of neuronal differentiation marker β3-tubulin were detected by immunoblotting. Quantification of representative blot is shown from n=3.

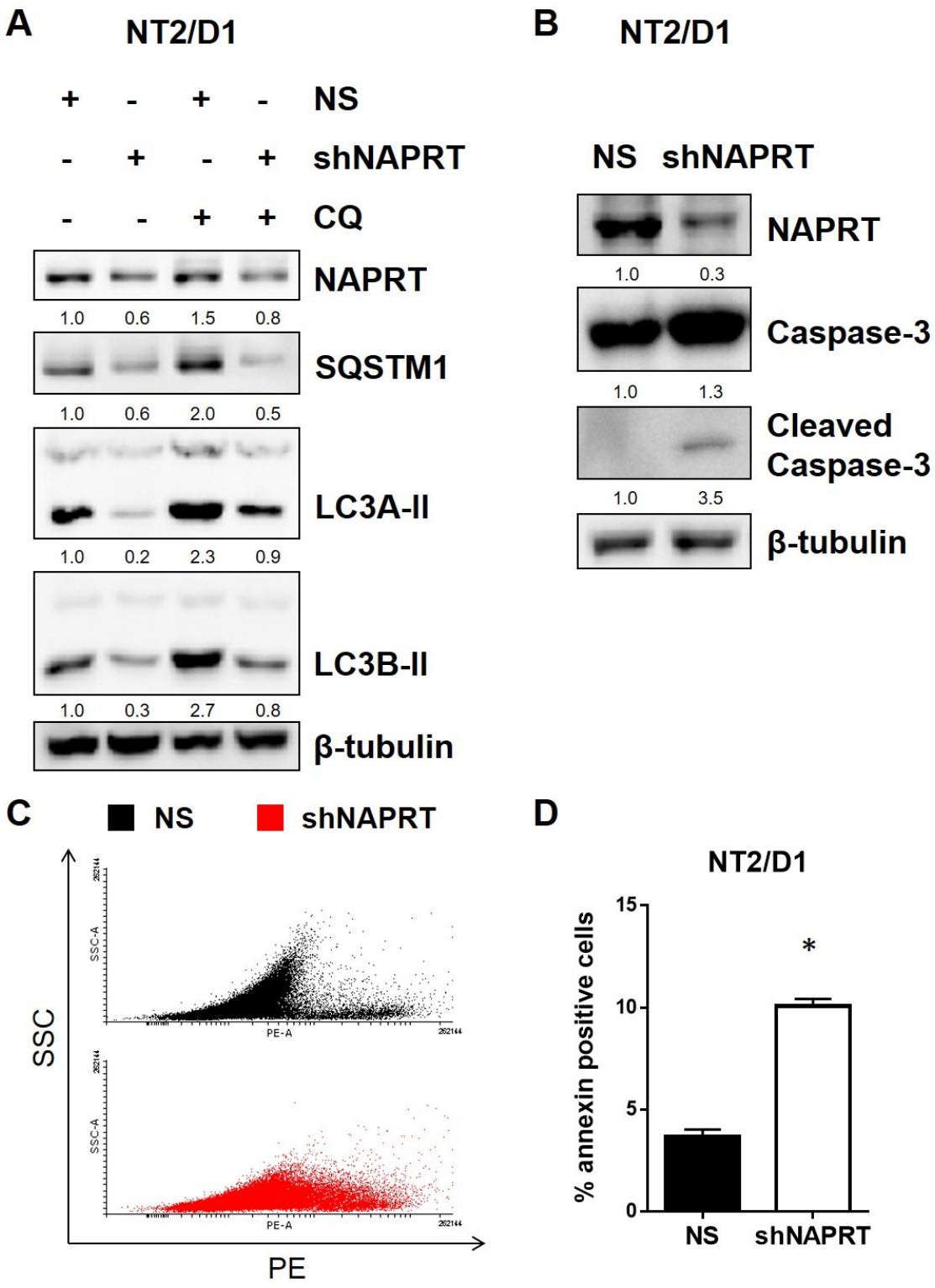
A
NT2/D1
+ - + - NS
- + - + shNAPRT
- - + + CQ
NAPRT
1.0 0.6 1.5 0.8
SQSTM1
1.0 0.6 2.0 0.5
LC3A-II
1.0 0.2 2.3 0.9
LC3B-II
1.0 0.3 2.7 0.8
β-tubulin
B
NT2/D1
NS shNAPRT
NAPRT
1.0 0.3
Caspase-3
1.0 1.3
Cleaved Caspase-3
1.0 3.5
β-tubulin
C
NS
shNAPRT
SSC
PE
SSC-A
PE-A
D
NT2/D1
% annexin positive cells
15
10
5
0
*
NS
shNAPRT

Figure 3.7

Figure 3.7. NAPRT knockdown promotes cell death but not autophagy in NT2/D1 cells.

(A) NT2/D1 cells that were transduced with shNAPRT or control shRNA (NS) were treated or not treated with chloroquine (CQ) for 24 hours. Whole cell lysates were subjected to SDS-PAGE and immunoblotted for the levels of autophagy proteins (SQSTM1, LC3A, and LC3B). (B) Whole cell lysates of NT2/D1 were subjected to SDS-PAGE for detection of Caspase-3. Quantification of representative blot is shown from n=3. (C) NT2/D1 cells were stained with PE-conjugated annexin V and analyzed by flow cytometry. Representative dot plots are shown from n=3. (D) The percentage of NT2/D1 NS or shNAPRT cells that were positive for annexin was measured using Flowing software. Results shown as mean±SD, *p-value<0.05 obtained by a Student's t-test comparing the knockdown with NS control.

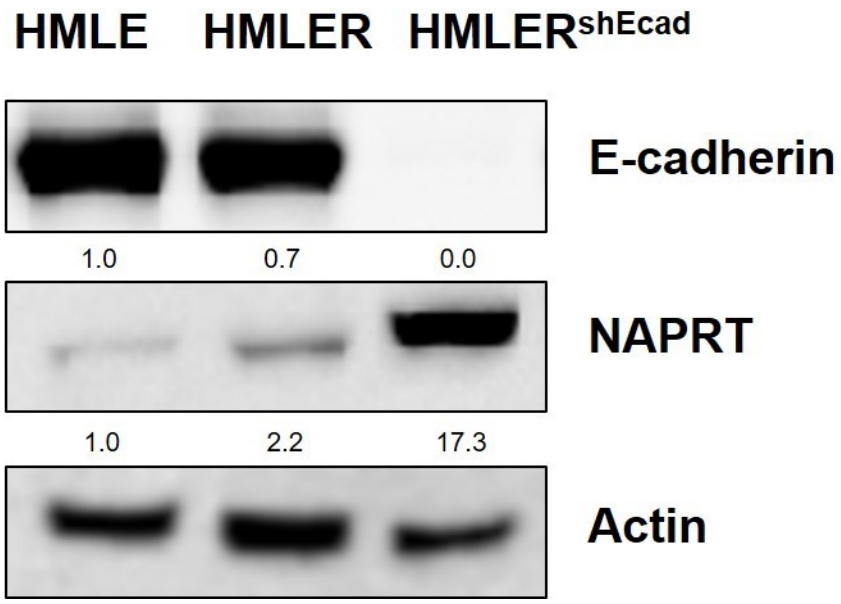

Figure 3.8. HMLER-shEcad CSLCs express higher levels of NAPRT than non-transformed and non-CSLC counterparts.

Whole cell lysates of HMLE (normal cells), HMLER (cancer cells), and HMLER-shEcad (CSLCs) were subjected to SDS-PAGE and immunoblotted for levels of NAPRT. Quantification of representative blot is shown from n=3.

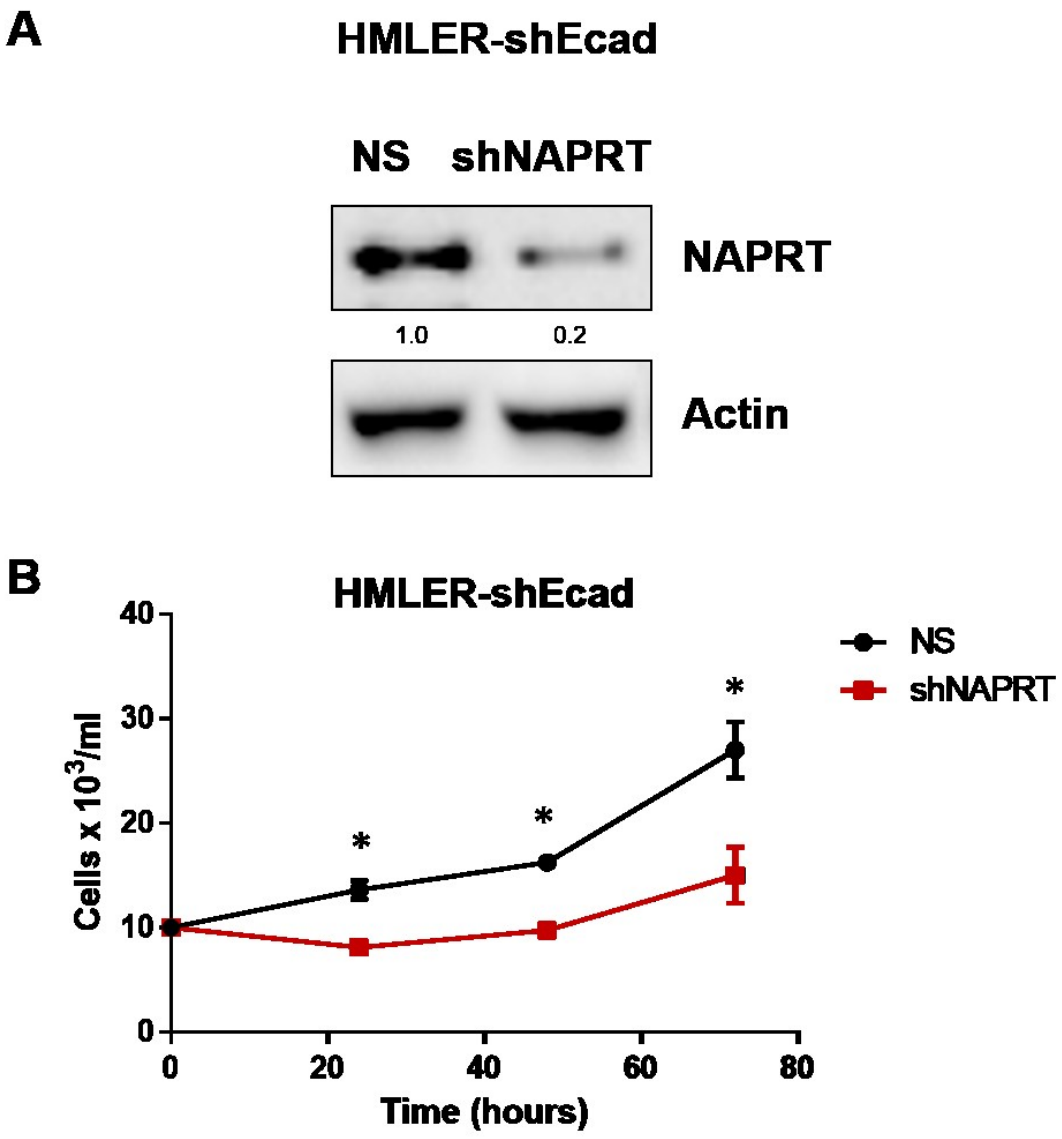

Figure 3.9. NAPRT knockdown inhibits the proliferation of HMLER-shEcad cells. (A) HMLER-shEcad that were transduced with shNAPRT or NS were subjected to SDS-PAGE. The levels of NAPRT were detected by immunoblotting. Quantification of representative blot is shown from n=3. (B) The number of viable cells were determined by trypan blue exclusion in a 72-hour time-course assay and presented as a proliferation curve. Results shown as mean±SD, *p-value<0.05 obtained by a Student's t-test comparing the knockdown with NS control, n=3.

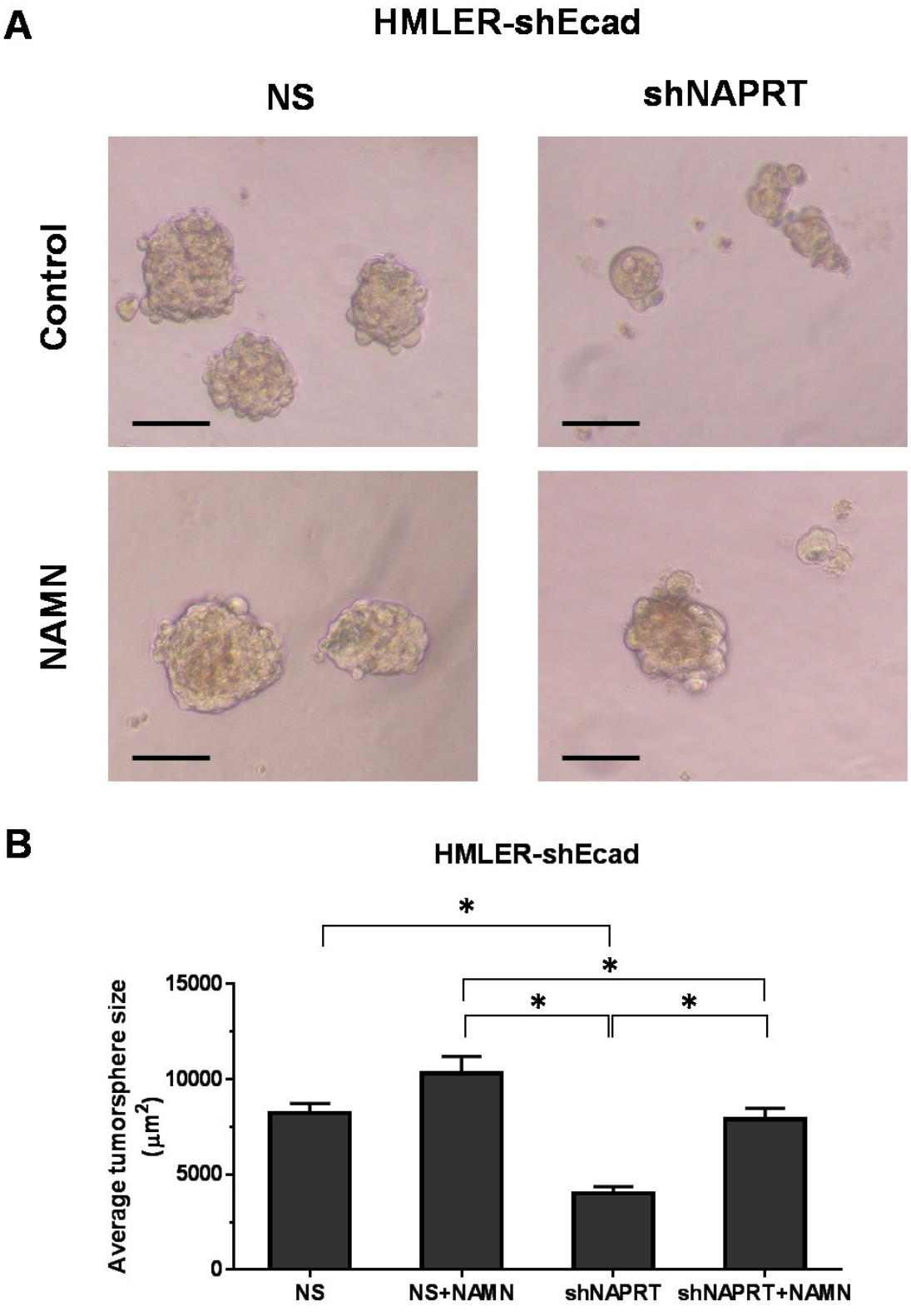
A
HMLER-shEcad
NS
shNAPRT
Control
NAMN
B
HMLER-shEcad
Average tumorsphere size (μm²)
15000
10000
5000
0
*
*
*
*
NS
NS+NAMN
shNAPRT
shNAPRT+NAMN

Figure 3.10

Figure 3.10. NAPRT knockdown decreases tumorsphere size of HMLER-shEcad cells.

(A) HMLER-shEcad cells that were transduced with shNAPRT or control shRNA (NS) were plated in nonadherent conditions and treated or not treated with 100 μM of NAMN. Tumorspheres were allowed to form for 5 days. Photos were taken over multiple fields of view. Representative images are shown from n=3. Scale bars 100 μm. (B) Average area of tumorspheres (μm^2) that were equal or greater than 50 μm were analyzed over multiple images. Results shown as mean±SEM, *p-value<0.05 obtained using two-way ANOVA with a Tukey posttest.

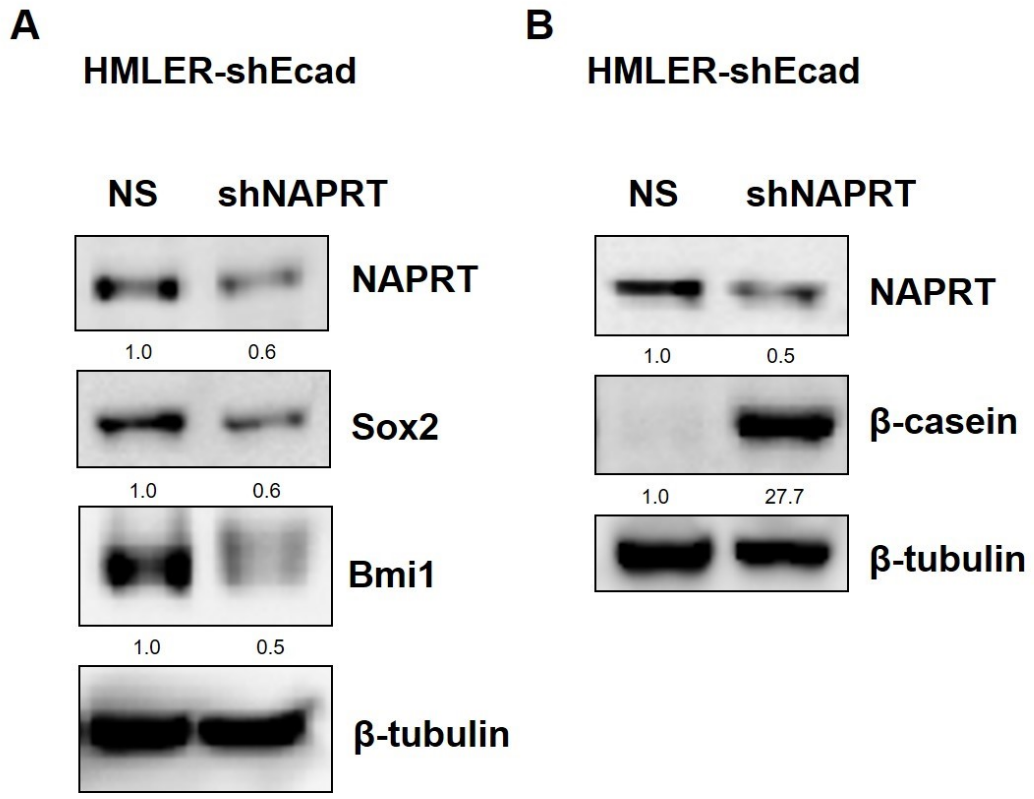

Figure 3.11. NAPRT knockdown decreases stemness and increases differentiation markers in HMLER-shEcad cells.

(A) Whole cell lysates of HMLER-shEcad cells that were transduced with shNAPRT or control shRNA (NS) were subjected to SDS-PAGE. The levels of stemness markers (Sox2 and Bmi1) were detected by immunoblotting. (B) SDS-PAGE of NS and shNAPRT whole cell lysates were immunoblotted for levels of epithelial mammary differentiation marker β-casein. Quantification of representative blot is shown from n=3.

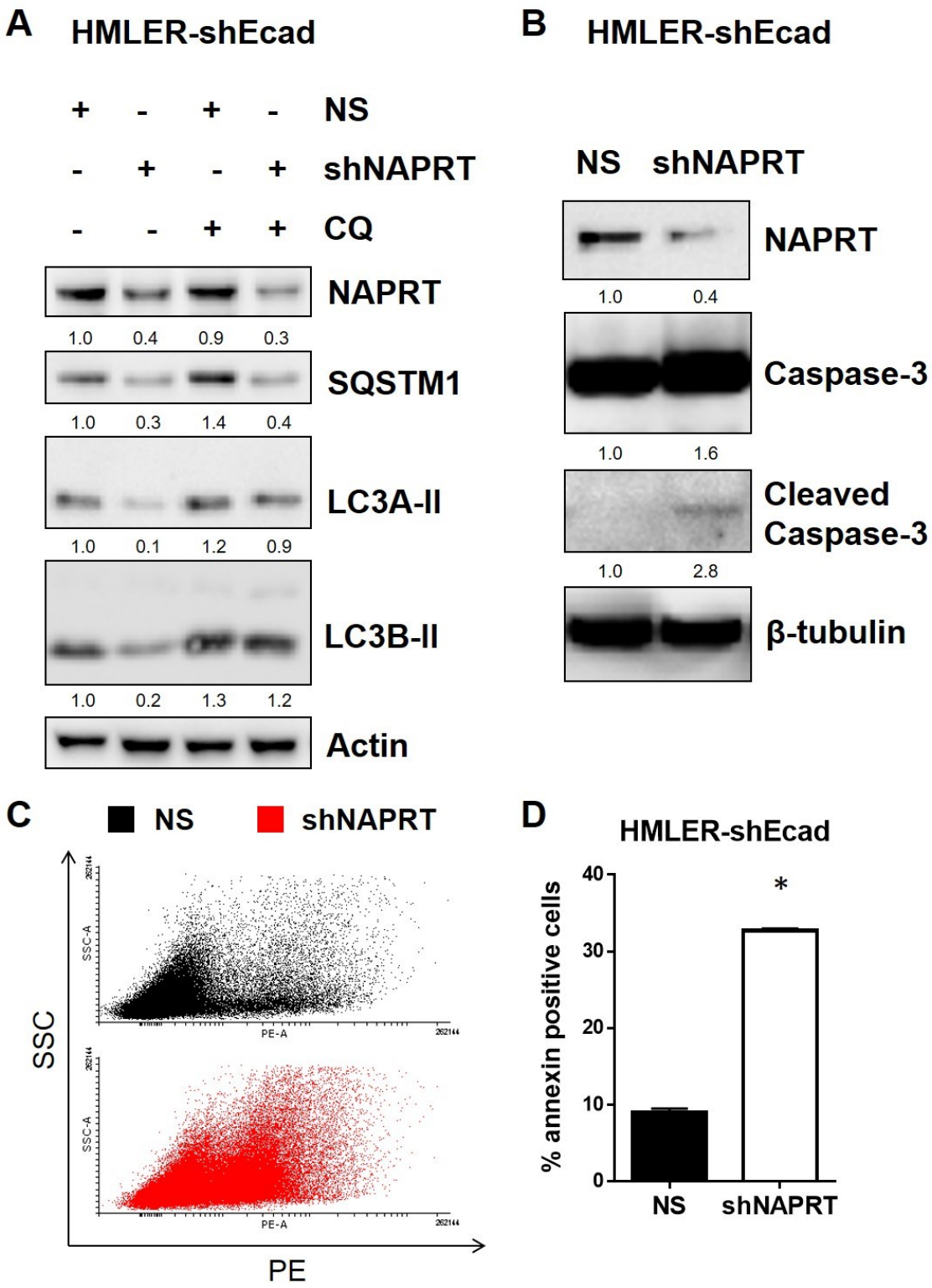
A
HMLER-shEcad
+ - + - NS
- + - + shNAPRT
- - + + CQ
NAPRT
1.0 0.4 0.9 0.3
SQSTM1
1.0 0.3 1.4 0.4
LC3A-II
1.0 0.1 1.2 0.9
LC3B-II
1.0 0.2 1.3 1.2
Actin
B
HMLER-shEcad
NS shNAPRT
NAPRT
1.0 0.4
Caspase-3
1.0 1.6
Cleaved Caspase-3
1.0 2.8
β-tubulin
C
NS shNAPRT
SSC
PE
SSC-A
PE-A
D
HMLER-shEcad
% annexin positive cells
40
30
20
10
0
*
NS shNAPRT

Figure 3.12

Figure 3.12. NAPRT knockdown promotes autophagy and cell death in HMLER-shEcad cells.

(A) HMLER-shEcad cells that were transduced with shNAPRT or control shRNA (NS) were treated or not treated with chloroquine (CQ) for 24 hours. Whole cell lysates were subjected to SDS-PAGE and immunoblotted for the levels of autophagy proteins (SQSTM1, LC3A, and LC3B). (B) Whole cell lysates of HMLER-shEcad were subjected to SDS-PAGE for detection of Caspase-3. Quantification of representative blot is shown from n=3. (C) HMLER-shEcad cells were stained with PE-conjugated annexin V and analyzed by flow cytometry. Representative dot plots are shown from n=3. (D) The percentage of HMLER-shEcad NS or shNAPRT cells that were positive for annexin was measured using Flowing software. Results shown as mean±SD, *p-value<0.05 obtained by a Student's t-test comparing the knockdown with NS control.

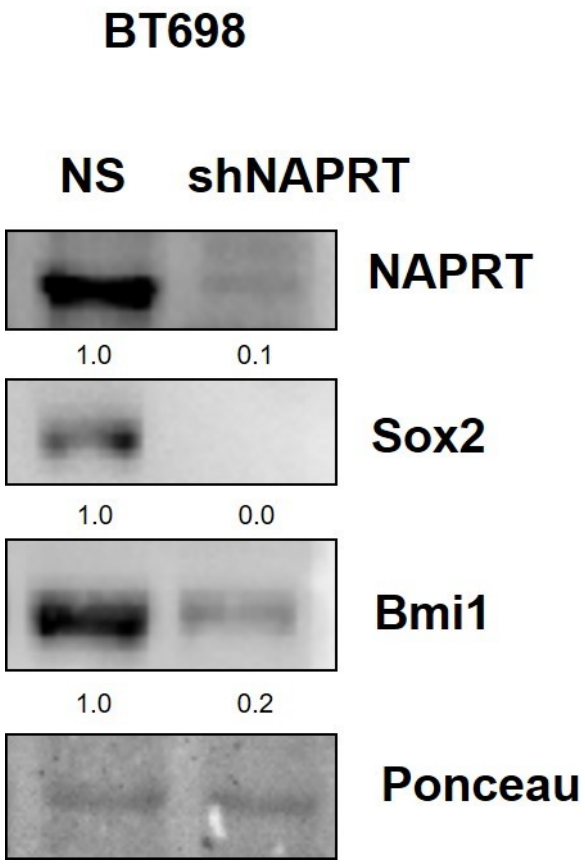

Figure 3.13. NAPRT knockdown decreases expression of stemness markers in BT698 BTICs.

BT698 cells were transduced with shNAPRT or control shRNA (NS). Whole cell lysates were subjected to SDS-PAGE and the levels of stemness markers (Sox2 and Bmi1) were detected by immunoblotting. Quantification of n=1 shown.

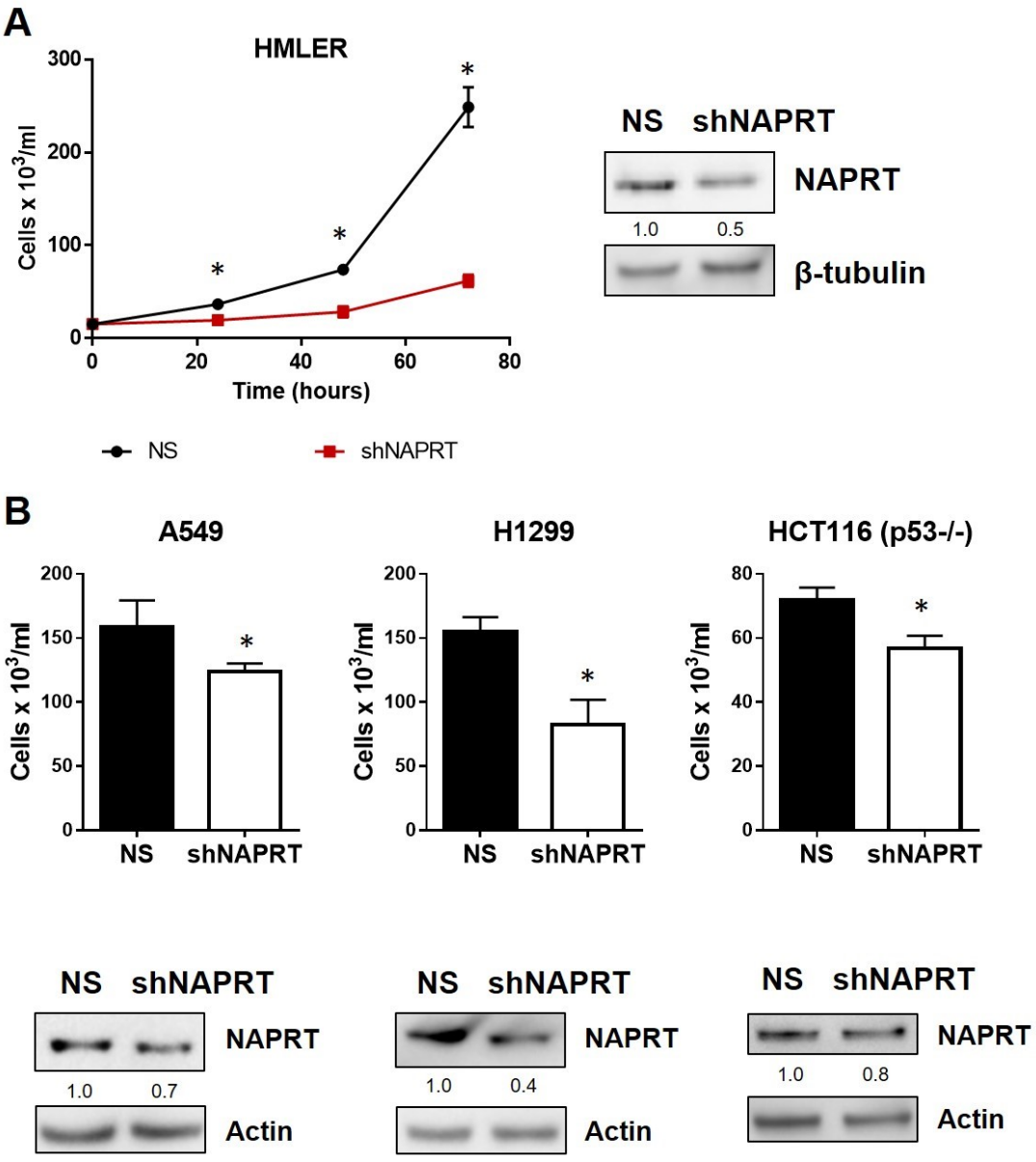
A
HMLER
Cells x 10^3/ml
Time (hours)
NS
shNAPRT
NS shNAPRT
NAPRT
1.0 0.5
β-tubulin
B
A549
H1299
HCT116 (p53-/-)
Cells x 10^3/ml
NS shNAPRT
NS shNAPRT
NAPRT
1.0 0.7
Actin
NS shNAPRT
NAPRT
1.0 0.4
Actin
NS shNAPRT
NAPRT
1.0 0.8
Actin

Figure 3.14

Figure 3.14. NAPRT knockdown inhibits the proliferation of differentiated cancer cells. HMLER, A549, H1299, and HCT116 (p53 -/-) cells were transduced with shNAPRT or control shRNA (NS). (A) The number of viable HMLER cells were determined by trypan blue exclusion in a 72-hour time-course assay and presented as a proliferation curve (left panel). The levels of NAPRT were detected by immunoblotting (right panel). (B) The number of viable A549, H1299, and HCT116 (p53 -/-) cells were counted by trypan blue exclusion after 72 hours (top panel). The levels of NAPRT were detected by immunoblotting (bottom panel). Results shown as mean±SD, *p-value<0.05 obtained by a Student's t-test comparing the knockdown with NS control, n=3.

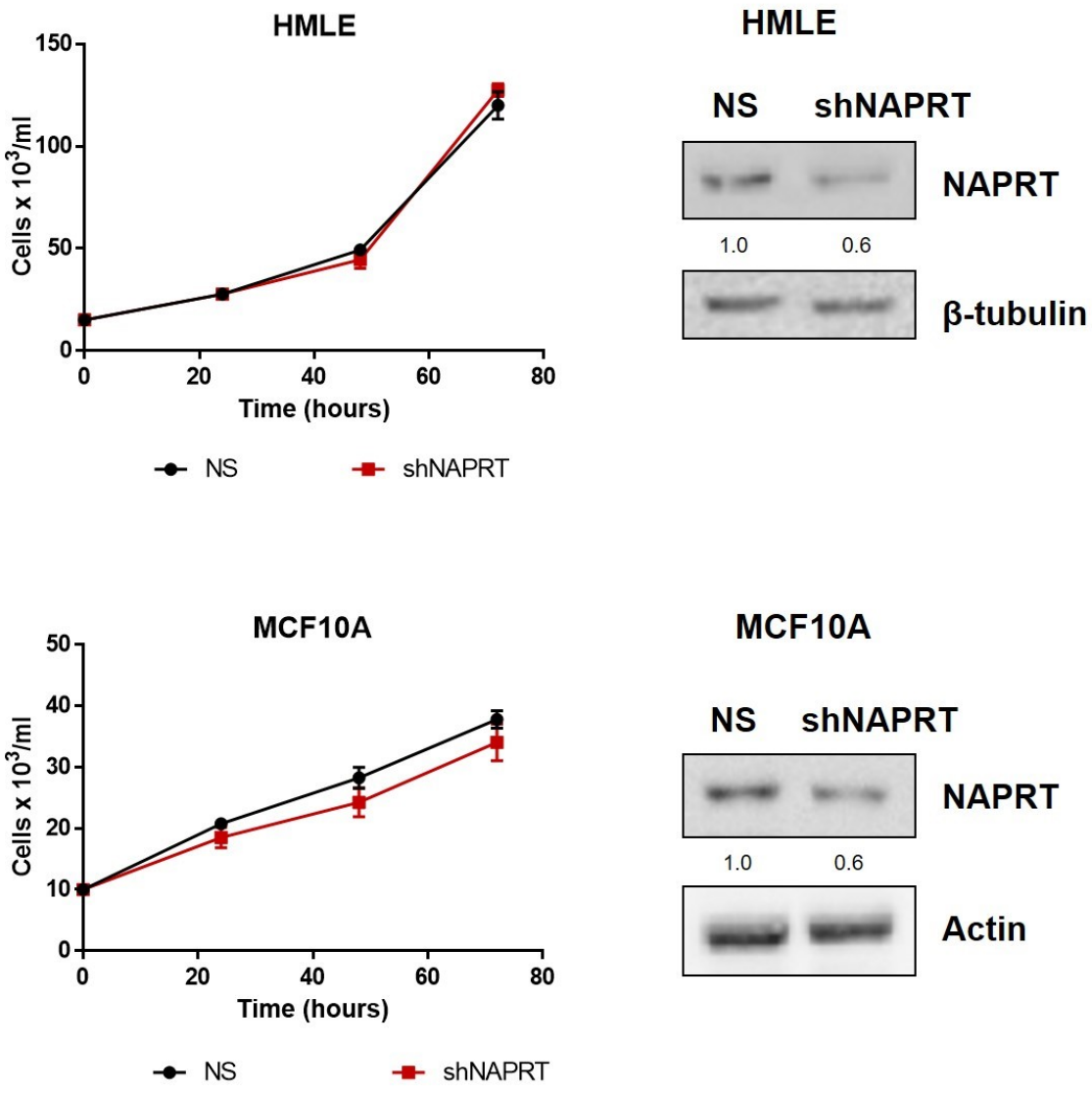

Figure 3.15. NAPRT knockdown only marginally affects the proliferation of normal non-transformed cells.

HMLE and MCF10A cells were transduced with shNAPRT or control shRNA (NS). The number of viable cells were determined by trypan blue exclusion in a 72-hour time-course assay and presented as a proliferation curve (left panel). The levels of NAPRT were detected by immunoblotting (right panel). Results shown as mean±SD, *p-value<0.05 obtained by a Student's t-test comparing the knockdown with NS control, n=3.

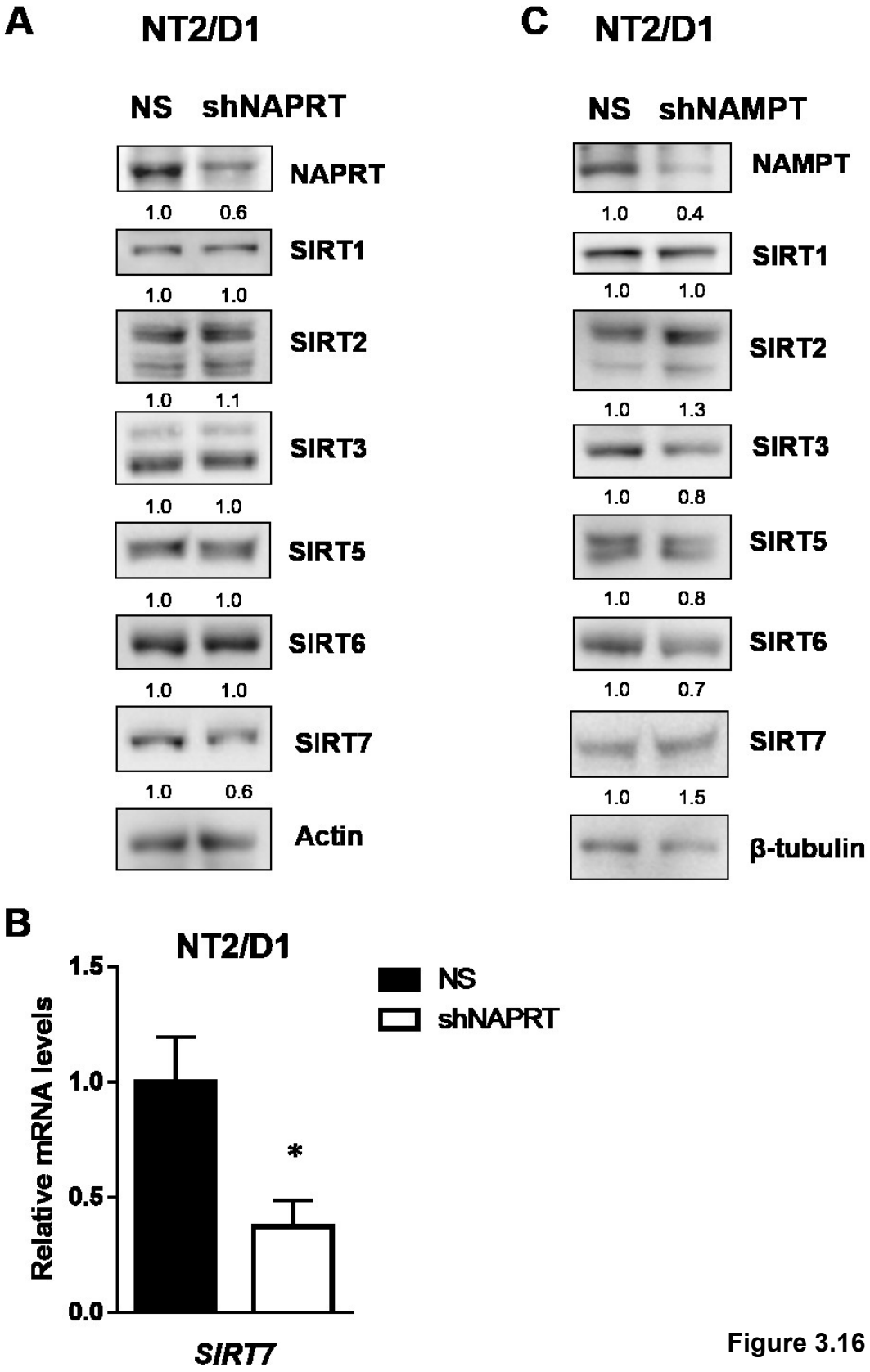
A
NT2/D1
NS
shNAPRT
NAPRT
1.0
0.6
SIRT1
1.0
1.0
SIRT2
1.0
1.1
SIRT3
1.0
1.0
SIRT5
1.0
1.0
SIRT6
1.0
1.0
SIRT7
1.0
0.6
Actin
C
NT2/D1
NS
shNAMPT
NAMPT
1.0
0.4
SIRT1
1.0
1.0
SIRT2
1.0
1.3
SIRT3
1.0
0.8
SIRT5
1.0
0.8
SIRT6
1.0
0.7
SIRT7
1.0
1.5
β-tubulin
B
NT2/D1
NS
shNAPRT
Relative mRNA levels
1.5
1.0
0.5
0.0
*
SIRT7

Figure 3.16

Figure 3.16. NAPRT knockdown selectively downregulates SIRT7 expression in NT2/D1 cells.

Whole cell lysates of NT2/D1 cells that were transduced with shNAPRT or control shRNA (NS) were subjected to SDS-PAGE to measure the levels of SIRTs. (B) qRT-PCR analysis was performed to measure *SIRT7* levels. (C) Whole cell lysates of NT2/D1 cells that were transduced with shNAMPT or NS were subjected to SDS-PAGE to measure the levels of SIRTs. Quantification of representative blot is shown from n=3. Results shown as mean±SEM, *p-value<0.05 obtained by a Student's t-test comparing the knockdown with NS control, n=3.

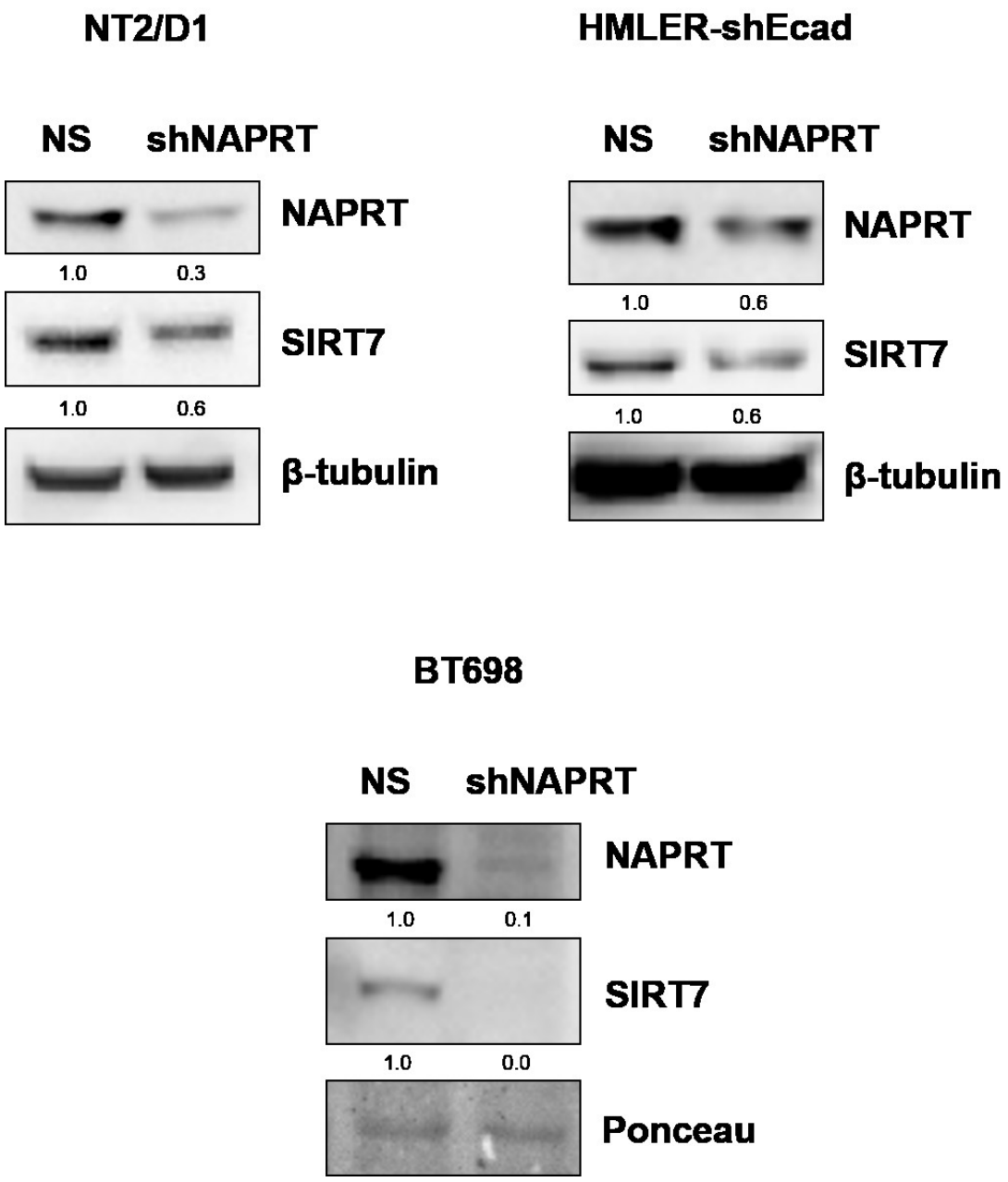

Figure 3.17. NAPRT knockdown decreases SIRT7 expression in CSLCs.
Whole cell lysates of NT2/D1, HMLER-shEcad, and BT698 cells that were transduced with shNAPRT or control shRNA (NS) were subjected to SDS-PAGE to detect levels of SIRT7. Quantification of representative blot is shown from n=3 for NT2/D1 and HMLER-shEcad, and n=1 for BT698.

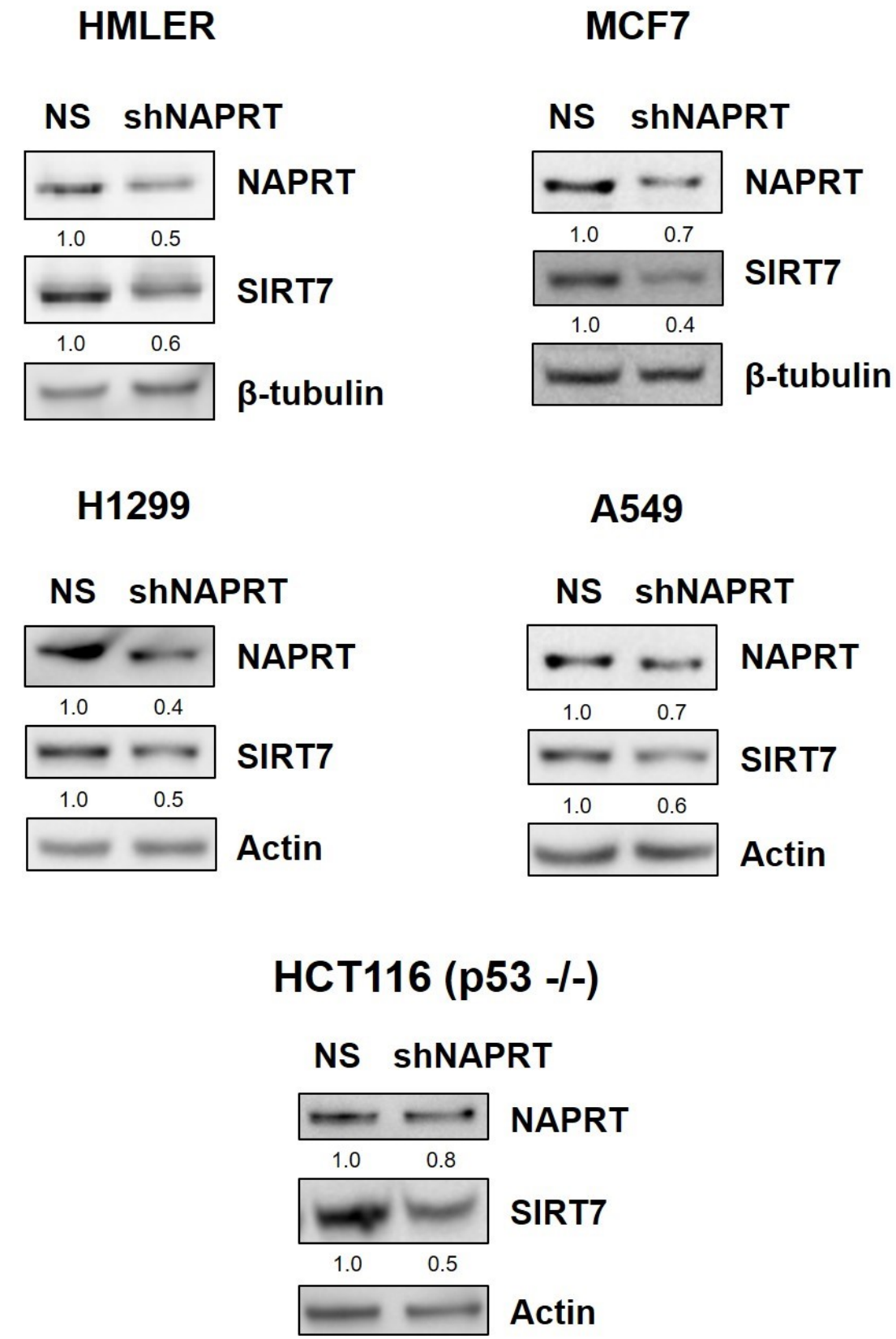
HMLER
NS shNAPRT
NAPRT
1.0 0.5
SIRT7
1.0 0.6
β-tubulin
MCF7
NS shNAPRT
NAPRT
1.0 0.7
SIRT7
1.0 0.4
β-tubulin
H1299
NS shNAPRT
NAPRT
1.0 0.4
SIRT7
1.0 0.5
Actin
A549
NS shNAPRT
NAPRT
1.0 0.7
SIRT7
1.0 0.6
Actin
HCT116 (p53 -/-)
NS shNAPRT
NAPRT
1.0 0.8
SIRT7
1.0 0.5
Actin

Figure 3.18

Figure 3.18. NAPRT knockdown decreases SIRT7 expression in differentiated cancer cells.

Breast cancer cells (HMLER and MCF7), lung cancer cells (H1299 and A549) and colorectal cancer cells (HCT116 p53 -/-) were transduced with shNAPRT or control shRNA (NS). Whole cell lysates were subjected to SDS-PAGE to detect levels of SIRT7. Quantification of representative blot is shown from n=3.

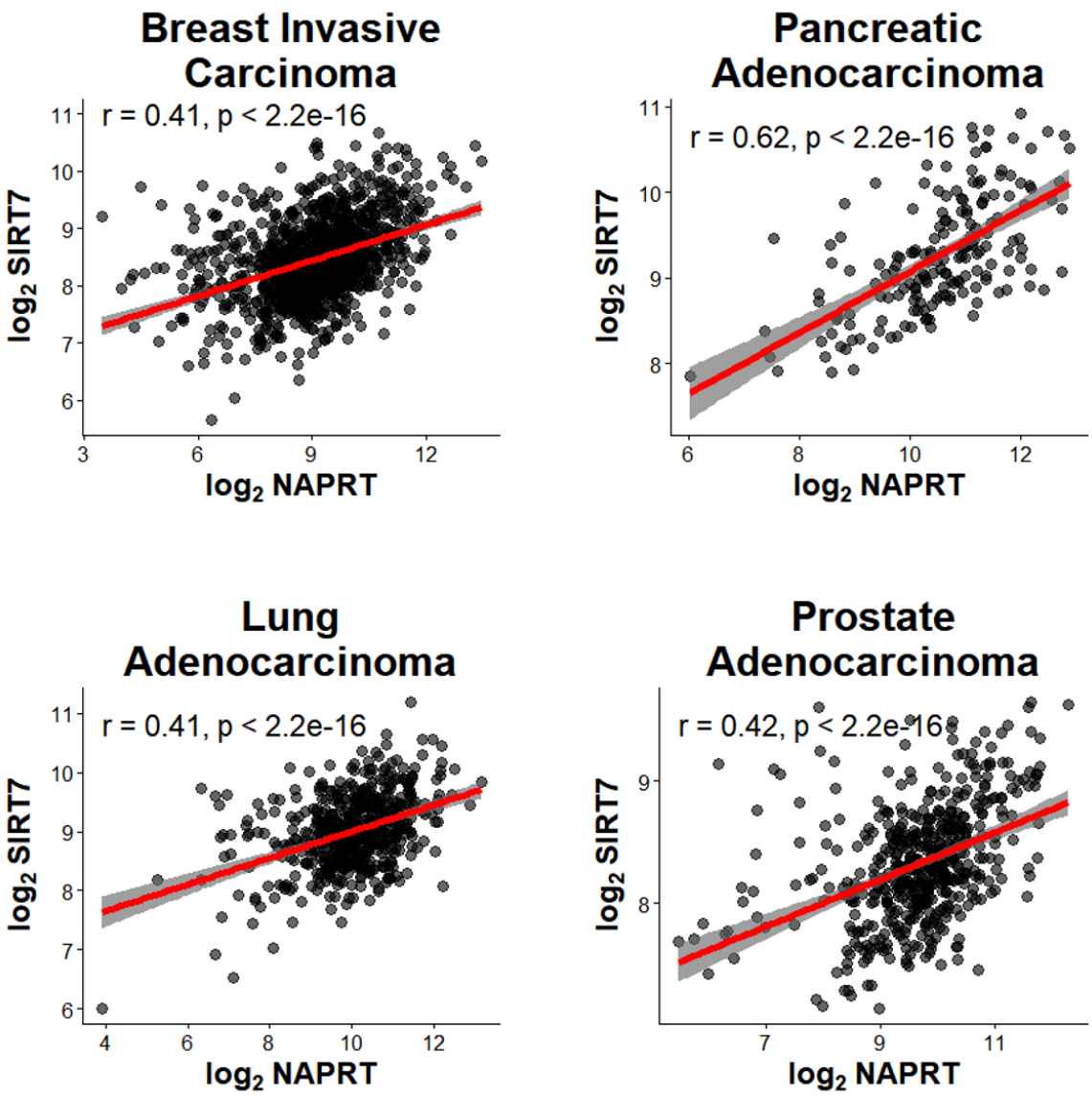

Figure 3.19. NAPRT expression positively correlates with SIRT7 expression in various cancers.

TCGA dataset of breast invasive carcinoma, pancreatic adenocarcinoma, lung adenocarcinoma, and prostate adenocarcinoma were used to correlate the mRNA expression of NAPRT with SIRT7. A Pearson correlation index and p-value were calculated using R software. Shaded area showing 95% confidence interval.

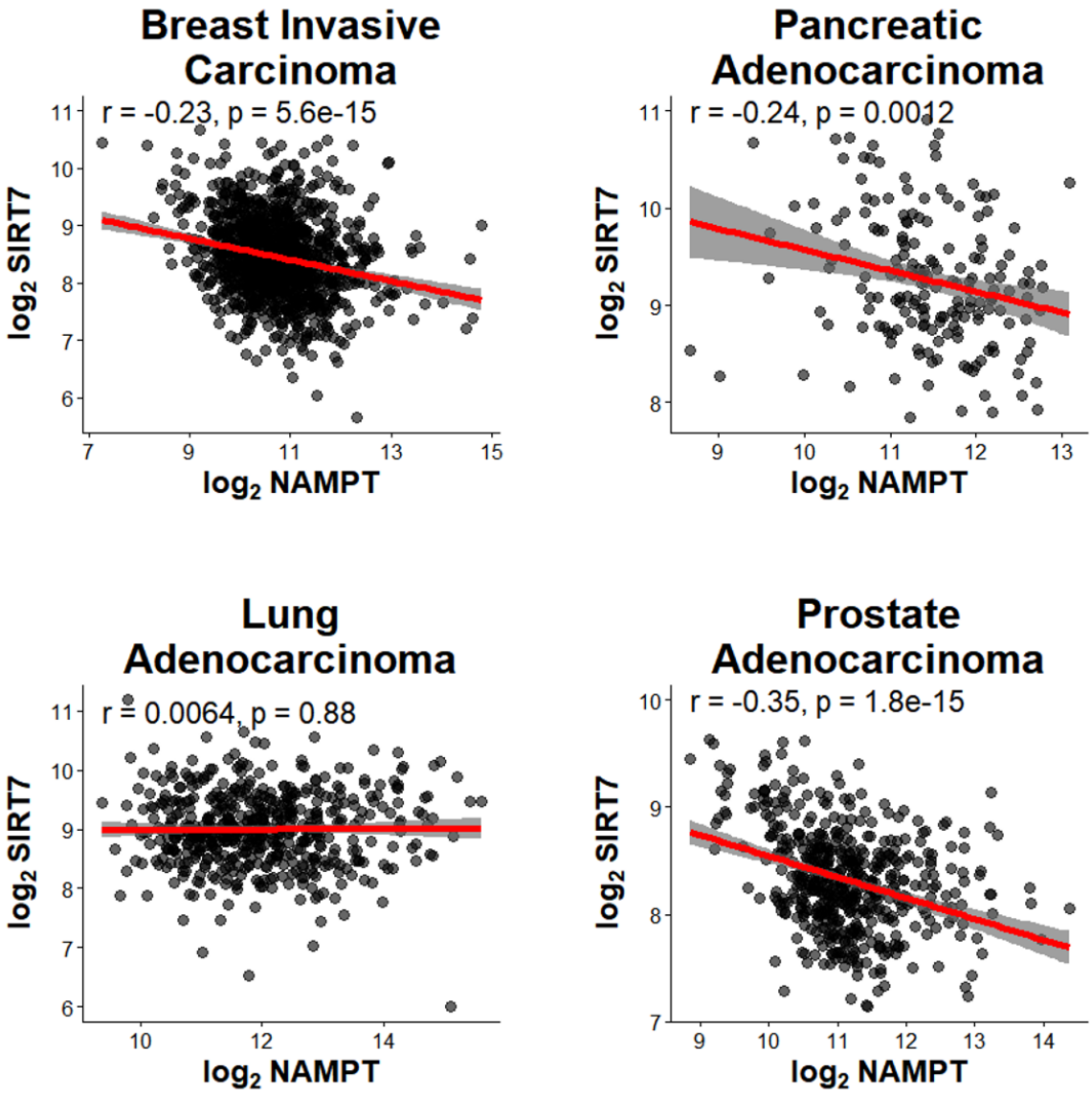

Figure 3.20. NAMPT expression has no positive correlation with SIRT7 expression. TCGA dataset of breast invasive carcinoma, pancreatic adenocarcinoma, lung adenocarcinoma, and prostate adenocarcinoma were used to correlate the mRNA expression of NAMPT with SIRT7. A Pearson correlation index and p-value were calculated using R software. Shaded area showing 95% confidence interval.

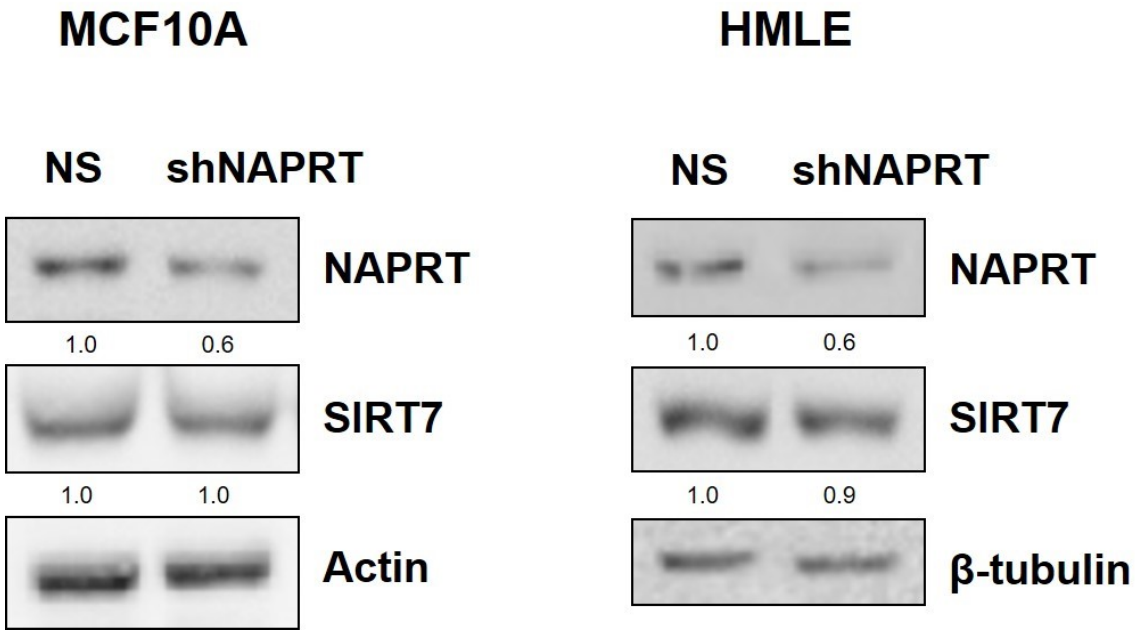

Figure 3.21. NAPRT knockdown does not affect SIRT7 expression in normal non-transformed cells.

Normal non-transformed breast cell lines, MCF10A and HMLE, were transduced with shNAPRT or control shRNA (NS). Whole cell lysates were subjected to SDS-PAGE to detect levels of SIRT7. Quantification of representative blot is shown from n=3.

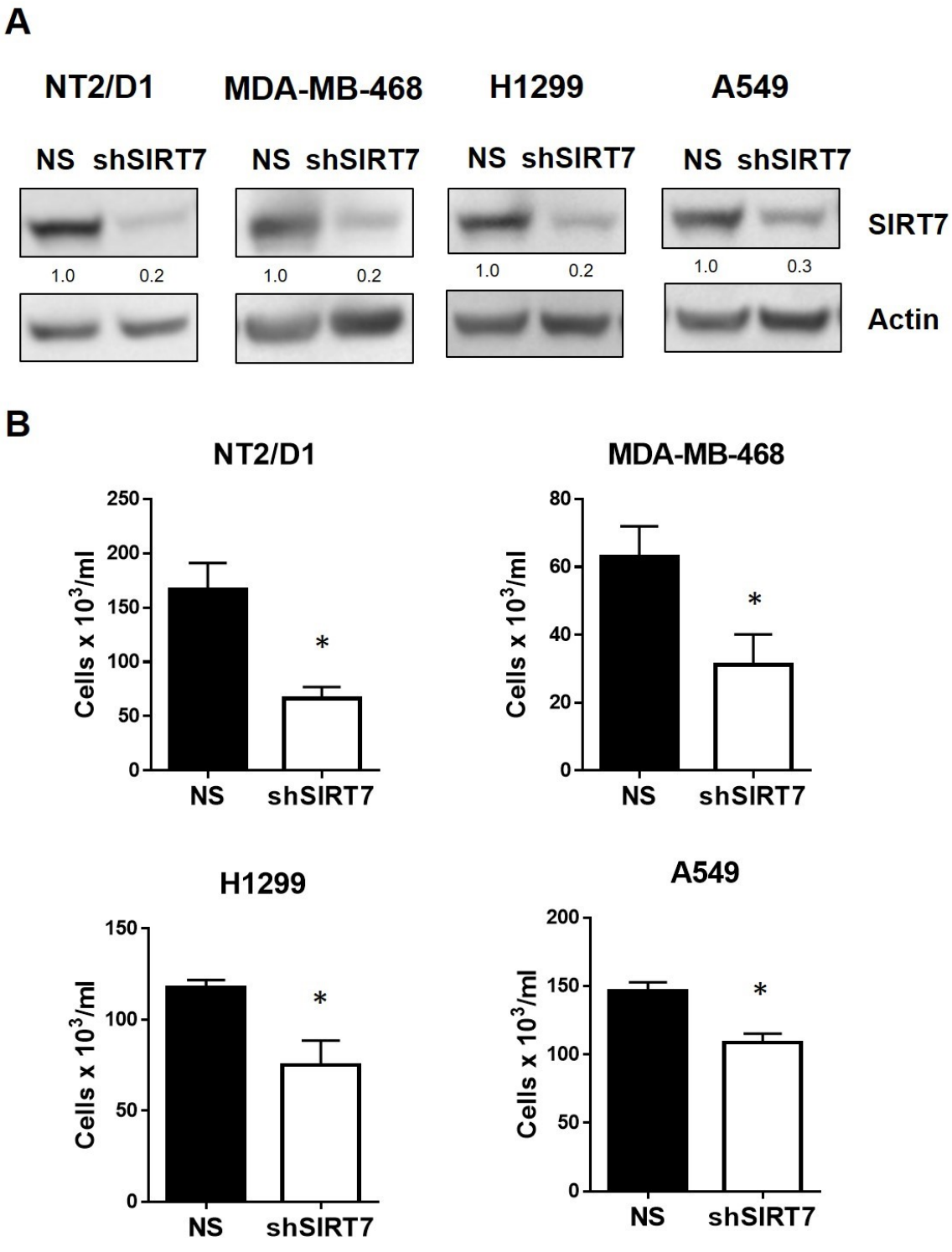
A
NT2/D1
MDA-MB-468
H1299
A549
NS shSIRT7
NS shSIRT7
NS shSIRT7
NS shSIRT7
1.0 0.2
1.0 0.2
1.0 0.2
1.0 0.3
SIRT7
Actin
B
NT2/D1
MDA-MB-468
H1299
A549
Cells x 10^3/ml
NS
shSIRT7
*

Figure 3.22

Figure 3.22. SIRT7 knockdown inhibits the proliferation of various cancer cells. (A) NT2/D1, MDA-MB-468, H1299, and A549 cells were transduced with shSIRT7 or control shRNA (NS). The levels of SIRT7 were detected by immunoblotting. (B) The number of viable cells were counted by trypan blue exclusion after 72 hours. Results shown as mean±SD, *p-value<0.05 obtained by a Student's t-test comparing the knockdown with NS control, n=3.

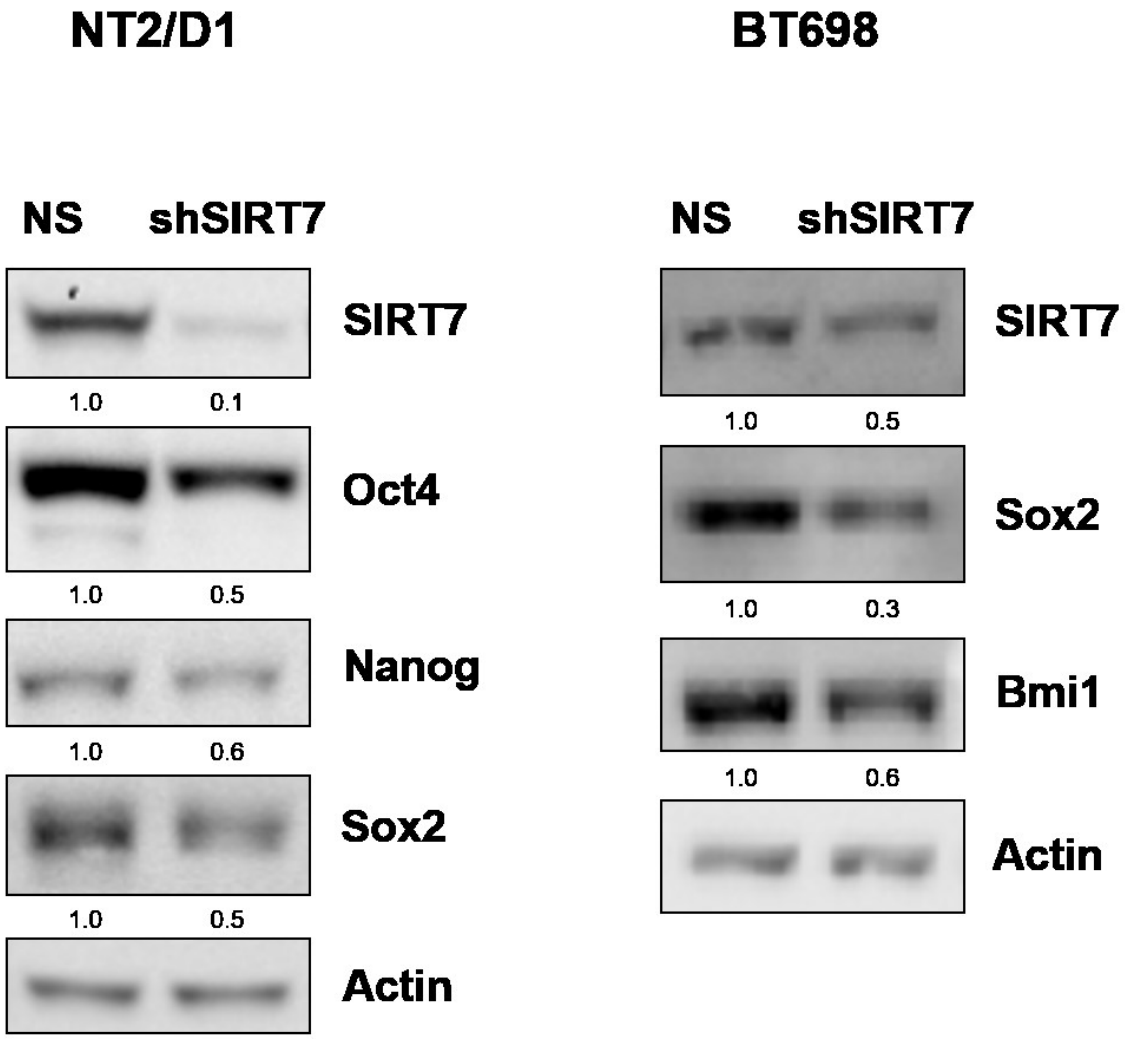

Figure 3.23. SIRT7 knockdown decreases expression of stemness markers in CSLCs. NT2/D1 and BT698 cells were transduced with shSIRT7 or control shRNA (NS). Whole cell lysates were subjected to SDS-PAGE and the levels of stemness markers (Oct4, Nanog, Sox2, and Bmi1) were detected by immunoblotting. Quantification of representative blot is shown from n=3 for NT2/D1 and n=1 for BT698.

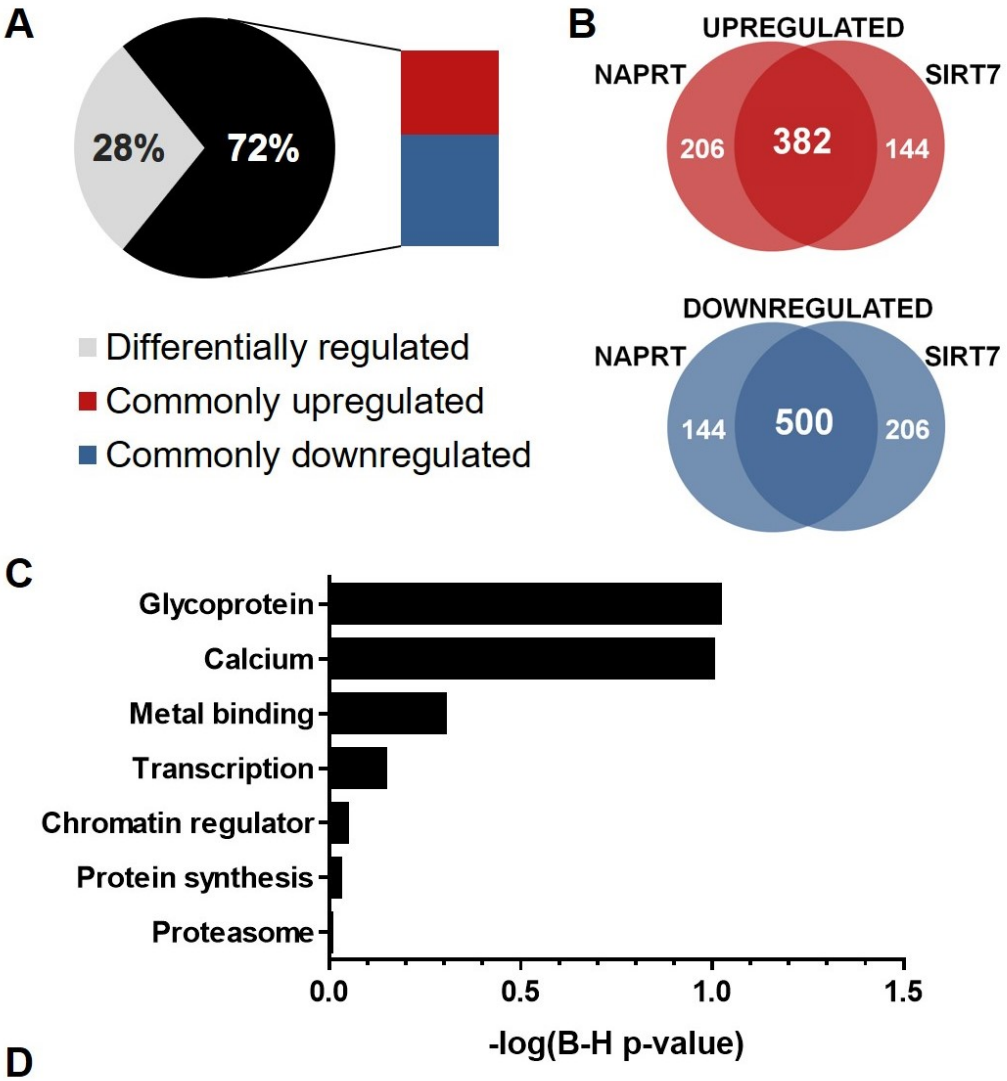
A
28%
72%
Differentially regulated
Commonly upregulated
Commonly downregulated
B
UPREGULATED
NAPRT
SIRT7
206
382
144
DOWNREGULATED
NAPRT
SIRT7
144
500
206
C
Glycoprotein
Calcium
Metal binding
Transcription
Chromatin regulator
Protein synthesis
Proteasome
0.0
0.5
1.0
1.5
-log(B-H p-value)
D
Transcription
NS
shNAPRT
shSIRT7
Proteasome
NS
shNAPRT
shSIRT7
0.08 0.16 0.24

Figure 3.24

Figure 3.24. Cells with NAPRT and SIRT7 knockdown share comparable proteomic profiles.

NT2/D1 cells that were transduced with shNAPRT, shSIRT7, or control shRNA (NS) were subjected to proteomics analysis, n=2. (A) Of the proteins which had significant changes in expression as compared to levels in control cells, 72% were commonly upregulated or downregulated by NAPRT and SIRT7 knockdown, while 28% were differentially regulated. (B) Venn diagram showing 382 proteins that were upregulated in both NAPRT and SIRT7 knockdown cells, 500 proteins that were downregulated in both NAPRT and SIRT7 knockdown cells, 206 proteins that were upregulated in NAPRT knockdown but downregulated in SIRT7 knockdown, and 144 proteins that were upregulated in SIRT7 knockdown but downregulated in NAPRT knockdown. (C) An integrated signature of the commonly regulated proteins was analyzed using DAVID software for pathway enrichment analysis. Enriched pathways are shown with bars representing –log(B-H adjusted p-values of the enriched pathway). (D) Mean relative expression of proteins from the integrated signature that belonged to a transcription or proteasome function were visualized by heatmaps generated by MEV software.

CHAPTER 4: DISCUSSION

Cancer is the leading cause of death and a tremendous healthcare burden worldwide, regardless of a country's economic development. Overall, the burden of cancer totaled 6.2 million deaths in 2000, 8.2 million in 2012, and 8.8 million in 2015.[165–167] This is expected to increase as the world population ages and adopts lifestyle behaviors that are risk factors. Lung cancer is the leading cause of cancer death due to the high number of cases and high fatality. Breast cancer, which has the second highest incidence rate, is the most prevalent cancer due to its relatively more favorable prognosis.[165,166] While cancer mortality has been on the decline over the past 20 years, it can largely be attributed to early diagnosis and reduced tobacco use, and is not necessarily an indication of advancements in cancer treatments.[168]

Despite the development of numerous cancer therapy agents, complete remission of cancer has remained difficult to attain. One reason that many cancer therapies are unsuccessful is due to the inherent heterogeneity of tumors. Cancer cells accumulate mutations due to their genetic instability, and consequently produce a variant of subpopulations within tumors. The diverse genetic profiles of cancer cells implicate that some populations will be susceptible to treatment, while others will be resistant and be able to withstand the selection pressure of therapy. Thus, the cancer does not only persist but will be composed of cells with increased fitness for survival.[169,170] Moreover, even in patients who achieve complete remission, where no evidence of cancer can be detected, a relapse of cancer can emerge years later.[152,171] A fundamental driver of these therapeutic challenges has relatively recently been explained by the existence of CSCs. CSCs are a small subpopulation of cancer cells that have stem-like activity such as self-renewal and high tumorigenicity.[170] They contribute to tumor heterogeneity through differentiation into diverse nontumorigenic cancer cells, and tend to be more resistant to therapy than their differentiated progeny.[172] For example, $CD44^{high}/CD24^{low}$ breast CSLCs are more resistant to docetaxel chemotherapy and the population of these CSLCs is enriched after treatment.[173] Similarly, thyroid carcinoma and colorectal CSLCs are less sensitive to doxorubicin and oxaliplatin than differentiated cancer cells.[174–176] The survival of these

CSLCs can lead to re-growth of the tumor, and the enrichment of these cells implicate that the cancer relapse will be resistant to the previously used therapy. [177]

For these reasons, it is important to better understand the molecular biology of CSCs so that therapies targeting them can be effectively designed to eradicate cancer. The stemness characteristic of CSLCs which distinguishes them from other cancer cells is ascribed to a transcriptional program that closely resembles that of ESCs. Induction of an ESC-like signature creates highly tumorigenic cells, supporting the function of these genes in the CSLC phenotype.[178] Moreover, tumors that fit an ESC-like profile are poorly differentiated, more aggressive, and are associated with poorer diagnosis. The molecular profile of these ESC-like tumors consists of targets of core stem cell-associated transcription factors (Oct4, Nanog, and Sox2) and Polycomb complex genes (Bmi1, Ezh2) which are also central to stem cell function.[23] Hence, the targeting of genes responsible for cancer stemness properties is a novel approach in cancer therapy. For example, inhibition of Stat3, a gene important for cancer stemness, was found to deplete the CSLC population and thereby prevent metastasis and relapse *in vivo*.[152] Inhibition of another protein involved in stemness, c-Met, was also shown to slow tumor growth and decrease the population of CSLCs.[179]

Studies on other aberrant pathways in CSCs are also important to yield novel therapeutic targets. A well-recognized hallmark of cancer is deregulated metabolism and related energetic pathways, among which is the Warburg effect. This phenomenon describes the preferential use of glycolysis in cancer cells, which is unusual given that OXPHOS is a more efficient energy production pathway. The reasons for this are thought to be for generation of glycolytic intermediates that can be used for growth, and because cancer cells may have impairments in their OXPHOS pathway.[43,45] Nevertheless, even in cancer cells that have defects in mitochondrial respiration, OXPHOS can also contribute to energy production. Furthermore, under certain environmental pressures, cancer cells may shift from a glycolytic phenotype to an OXPHOS phenotype.[43] In CSLCs, there is less consensus on which metabolic processes are preferred and it may depend on the tumor type.[180] Pancreatic and glioma CSLCs have been shown to express more mitochondrial genes and depend more on OXPHOS than glycolysis.[181–183] In contrast,

studies of breast and lung cancers showed that CSLCs had higher glycolysis activity than non-CSLCs.[184,185] Due to the likely plasticity of CSLCs and differentiated cancer cells to utilize additional metabolic pathways, therapeutic strategies that can target both glycolysis and OXPHOS may be beneficial. NAD^+ and its reduced form, NADH, participate as redox molecules in both of these energy production pathways. In glycolysis, NAD^+ is required to produce 1,3-BPG and is converted to NADH, which is then used during OXPHOS to help establish a proton gradient across the mitochondrial membrane.[61] Metformin has been shown to prevent cancer cell proliferation by inhibiting the regeneration of NAD^+ at complex I, affecting cellular respiration and aspartate synthesis.[186,187] In the present study, NAPRT is investigated as a potential therapeutic target. NAPRT is one of the enzymes involved in the synthesis of NAD^+, which is a molecule required for both glycolysis and OXPHOS. Among the NAD^+-synthesizing enzymes, extensive studies have been conducted on NAMPT, which have revealed its roles in cancer malignancy and led to the development of pharmaceutical inhibitors. Remarkably, NAPRT has not been given due consideration and has been scarcely studied in cancer, possibly overlooking its importance in cellular processes and its potential for anticancer therapeutic modulation.

Here, NT2/D1 embryonic carcinoma cells (which have a molecular resemblance to the ESC-like stemness signature), HMLER-shEcad breast cancer cells (which have EMT-induced stem cell properties), and BT698 patient-derived BTICs were used to investigate the role of NAPRT in CSLCs. It was demonstrated that the consequence of knocking down NAPRT in NT2/D1 and HMLER-shEcad cells was significant enough to affect cell proliferation, inducing senescence or promoting cell death in different subsets of cells. Expression of stemness markers was reduced following NAPRT knockdown in CSLC models, including in patient-derived BT698 cells. Accompanying loss of stemness was an increase in differentiation markers. A plausible mechanism for these NAPRT-related effects was identified to be via the regulation of SIRT7.

In line with their stemness features, CSCs have mechanisms that make them more resistant to therapy. To effectively treat cancer, CSC properties such as self-renewal and lack of differentiation need to be targeted.[188,189] NAPRT knockdown in three CSLC

models (NT2/D1, HLMER-shEcad, and BT698 cells) decreased the expression of critical transcriptional factors involved in stemness (Oct4, Nanog, Sox2, and Bmi1, as applicable).[23] Indeed, the ability to form tumorspheres, which is one of the accepted measures of stemness,[190] was diminished following NAPRT knockdown in NT2/D1 and HMLER-shEcad cells. The inhibition of stem cell markers has been demonstrated as a relevant strategy to target CSCs. Knockdown of Sox2 in skin tumors decreased their ability to initiate tumors during serial transplantations, and deletion of Sox2 in pre-existing tumors resulted in their drastic regression *in vivo*.[191] In pancreatic cancer cells, double knockdown of Oct4 and Nanog reduced the tumorigenesis and chemoresistance of CSLCs.[192] Similarly, Bmi1 inhibition has also been demonstrated to be an attractive strategy against CSLCs, due to its role in self-renewal, viability, and proliferation. Transient treatment using a Bmi1 inhibitor was sufficient to irreversibly decrease the tumor initiating capacity of colorectal CSLCs *in vivo*.[193] These studies confirm Oct4, Nanog, Sox2, and Bmi1 as regulators of CSLCs and suggest that treatments that can affect stemness markers, such as depletion of NAPRT, can also control tumor growth and be valuable anticancer approaches.

Interestingly, such loss of stemness in NAPRT knockdown cells was accompanied with increase in differentiation. NT2/D1 cells differentiated towards a neuronal lineage, while HMLER-shEcad cells differentiated towards to a mammary epithelial lineage. The potential of differentiation induction as a strategy to eliminate CSLC stemness has been used for decades with retinoic acid, which continues to be the standard of care for acute promyelocytic leukemia.[180] Retinoic acid was also shown to induce differentiation of glioblastoma CSCLs, which decreased their migratory and angiogenic activity, and reduced their tumorigenicity *in vivo*.[194] The value of differentiation therapy was again demonstrated by BMP4, a neural stem cell regulator that triggered glioblastoma CSLCs differentiation, depleting their population and hindering tumorigenicity.[195] Inducing CSC differentiation causes them to lose stemness and malignancy-related properties that make them chemoresistant, rendering them more susceptible to further treatments. For example, use of differentiation-inducing agents shows great potential in combination therapies that can increase the efficacy of cytotoxic compounds such as 5-fluorouracil.[196,197]

Autophagy has emerged as an important process in cancer, although its specific roles in tumor suppression or tumorigenesis are still unclear.[53] Given the links between autophagy and many aspects of cancer metabolism, current research recognizes the potential of modulating autophagy to target cancer cells.[198] From its role in Ras transformation to sustaining glycolysis and mitochondrial metabolism, autophagy is implicated in both tumor initiation and tumor maintenance.[199] Inhibition of autophagy in certain settings can hinder cancer cell growth or tumor growth *in vivo*.[198] Autophagy can also help cells adapt to metabolic stresses such as nutrient or oxygen deprivation, which are conditions that may be created from administration of therapies.[200] For example, colorectal CSLCs have resisted chemotherapy-induced apoptosis by promoting autophagy, resulting in enrichment of the CSLC population.[56] In contrast, induction of autophagic cell death is also a valuable therapeutic method.[200] Thus, understanding the role of autophagy in cancer is important for exploiting it as the primary treatment method, and knowing how cancer cells use autophagy as a compensatory mechanism during treatment can help us devise more effective therapeutic strategies to avert this response.

Basal autophagy under normal nutrient-rich conditions functions to maintain homeostasis, selectively eliminating protein aggregates and organelles. The inclusion of specific cargo into autophagosomes is mediated by adaptor proteins such as SQSTM1, which recognizes cargo that is tagged by ubiquitin and links them to LC3 proteins on the autophagosome.[201] During nutrient deprivation, the autophagy process becomes more nonselective and degrades bulk cytoplasmic constituents to be recycled.[201] As a deficiency in NAPRT likely disrupts cellular energetics, it was expected that cells would respond to the stress with induction of autophagy. In both NT2/D1 and HMLER-shEcad cells, a turnover of SQSTM1 could be detected under basal conditions, relating to the upkeep of the cell. Following NAPRT knockdown, the turnover of SQSTM1 was not only reduced, but its levels in the untreated knockdown cells indicate that SQSTM1 was perhaps downregulated at a transcriptional level. This indicated that selective autophagy facilitated by SQSTM1 was decreased, which can be consistent with a stress response. However, the overall autophagy data suggested that classic starvation-induced autophagy was not necessarily occurring following NAPRT knockdown. In NT2/D1 cells, both autophagy activity and activation of autophagic machinery were decreased following

NAPRT knockdown, as indicated by the reduced flux and cumulative autophagy protein levels. Conversely, in HMLER-shEcad cells, NAPRT knockdown promoted autophagic flux but did not additionally upregulate autophagic machinery. Thus, NAPRT knockdown in NT2/D1 and HMLER-shEcad cells stimulated different autophagic responses. This could be explained by the varying levels of basal autophagy and sensitivity to induce autophagy between cell lines.

In order to exploit the autophagic response during NAPRT knockdown, its role in certain cancers and its relation to cell death need to be better understood. Despite the differential regulation of autophagy in shNAPRT cells, the evidence showing that both NT2/D1 and HMLER-shEcad cells underwent cell death could signify that both autophagic responses failed to act as a survival mechanism. In NT2/D1 shNAPRT cells, the reduction in autophagic machinery could be confirmed at the transcriptional level, probing for autophagy related genes (ATGs). If further investigation reveals the mechanism by which autophagy suppression occurs, such as signaling via mTOR, mTOR could be inhibited to determine whether restoration of autophagy circumvents cell death. This would provide insight on whether the loss of NT2/D1 cell viability was due to a failure in activating the survival functions of autophagy during NAPRT knockdown. Alternatively, to clarify whether autophagy downregulation served as a coping mechanism, autophagy could be further inhibited in NAPRT knockdown cells by depleting ATGs. If cells are protected against cell death, it can be hypothesized that autophagy was downregulated in an effort to prevent autophagic cell death. Similarly, in HMLER-shEcad cells with NAPRT knockdown, autophagy could be related to cell death if the levels of autophagy were insufficient to cope with the energy stress. It also remains possible that autophagic cell death was involved even without any excessive autophagy degradation observed. Thus, investigation of autophagy in HMLER-shEcad cells could be approached in a similar method as in NT2/D1, where mTOR inhibition is used to further induce autophagy and measure its protective or destructive effects in NAPRT knockdown cells.

Furthermore, the effect of autophagy manipulation can be investigated concomitantly with the regulation of senescence. In many cancer models, autophagy has

been shown to have a positive correlation with senescence, whereby inhibition of autophagy delays senescence. It is speculated that autophagy can serve a protective role to divert cells towards senescence instead of cell death.[202] On the other hand, inhibition of autophagy in normal stem cells promoted senescence, although the downregulation of autophagy in that study was not in response to another treatment.[203] Supporting these studies is one conducted in NT2/D1 cells which showed that any disruption in autophagy induces senescence.[60] How autophagy regulates cell death and senescence appears to be complex and cell type-dependent.

The aim of cancer therapies is to either promote cytotoxicity or arrest cancer cell growth to stop their spread. Senescence and apoptosis are both common cell responses to prevent transformation, but the processes can be deregulated in transformed cells.[188,204] Although apoptosis seems to be the more effective anticancer mechanism, senescence also has its own advantages. Cytotoxic treatments may cause more severe side effects in cancer patients than senescence, which is the pathway initiated by cells when the damage imposed is insufficient.[204,205] The principle of invoking senescence is to facilitate tumor clearance by the host's immune system, whereas apoptosis does not initiate an immune response.[205] Furthermore, if only a limited number of cells will be affected by the treatment, senescence-elicited mobilization of immune response will be more effective for tumor clearance as cells neighboring senescent cells can be induced via paracrine signaling to also senescence.[204–206] Modulation of p53 in liver cancer was shown to result in complete tumor regression *in vivo*, not through apoptosis but through the senescence program.[207] NAPRT knockdown in NT2/D1 induced senescence in the majority of cells, and promoted cell death in a subset of cells, as evidenced by the detection of cleaved Caspase-3 and the staining of Annexin V. Because there are Caspase-3-independent modes of apoptosis and Caspase-3 may also function in other processes such as differentiation, its involvement in cell death and differentiation should be confirmed by treating NAPRT knockdown cells with Caspase inhibitor.[146,159] In HMLER-shEcad cells, NAPRT knockdown also promoted cell death, and the effect was even more drastic than in NT2/D1 cells. Overall, the findings show that NAPRT knockdown can mediate tumor-suppressing effects through different modes of irreversible growth inhibition.

Given the function of NAPRT as a NAD^+-synthesizing enzyme, it was expected that NAD^+ levels would be affected following NAPRT knockdown. To elucidate the mechanism by which NAPRT regulates CSLC processes, the consequence of NAPRT knockdown on NAD^+-dependent enzymes was examined. Specifically, SIRTs have extensive regulatory roles in cancer cell processes,[109] and may act as downstream effectors of NAPRT knockdown-related effects. Indeed, it was revealed that some NAPRT-related effects were possibly mediated by SIRT7. Among proteins that were regulated in common by NAPRT or SIRT7 knockdown were those associated with chromatin regulation, which corresponds to the nuclear localization of NAPRT and SIRT7. While the role of SIRT7 in cancer has been controversial for some time, its oncogenic properties are becoming clearer as its specific targets and mechanisms of function are being discovered. SIRT7 deacetylates lysine 18 of histone H3 (H3K18Ac) on the promoters of a set of genes linked to tumor suppression, resulting in their transcriptional repression. SIRT7 hence maintains the malignant phenotype of cancer cells, and knockdown of SIRT7 in U251 glioblastoma drastically inhibits tumor formation *in vivo*.[208] Notably, hypoacetylation of H3K18Ac is associated with higher cancer recurrence and poorer survival in prostate, lung, and kidney cancers.[209]

Of note, the integrated proteomic signature of NAPRT and SIRT7 knockdown cells also showed that the proteasome pathway was enriched. This is in accordance with the role of SIRT7 in the unfolded protein response (UPR), where misfolded proteins are degraded via the ubiquitin-proteasome pathway or via autophagy.[210] Thus, an investigation of the proteasome activity, with the regulation of autophagy, in NAPRT knockdown cells could be interesting. Selective autophagy was observed to be decreased, which could be due to a decrease in total ubiquitin-tagged protein substrates. However, given that the integrated signature of NAPRT and SIRT7 showed upregulation of several proteasomal proteins, it is more likely that protein aggregates were being directed from the autophagic pathway towards the proteasomal pathway for degradation instead. Nonetheless, an increased requirement for proteasomal degradation following NAPRT knockdown is an indication of increased cellular stress.

The regulation of NAPRT on SIRT7 should be further studied, including an investigation of whether NAPRT and SIRT7 mutually regulate each other. Since both proteins reside in the nucleus, a mechanism of regulation could be either direct or indirect transcription of relevant genes. While SIRT7 can exert transcriptional repression, NAPRT has not been shown to act as a transcription factor.[110] It is possible that the relationship between NAPRT and SIRT7 is similar to the regulation between NAMPT and SIRT1. NAMPT indirectly affects the activity of SIRT1 through the production of NAD^+. In turn, SIRT1 regulates NAMPT transcription via circadian clock proteins.[211] In this study, the expression levels of SIRT7 were affected by NAPRT knockdown, which could also be a feedback regulation from inhibition of NAD^+ production. The results from NAMN addition indeed suggest that the effects of NAPRT knockdown are related to reduced NAD^+ levels. To clarify the role and regulation of SIRT7, chromatin immunoprecipitation (ChIP) assays can be performed, along with examination of NAD^+ levels and additional rescue experiments to restore the NAD^+ content.

Finally, the minimal effects of NAPRT knockdown in normal cells were a good indication that a therapeutic strategy targeting NAPRT could have limited toxicity, at least to the breast tissue. However, the main toxic effect of NAMPT inhibitors was on hematopoietic cells that were more rapidly proliferating.[91] Interestingly, the expression levels of NAMPT and NAPRT in these cells suggest that NAPRT inhibition could be slightly better tolerated. While protein expression of both enzymes is low in the bone marrow, the RNA expression of NAMPT is 387.2 transcripts per million (TPM), while that of NAPRT is much lower at 9.6 TPM.[212,213] If hematopoietic cells do not have a dependency on NAPRT, then NAPRT inhibition should not affect them adversely. However, the effects of NAPRT inhibition on normal stem cells should be formally investigated to predict its clinical outcomes.

4.1 Limitations of Study and Future Directions

The field of CSCs is growing as researchers acknowledge the implications of these putative tumor-initiating cells in clinical settings. Yet, the research also remains controversial as there is no collective agreement on the exact definitions, appropriate models, and identification of CSLCs.[214]

All models have limitations in addition to their usefulness. The advantages of the current CSLC models in this study have already been presented, so their limitations will now be discussed. NT2/D1 and HMLER-shEcad cells are established cell lines which were immortalized for culturing *in vitro* and thus may have acquired additional mutations that stray from the original tumor. While patient-derived BTICs better reflect the properties of the original tumor and are more physiologically relevant, there can be large variation between cells from different patients and thus experiments must be repeated with multiple primary cells. Moreover, the current identification of BTICs hinges on their expression of CD133, which has been questioned as a CSLC marker as some studies have found that $CD133^-$ cancer cells were also able to initiate tumors *in vivo* with comparable efficiency.[215,216] While this study was not focused on demonstrating the difference between CSLCs and non-CSLCs, inclusion of $CD133^{low}$ BTICs can strengthen the conclusion that NAPRT should be considered as a therapeutic target. In view of the limitations with individual CSLC models, it would be beneficial to employ an even wider array of CSLC models, in order to obtain a comprehensive idea of NAPRT regulation on cancer stemness.

The gold standard to confirm the identity of CSCs is a serial transplantation assay. Obviously, future experiments that must be performed for the study of NAPRT and cancer stemness involve extensive validation of the findings by *in vivo* injections of the cells. There has been some debate about the accuracy of measuring CSC frequency using xenografts, as some studies have proposed that the tumor-initiating capacity of a cell is a reflection of its ability to adapt to a foreign environment.[217,218] Nonetheless, the definition of a CSC is not dependent on its frequency in a population and the tumor-initiating cells continue to have unique properties that make them important to study.[219]

Another consideration that must be taken into account is that the CSC population in a tumor is not fixed and their plasticity makes it a further challenge for cancer treatment.[170] It has been reported that differentiated cancer cells can dedifferentiate into CSLCs.[220,221] If treatment was specifically targeted towards CSLCs, then the plasticity of the bulk cancer cells would replenish the CSLC population and reconstitute the tumor. It is therefore imperative that therapeutic strategies are designed to be effective against both

CSLCs and differentiated cancer cell types. The findings of this study demonstrated that NAPRT is a novel therapeutic target and that its modulation already has the potential to impact both cell populations. To further develop NAPRT as a therapeutic strategy, combination therapies should be explored to mitigate the effects of cancer cell plasticity and more effectively treat the cancer in a concerted fashion. Overall, the possibilities of inhibiting NAPRT in cancer represent valuable therapeutic approaches that have the potential to target not only CSLCs but their differentiated progeny as well.

REFERENCES

1. Cooper, G. M. The Development and Causes of Cancer. in *The Cell: A Molecular Approach. 2nd edition* (Sinauer Associates, 2000).

2. Cancer statistics at a glance. *Canadian Cancer Society* Available at: http://www.cancer.ca/en/cancer-information/cancer-101/cancer-statistics-at-a-glance/?region=on. (Accessed: 28th February 2018)

3. Hanahan, D. & Weinberg, R. A. Hallmarks of Cancer: The Next Generation. *Cell* **144,** 646–674 (2011).

4. Hanahan, D. & Weinberg, R. A. The Hallmarks of Cancer. *Cell* **100,** 57–70 (2000).

5. Dagogo-Jack, I. & Shaw, A. T. Tumour heterogeneity and resistance to cancer therapies. *Nat. Rev. Clin. Oncol.* (2017). doi:10.1038/nrclinonc.2017.166

6. Kreso, A. & Dick, J. E. Evolution of the Cancer Stem Cell Model. *Cell Stem Cell* **14,** 275–291 (2014).

7. Vermeulen, L. *et al.* Single-cell cloning of colon cancer stem cells reveals a multi-lineage differentiation capacity. *Proc. Natl. Acad. Sci.* **105,** 13427–13432 (2008).

8. Visvader, J. E. & Lindeman, G. J. Cancer stem cells in solid tumours: accumulating evidence and unresolved questions. *Nat. Rev. Cancer* **8,** 755–768 (2008).

9. Clarke, M. F. *et al.* Cancer Stem Cells—Perspectives on Current Status and Future Directions: AACR Workshop on Cancer Stem Cells. *Cancer Res.* **66,** 9339–9344 (2006).

10. Hermann, P. C. *et al.* Distinct Populations of Cancer Stem Cells Determine Tumor Growth and Metastatic Activity in Human Pancreatic Cancer. *Cell Stem Cell* **1,** 313–323 (2007).

11. Atlasi, Y., Looijenga, L. & Fodde, R. Cancer Stem Cells, Pluripotency, and Cellular Heterogeneity. in *Current Topics in Developmental Biology* **107,** 373–404 (Elsevier, 2014).

12. Nguyen, L. V., Vanner, R., Dirks, P. & Eaves, C. J. Cancer stem cells: an evolving concept. *Nat. Rev. Cancer* **12,** 133–143 (2012).

13. Bonnet, D. & Dick, J. E. Human acute myeloid leukemia is organized as a hierarchy that originates from a primitive hematopoietic cell. *Nat. Med.* **3,** 730–737 (1997).

14. Singh, S. K. *et al.* Identification of a cancer stem cell in human brain tumors. *Cancer Res.* **63,** 5821–5828 (2003).

15. Al-Hajj, M., Wicha, M. S., Benito-Hernandez, A., Morrison, S. J. & Clarke, M. F. Prospective identification of tumorigenic breast cancer cells. *Proc. Natl. Acad. Sci.* **100,** 3983–3988 (2003).

16. O'Brien, C. A., Pollett, A., Gallinger, S. & Dick, J. E. A human colon cancer cell capable of initiating tumour growth in immunodeficient mice. *Nature* **445,** 106–110 (2007).

17. Stewart, J. M. *et al.* Phenotypic heterogeneity and instability of human ovarian tumor-initiating cells. *Proc. Natl. Acad. Sci.* **108,** 6468–6473 (2011).

18. McDonald, S. A. C., Graham, T. A., Schier, S., Wright, N. A. & Alison, M. R. Stem cells and solid cancers. *Virchows Arch.* **455,** 1–13 (2009).

19. Rosland, G. V. *et al.* Long-term Cultures of Bone Marrow-Derived Human Mesenchymal Stem Cells Frequently Undergo Spontaneous Malignant Transformation. *Cancer Res.* **69,** 5331–5339 (2009).

20. Foreman, K. E., Rizzo, P., Osipo, C. & Miele, L. The Cancer Stem Cell Hypothesis. in *Stem Cells and Cancer* (eds. Teicher, B. A. & Bagley, R. G.) 3–14 (Humana Press, 2009). doi:10.1007/978-1-60327-933-8_1

21. Wang, P., Wan, W., Xiong, S.-L., Feng, H. & Wu, N. Cancer stem-like cells can be induced through dedifferentiation under hypoxic conditions in glioma, hepatoma and lung cancer. *Cell Death Discov.* **3,** 16105 (2017).

22. Auffinger, B. *et al.* Conversion of differentiated cancer cells into cancer stem-like cells in a glioblastoma model after primary chemotherapy. *Cell Death Differ.* **21,** 1119–1131 (2014).

23. Ben-Porath, I. *et al.* An embryonic stem cell–like gene expression signature in poorly differentiated aggressive human tumors. *Nat. Genet.* **40,** 499–507 (2008).

24. Boyer, L. A. *et al.* Core Transcriptional Regulatory Circuitry in Human Embryonic Stem Cells. *Cell* **122,** 947–956 (2005).

25. Takahashi, K. & Yamanaka, S. Induction of Pluripotent Stem Cells from Mouse Embryonic and Adult Fibroblast Cultures by Defined Factors. *Cell* **126,** 663–676 (2006).

26. Kim, J. B. *et al.* Oct4-Induced Pluripotency in Adult Neural Stem Cells. *Cell* **136,** 411–419 (2009).

27. Liu, A., Yu, X. & Liu, S. Pluripotency transcription factors and cancer stem cells: small genes make a big difference. *Chin. J. Cancer* (2013). doi:10.5732/cjc.012.10282

28. Hu, T. *et al.* Octamer 4 Small Interfering RNA Results in Cancer Stem Cell-Like Cell Apoptosis. *Cancer Res.* **68,** 6533–6540 (2008).

29. Lin, Y. *et al.* Reciprocal Regulation of Akt and Oct4 Promotes the Self-Renewal and Survival of Embryonal Carcinoma Cells. *Mol. Cell* **48,** 627–640 (2012).

30. Kim, R.-J. & Nam, J.-S. OCT4 Expression Enhances Features of Cancer Stem Cells in a Mouse Model of Breast Cancer. *Lab. Anim. Res.* **27,** 147 (2011).

31. Jeter, C. R. *et al.* NANOG promotes cancer stem cell characteristics and prostate cancer resistance to androgen deprivation. *Oncogene* **30,** 3833–3845 (2011).

32. Jia, X. *et al.* SOX2 promotes tumorigenesis and increases the anti-apoptotic property of human prostate cancer cell. *J. Mol. Cell Biol.* **3,** 230–238 (2011).

33. Chang, C.-C. *et al.* Oct-3/4 Expression Reflects Tumor Progression and Regulates Motility of Bladder Cancer Cells. *Cancer Res.* **68,** 6281–6291 (2008).

34. Chou, Y.-T. *et al.* The Emerging Role of SOX2 in Cell Proliferation and Survival and Its Crosstalk with Oncogenic Signaling in Lung Cancer: SOX2 Regulates EGFR and BCL2L1 Signaling. *STEM CELLS* **31,** 2607–2619 (2013).

35. Wang, D. *et al.* Oct-4 and nanog promote the epithelial-mesenchymal transition of breast cancer stem cells and are associated with poor prognosis in breast cancer patients. *Oncotarget* **5,** (2014).

36. Liu, G. *et al.* Analysis of gene expression and chemoresistance of CD133+ cancer stem cells in glioblastoma. *Mol. Cancer* **5,** 67 (2006).

37. Frank, N. Y. *et al.* ABCB5-Mediated Doxorubicin Transport and Chemoresistance in Human Malignant Melanoma. *Cancer Res.* **65,** 4320–4333 (2005).

38. Mathews, L. A. *et al.* Increased Expression of DNA Repair Genes in Invasive Human Pancreatic Cancer Cells: *Pancreas* **40,** 730–739 (2011).

39. Singh, A. K. *et al.* Tumor heterogeneity and cancer stem cell paradigm: Updates in concept, controversies and clinical relevance: Tumor Heterogeneity and CSC Paradigm. *Int. J. Cancer* **136,** 1991–2000 (2015).

40. Jordan, C. T. Cancer Stem Cells: Controversial or Just Misunderstood? *Cell Stem Cell* **4,** 203–205 (2009).

41. Peacock, C. D. *et al.* Hedgehog signaling maintains a tumor stem cell compartment in multiple myeloma. *Proc. Natl. Acad. Sci.* **104,** 4048–4053 (2007).

42. Yuan, H.-X., Xiong, Y. & Guan, K.-L. Nutrient Sensing, Metabolism, and Cell Growth Control. *Mol. Cell* **49,** 379–387 (2013).

43. Zheng, J. Energy metabolism of cancer: Glycolysis versus oxidative phosphorylation (Review). *Oncol. Lett.* **4,** 1151–1157 (2012).

44. Alberts, B. *et al.* How Cells Obtain Energy from Food. in *Molecular Biology of the Cell. 4th edition* (Garland Science, 2002).

45. Liberti, M. V. & Locasale, J. W. The Warburg Effect: How Does it Benefit Cancer Cells? *Trends Biochem. Sci.* **41,** 211–218 (2016).

46. Vander Heiden, M. G., Cantley, L. C. & Thompson, C. B. Understanding the Warburg Effect: The Metabolic Requirements of Cell Proliferation. *Science* **324,** 1029–1033 (2009).

47. Altomare, D. A. & Testa, J. R. Perturbations of the AKT signaling pathway in human cancer. *Oncogene* **24,** 7455–7464 (2005).

48. Jin, F. *et al.* The miR-125a/HK2 axis regulates cancer cell energy metabolism reprogramming in hepatocellular carcinoma. *Sci. Rep.* **7,** (2017).

49. Dupuy, F. *et al.* PDK1-Dependent Metabolic Reprogramming Dictates Metastatic Potential in Breast Cancer. *Cell Metab.* **22,** 577–589 (2015).

50. He, C.-L. *et al.* Pyruvate Kinase M2 Activates mTORC1 by Phosphorylating AKT1S1. *Sci. Rep.* **6,** (2016).

51. DeBerardinis, R. J. & Chandel, N. S. Fundamentals of cancer metabolism. *Sci. Adv.* **2,** e1600200–e1600200 (2016).

52. Glick, D., Barth, S. & Macleod, K. F. Autophagy: cellular and molecular mechanisms. *J. Pathol.* **221,** 3–12 (2010).

53. Mathew, R., Karantza-Wadsworth, V. & White, E. Role of autophagy in cancer. *Nat. Rev. Cancer* **7,** 961–967 (2007).

54. Gong, C. *et al.* Beclin 1 and autophagy are required for the tumorigenicity of breast cancer stem-like/progenitor cells. *Oncogene* **32,** 2261–2272 (2013).

55. Galavotti, S. *et al.* The autophagy-associated factors DRAM1 and p62 regulate cell migration and invasion in glioblastoma stem cells. *Oncogene* **32,** 699–712 (2013).

56. Yang, H.-Z. *et al.* Autophagy contributes to the enrichment and survival of colorectal cancer stem cells under oxaliplatin treatment. *Cancer Lett.* **361,** 128–136 (2015).

57. Debnath, J., Baehrecke, E. H. & Kroemer, G. Does autophagy contribute to cell death? *Autophagy* **1,** 66–74 (2005).

58. Singh, B. N., Kumar, D., Shankar, S. & Srivastava, R. K. Rottlerin induces autophagy which leads to apoptotic cell death through inhibition of PI3K/Akt/mTOR pathway in human pancreatic cancer stem cells. *Biochem. Pharmacol.* **84,** 1154–1163 (2012).

59. Liang, X. H. *et al.* Induction of autophagy and inhibition of tumorigenesis by beclin 1. *Nature* **402,** 672–676 (1999).

60. Sharif, T. *et al.* Autophagic homeostasis is required for the pluripotency of cancer stem cells. *Autophagy* **13,** 264–284 (2017).

61. Cantó, C., Menzies, K. J. & Auwerx, J. NAD+ Metabolism and the Control of Energy Homeostasis: A Balancing Act between Mitochondria and the Nucleus. *Cell Metab.* **22,** 31–53 (2015).

62. Maayan, M. L. Nad+-Glycohydrolase of Thyroid Homogenates. *Nature* **204,** 1169–1170 (1964).

63. Borradaile, N. M., Watson, A. & Pickering, J. G. Regeneration and Aging: Regulation by Sirtuins and the NAD+ Salvage Pathway. in *Regenerative Nephrology* 289–298 (Elsevier, 2011). doi:10.1016/B978-0-12-380928-5.10019-3

64. Imai, S., Armstrong, C. M., Kaeberlein, M. & Guarente, L. Transcriptional silencing and longevity protein Sir2 is an NAD-dependent histone deacetylase. *Nature* **403,** 795–800 (2000).

65. Berger, F. The new life of a centenarian: signalling functions of NAD(P). *Trends Biochem. Sci.* **29,** 111–118 (2004).

66. Terzi, M. Y., Izmirli, M. & Gogebakan, B. The cell fate: senescence or quiescence. *Mol. Biol. Rep.* **43,** 1213–1220 (2016).

67. López-Otín, C., Blasco, M. A., Partridge, L., Serrano, M. & Kroemer, G. The Hallmarks of Aging. *Cell* **153,** 1194–1217 (2013).

68. Imai, S. & Guarente, L. It takes two to tango: NAD+ and sirtuins in aging/longevity control. *Npj Aging Mech. Dis.* **2,** (2016).

69. Zhang, H. *et al.* NAD+ repletion improves mitochondrial and stem cell function and enhances life span in mice. *Science* **352,** 1436–1443 (2016).

70. Bogan, K. L. & Brenner, C. Nicotinic Acid, Nicotinamide, and Nicotinamide Riboside: A Molecular Evaluation of NAD $^{+}$ Precursor Vitamins in Human Nutrition. *Annu. Rev. Nutr.* **28,** 115–130 (2008).

71. Chen, Y. & Guillemin, G. J. Kynurenine pathway metabolites in humans: disease and healthy States. *Int. J. Tryptophan Res. IJTR* **2,** 1–19 (2009).

72. Dai, X. & Zhu, B. T. Indoleamine 2,3-dioxygenase tissue distribution and cellular localization in mice: implications for its biological functions. *J. Histochem. Cytochem. Off. J. Histochem. Soc.* **58,** 17–28 (2010).

73. Wu, W. *et al.* Expression of Tryptophan 2,3-Dioxygenase and Production of Kynurenine Pathway Metabolites in Triple Transgenic Mice and Human Alzheimer's Disease Brain. *PLoS ONE* **8,** e59749 (2013).

74. Houtkooper, R. H., Cantó, C., Wanders, R. J. & Auwerx, J. The Secret Life of NAD+: An Old Metabolite Controlling New Metabolic Signaling Pathways. *Endocr. Rev.* **31,** 194–223 (2010).

75. Chiarugi, A., Dölle, C., Felici, R. & Ziegler, M. The NAD metabolome — a key determinant of cancer cell biology. *Nat. Rev. Cancer* **12,** 741 (2012).

76. Bieganowski, P. & Brenner, C. Discoveries of Nicotinamide Riboside as a Nutrient and Conserved NRK Genes Establish a Preiss-Handler Independent Route to NAD+ in Fungi and Humans. *Cell* **117,** 495–502 (2004).

77. Nikiforov, A., Dölle, C., Niere, M. & Ziegler, M. Pathways and Subcellular Compartmentation of NAD Biosynthesis in Human Cells FROM ENTRY OF EXTRACELLULAR PRECURSORS TO MITOCHONDRIAL NAD GENERATION. *J. Biol. Chem.* **286,** 21767–21778 (2011).

78. Cole, J. *et al.* Novel NAPRT specific antibody identifies small cell lung cancer and neuronal cancers as promising clinical indications for a NAMPT inhibitor/niacin co-administration strategy. *Oncotarget* **8,** (2017).

79. Preiss, J. & Handler, P. Biosynthesis of diphosphopyridine nucleotide. I. Identification of intermediates. *J. Biol. Chem.* **233,** 488–492 (1958).

80. Tsubota, K. The first human clinical study for NMN has started in Japan. *Npj Aging Mech. Dis.* **2,** (2016).

81. Hasmann, M. & Schemainda, I. FK866, a highly specific noncompetitive inhibitor of nicotinamide phosphoribosyltransferase, represents a novel mechanism for induction of tumor cell apoptosis. *Cancer Res.* **63,** 7436–7442 (2003).

82. Watson, M. *et al.* The Small Molecule GMX1778 Is a Potent Inhibitor of NAD+ Biosynthesis: Strategy for Enhanced Therapy in Nicotinic Acid Phosphoribosyltransferase 1-Deficient Tumors. *Mol. Cell. Biol.* **29,** 5872–5888 (2009).

83. Lucena-Cacace, A., Otero-Albiol, D., Jimenez-Garcia, M. p, Muñoz-Galvan, S. & Carnero, A. NAMPT is a Potent Oncogene in Colon Cancer Progression that Modulates Cancer Stem Cell Properties and resistance to therapy through Sirt1 and PARP. *Clin. Cancer Res.* clincanres.2575.2017 (2017). doi:10.1158/1078-0432.CCR-17-2575

84. Wang, B. *et al.* NAMPT overexpression in prostate cancer and its contribution to tumor cell survival and stress response. *Oncogene* **30,** 907–921 (2011).

85. Chini, C. C. S. *et al.* Targeting of NAD Metabolism in Pancreatic Cancer Cells: Potential Novel Therapy for Pancreatic Tumors. *Clin. Cancer Res.* **20,** 120–130 (2014).

86. Xiao, Y. *et al.* Dependence of tumor cell lines and patient-derived tumors on the NAD salvage pathway renders them sensitive to NAMPT inhibition with GNE-618. *Neoplasia N. Y. N* **15,** 1151–1160 (2013).

87. Moon, Y. W., Hajjar, J., Hwu, P. & Naing, A. Targeting the indoleamine 2,3-dioxygenase pathway in cancer. *J. Immunother. Cancer* **3,** (2015).

88. Johnson, T. S. & Munn, D. H. Host Indoleamine 2,3-Dioxygenase: Contribution to Systemic Acquired Tumor Tolerance. *Immunol. Invest.* **41,** 765–797 (2012).

89. Shackelford, R. E., Mayhall, K., Maxwell, N. M., Kandil, E. & Coppola, D. Nicotinamide Phosphoribosyltransferase in Malignancy: A Review. *Genes Cancer* **4,** 447–456 (2013).

90. Duarte-Pereira, S. *et al.* Extensive regulation of nicotinate phosphoribosyltransferase (NAPRT) expression in human tissues and tumors. *Oncotarget* **7,** (2016).

91. von Heideman, A., Berglund, Å., Larsson, R. & Nygren, P. Safety and efficacy of NAD depleting cancer drugs: results of a phase I clinical trial of CHS 828 and overview of published data. *Cancer Chemother. Pharmacol.* **65,** 1165–1172 (2010).

92. Holen, K., Saltz, L. B., Hollywood, E., Burk, K. & Hanauske, A.-R. The pharmacokinetics, toxicities, and biologic effects of FK866, a nicotinamide adenine dinucleotide biosynthesis inhibitor. *Invest. New Drugs* **26,** 45–51 (2008).

93. Goldinger, S. M. *et al.* Efficacy and Safety of APO866 in Patients With Refractory or Relapsed Cutaneous T-Cell Lymphoma: A Phase 2 Clinical Trial. *JAMA Dermatol.* **152,** 837 (2016).

94. Hara, N. *et al.* Elevation of Cellular NAD Levels by Nicotinic Acid and Involvement of Nicotinic Acid Phosphoribosyltransferase in Human Cells. *J. Biol. Chem.* **282,** 24574–24582 (2007).

95. Shames, D. S. *et al.* Loss of NAPRT1 Expression by Tumor-Specific Promoter Methylation Provides a Novel Predictive Biomarker for NAMPT Inhibitors. *Clin. Cancer Res.* **19,** 6912–6923 (2013).

96. Olesen, U. H., Hastrup, N. & Sehested, M. Expression patterns of nicotinamide phosphoribosyltransferase and nicotinic acid phosphoribosyltransferase in human malignant lymphomas: NAMPT AND NAPRT IN MALIGNANT LYMPHOMAS. *APMIS* **119,** 296–303 (2011).

97. Olesen, U. H., Thougaard, A. V., Jensen, P. B. & Sehested, M. A Preclinical Study on the Rescue of Normal Tissue by Nicotinic Acid in High-Dose Treatment with APO866, a Specific Nicotinamide Phosphoribosyltransferase Inhibitor. *Mol. Cancer Ther.* **9,** 1609–1617 (2010).

98. O'Brien, T. *et al.* Supplementation of nicotinic acid with NAMPT inhibitors results in loss of in vivo efficacy in NAPRT1-deficient tumor models. *Neoplasia N. Y. N* **15,** 1314–1329 (2013).

99. Piacente, F. *et al.* Nicotinic Acid Phosphoribosyltransferase Regulates Cancer Cell Metabolism, Susceptibility to NAMPT Inhibitors, and DNA Repair. *Cancer Res.* **77,** 3857–3869 (2017).

100. Nomura, F. *et al.* Enhancement of poly-adenosine diphosphate-ribosylation in human hepatocellular carcinoma. *J. Gastroenterol. Hepatol.* **15,** 529–535 (2000).

101. Morales, J. *et al.* Review of poly (ADP-ribose) polymerase (PARP) mechanisms of action and rationale for targeting in cancer and other diseases. *Crit. Rev. Eukaryot. Gene Expr.* **24,** 15–28 (2014).

102. Ricks, T. K. *et al.* Successes and Challenges of PARP Inhibitors in Cancer Therapy. *Front. Oncol.* **5,** (2015).

103. Hu, J., Jing, H. & Lin, H. Sirtuin inhibitors as anticancer agents. *Future Med. Chem.* **6,** 945–966 (2014).

104. Dang, W. The controversial world of sirtuins. *Drug Discov. Today Technol.* **12,** e9–e17 (2014).

105. Seto, E. & Yoshida, M. Erasers of Histone Acetylation: The Histone Deacetylase Enzymes. *Cold Spring Harb. Perspect. Biol.* **6,** a018713–a018713 (2014).

106. Chen, W., Yuan, H. & Su, L. The emerging and diverse roles of sirtuins in cancer: a clinical perspective. *OncoTargets Ther.* 1399 (2013). doi:10.2147/OTT.S37750

107. Imai, S. & Guarente, L. NAD+ and sirtuins in aging and disease. *Trends Cell Biol.* **24,** 464–471 (2014).

108. Canto, C. & Auwerx, J. Targeting Sirtuin 1 to Improve Metabolism: All You Need Is NAD+? *Pharmacol. Rev.* **64,** 166–187 (2012).

109. Chalkiadaki, A. & Guarente, L. The multifaceted functions of sirtuins in cancer. *Nat. Rev. Cancer* **15,** 608–624 (2015).

110. Palmirotta, R. *et al.* Sirtuins and Cancer: Role in the Epithelial-Mesenchymal Transition. *Oxid. Med. Cell. Longev.* **2016,** 1–9 (2016).

111. Paredes, S., Villanova, L. & Chua, K. F. Molecular Pathways: Emerging Roles of Mammalian Sirtuin SIRT7 in Cancer. *Clin. Cancer Res.* **20,** 1741–1746 (2014).

112. Zhang, S. *et al.* Sirt7 promotes gastric cancer growth and inhibits apoptosis by epigenetically inhibiting miR-34a. *Sci. Rep.* **5,** (2015).

113. Yu, H. *et al.* Overexpression of Sirt7 Exhibits Oncogenic Property and Serves as a Prognostic Factor in Colorectal Cancer. *Clin. Cancer Res.* **20,** 3434–3445 (2014).

114. Deshmukh, A., Deshpande, K., Arfuso, F., Newsholme, P. & Dharmarajan, A. Cancer stem cell metabolism: a potential target for cancer therapy. *Mol. Cancer* **15,** (2016).

115. Blelloch, R. H. Nuclear cloning of embryonal carcinoma cells. *Proc. Natl. Acad. Sci.* (2004). doi:10.1073/pnas.0405015101

116. Fujimori, H., Shikanai, M., Teraoka, H., Masutani, M. & Yoshioka, K. Induction of Cancerous Stem Cells during Embryonic Stem Cell Differentiation. *J. Biol. Chem.* **287,** 36777–36791 (2012).

117. Sutiwisesak, R. *et al.* Induced pluripotency enables differentiation of human nullipotent embryonal carcinoma cells N2102Ep. *Biochim. Biophys. Acta BBA - Mol. Cell Res.* **1843,** 2611–2619 (2014).

118. Vega-Naredo, I. *et al.* Mitochondrial metabolism directs stemness and differentiation in P19 embryonal carcinoma stem cells. *Cell Death Differ.* **21,** 1560–1574 (2014).

119. Damjanov, I. & Andrews, P. W. The terminology of teratocarcinomas and teratomas. *Nat. Biotechnol.* **25,** 1212–1212 (2007).

120. Blum, B. & Benvenisty, N. The Tumorigenicity of Human Embryonic Stem Cells. in *Advances in Cancer Research* **100,** 133–158 (Elsevier, 2008).

121. Kleinsmith, L. J. & Pierce, G. B. Multipotentiality of Single Embryonal Carcinoma Cells. *Cancer Res.* **24,** 1544–1551 (1964).

122. Illmensee, K. & Mintz, B. Totipotency and normal differentiation of single teratocarcinoma cells cloned by injection into blastocysts. *Proc. Natl. Acad. Sci. U. S. A.* **73,** 549–553 (1976).

123. Kelly, G. M. & Gatie, M. I. Mechanisms Regulating Stemness and Differentiation in Embryonal Carcinoma Cells. *Stem Cells Int.* **2017,** 1–20 (2017).

124. Park, E. K. *et al.* Transcriptional repression of cancer stem cell marker CD133 by tumor suppressor p53. *Cell Death Dis.* **6,** e1964–e1964 (2015).

125. You, J. S. *et al.* Depletion of Embryonic Stem Cell Signature by Histone Deacetylase Inhibitor in NCCIT Cells: Involvement of Nanog Suppression. *Cancer Res.* **69,** 5716–5725 (2009).

126. Musch, T., Öz, Y., Lyko, F. & Breiling, A. Nucleoside Drugs Induce Cellular Differentiation by Caspase-Dependent Degradation of Stem Cell Factors. *PLoS ONE* **5,** e10726 (2010).

127. Watanabe, K. *et al.* Cripto-1 Is a Cell Surface Marker for a Tumorigenic, Undifferentiated Subpopulation in Human Embryonal Carcinoma Cells. *STEM CELLS* **28,** 1303–1314 (2010).

128. Chadalavada, R. S. V. *et al.* Constitutive Gene Expression Predisposes Morphogen-Mediated Cell Fate Responses of NT2/D1 and 27X-1 Human Embryonal Carcinoma Cells. *STEM CELLS* **25,** 771–778 (2006).

129. Coyle, D. E., Li, J. & Baccei, M. Regional Differentiation of Retinoic Acid-Induced Human Pluripotent Embryonic Carcinoma Stem Cell Neurons. *PLoS ONE* **6,** e16174 (2011).

130. Pal, R. & Ravindran, G. Assessment of pluripotency and multilineage differentiation potential of NTERA-2 cells as a model for studying human embryonic stem cells. *Cell Prolif.* **39,** 585–598 (2006).

131. Prat, A. *et al.* Characterization of cell lines derived from breast cancers and normal mammary tissues for the study of the intrinsic molecular subtypes. *Breast Cancer Res. Treat.* **142,** 237–255 (2013).

132. Guen, V. J. *et al.* EMT programs promote basal mammary stem cell and tumor-initiating cell stemness by inducing primary ciliogenesis and Hedgehog signaling. *Proc. Natl. Acad. Sci.* **114,** E10532–E10539 (2017).

133. Gupta, P. B. *et al.* Identification of Selective Inhibitors of Cancer Stem Cells by High-Throughput Screening. *Cell* **138,** 645–659 (2009).

134. Mani, S. A. *et al.* The Epithelial-Mesenchymal Transition Generates Cells with Properties of Stem Cells. *Cell* **133,** 704–715 (2008).

135. Onder, T. T. *et al.* Loss of E-Cadherin Promotes Metastasis via Multiple Downstream Transcriptional Pathways. *Cancer Res.* **68,** 3645–3654 (2008).

136. Singh, S. K. *et al.* Identification of human brain tumour initiating cells. *Nature* **432,** 396–401 (2004).

137. Lee, J. *et al.* Tumor stem cells derived from glioblastomas cultured in bFGF and EGF more closely mirror the phenotype and genotype of primary tumors than do serum-cultured cell lines. *Cancer Cell* **9,** 391–403 (2006).

138. Hu, Y. *et al.* mTOR and autophagy in regulation of acute lung injury: a review and perspective. *Microbes Infect.* **16,** 727–734 (2014).

139. Quan, W. & Lee, M.-S. Role of Autophagy in the Control of Body Metabolism. *Endocrinol. Metab.* **28,** 6 (2013).

140. Zhao, Y. *et al.* RACK1 Promotes Autophagy by Enhancing the Atg14L-Beclin 1-Vps34-Vps15 Complex Formation upon Phosphorylation by AMPK. *Cell Rep.* **13,** 1407–1417 (2015).

141. Sharif, T. *et al.* Regulation of Cancer and Cancer-Related Genes via NAD^+. *Antioxid. Redox Signal.* (2018). doi:10.1089/ars.2017.7478

142. Strober, W. Trypan Blue Exclusion Test of Cell Viability. in *Current Protocols in Immunology* (eds. Coligan, J. E., Bierer, B. E., Margulies, D. H., Shevach, E. M. & Strober, W.) (John Wiley & Sons, Inc., 2001). doi:10.1002/0471142735.ima03bs21

143. Liao, M.-J. *et al.* Enrichment of a Population of Mammary Gland Cells that Form Mammospheres and Have In vivo Repopulating Activity. *Cancer Res.* **67,** 8131–8138 (2007).

144. Quah, B. J. C. & Parish, C. R. The Use of Carboxyfluorescein Diacetate Succinimidyl Ester (CFSE) to Monitor Lymphocyte Proliferation. *J. Vis. Exp.* (2010). doi:10.3791/2259

145. Maier, A. B., Westendorp, R. G. J. & Van Heemst, D. beta-Galactosidase Activity as a Biomarker of Replicative Senescence during the Course of Human Fibroblast Cultures. *Ann. N. Y. Acad. Sci.* **1100,** 323–332 (2007).

146. Cummings, B. S. & Schnellmann, R. G. Measurement of Cell Death in Mammalian Cells. in *Current Protocols in Pharmacology* (eds. Enna, S. J. et al.) (John Wiley & Sons, Inc., 2004). doi:10.1002/0471141755.ph1208s25

147. Asai, K., Buurman, W. A., Reutelingsperger, C. P. M., Schutte, B. & Kaminishi, M. Low concentrations of ethanol induce apoptosis in human intestinal cells. *Scand. J. Gastroenterol.* **38,** 1154–1161 (2003).

148. Murphy, J. P., Stepanova, E., Everley, R. A., Paulo, J. A. & Gygi, S. P. Comprehensive Temporal Protein Dynamics during the Diauxic Shift in *Saccharomyces cerevisiae*. *Mol. Cell. Proteomics* **14,** 2454–2465 (2015).

149. Rappsilber, J., Ishihama, Y. & Mann, M. Stop and go extraction tips for matrix-assisted laser desorption/ionization, nanoelectrospray, and LC/MS sample pretreatment in proteomics. *Anal. Chem.* **75,** 663–670 (2003).

150. Ting, L., Rad, R., Gygi, S. P. & Haas, W. MS3 eliminates ratio distortion in isobaric multiplexed quantitative proteomics. *Nat. Methods* **8,** 937–940 (2011).

151. Eccles, M. & Li, C. Senescence Associated **?**-galactosidase Staining. *BIO-Protoc.* **2,** (2012).

152. Li, Y. *et al.* Suppression of cancer relapse and metastasis by inhibiting cancer stemness. *Proc. Natl. Acad. Sci.* **112,** 1839–1844 (2015).

153. Bertolini, G. *et al.* Highly tumorigenic lung cancer CD133+ cells display stem-like features and are spared by cisplatin treatment. *Proc. Natl. Acad. Sci.* **106,** 16281–16286 (2009).

154. Dontu, G. In vitro propagation and transcriptional profiling of human mammary stem/progenitor cells. *Genes Dev.* **17,** 1253–1270 (2003).

155. Dráberová, E. *et al.* Class III β-Tubulin Is Constitutively Coexpressed With Glial Fibrillary Acidic Protein and Nestin in Midgestational Human Fetal Astrocytes: Implications for Phenotypic Identity. *J. Neuropathol. Exp. Neurol.* **67,** 341–354 (2008).

156. Mizushima, N., Yoshimori, T. & Levine, B. Methods in Mammalian Autophagy Research. *Cell* **140,** 313–326 (2010).

157. Metz, P. *et al.* Dengue Virus Inhibition of Autophagic Flux and Dependency of Viral Replication on Proteasomal Degradation of the Autophagy Receptor p62. *J. Virol.* **89,** 8026–8041 (2015).

158. Porter, A. G. & Jänicke, R. U. Emerging roles of caspase-3 in apoptosis. *Cell Death Differ.* **6,** 99–104 (1999).

159. Galluzzi, L. *et al.* No death without life: vital functions of apoptotic effectors. *Cell Death Differ.* **15,** 1113–1123 (2008).

160. Chen, D. *et al.* Targeting BMI1 + Cancer Stem Cells Overcomes Chemoresistance and Inhibits Metastases in Squamous Cell Carcinoma. *Cell Stem Cell* **20,** 621–634.e6 (2017).

161. Pujuguet, P., Radisky, D., Levy, D., Lacza, C. & Bissell, M. J. Trichostatin A inhibits beta-casein expression in mammary epithelial cells. *J. Cell. Biochem.* **83,** 660–670 (2001).

162. Bajrami, I. *et al.* Synthetic lethality of PARP and NAMPT inhibition in triple-negative breast cancer cells: Synthetic lethality between NAMPT and PARPi. *EMBO Mol. Med.* **4,** 1087–1096 (2012).

163. Basel, M. T. *et al.* Developing a xenograft human tumor model in immunocompetent mice. *Cancer Lett.* **412,** 256–263 (2018).

164. Semenkow, S. *et al.* An immunocompetent mouse model of human glioblastoma. *Oncotarget* **8,** (2017).

165. Parkin, D. M., Bray, F., Ferlay, J. & Pisani, P. Estimating the world cancer burden: Globocan 2000. *Int. J. Cancer* **94,** 153–156 (2001).

166. Torre, L. A. *et al.* Global cancer statistics, 2012: Global Cancer Statistics, 2012. *CA. Cancer J. Clin.* **65,** 87–108 (2015).

167. Cancer. *World Health Organization* Available at: http://www.who.int/news-room/fact-sheets/detail/cancer. (Accessed: 7th June 2018)

168. Siegel, R. L., Miller, K. D. & Jemal, A. Cancer statistics, 2018: Cancer Statistics, 2018. *CA. Cancer J. Clin.* **68,** 7–30 (2018).

169. Fisher, R., Pusztai, L. & Swanton, C. Cancer heterogeneity: implications for targeted therapeutics. *Br. J. Cancer* **108,** 479–485 (2013).

170. Saunders, N. A. *et al.* Role of intratumoural heterogeneity in cancer drug resistance: molecular and clinical perspectives: Contribution of intratumoural heterogeneity to drug resistance. *EMBO Mol. Med.* **4,** 675–684 (2012).

171. Vose, J. M. *et al.* Relapse from Complete Remission More Than 5 Years after Therapy for Diffuse Large B-Cell Lymphoma (DLBCL): Relapse Histology Most Commonly DLBCL with a Germinal Center B-Cell (GCB) Phenotype. *Blood* **110,** 3430–3430 (2007).

172. Shackleton, M., Quintana, E., Fearon, E. R. & Morrison, S. J. Heterogeneity in Cancer: Cancer Stem Cells versus Clonal Evolution. *Cell* **138,** 822–829 (2009).

173. Li, X. *et al.* Intrinsic Resistance of Tumorigenic Breast Cancer Cells to Chemotherapy. *JNCI J. Natl. Cancer Inst.* **100,** 672–679 (2008).

174. Wielenga, M. C. B. *et al.* ER-Stress-Induced Differentiation Sensitizes Colon Cancer Stem Cells to Chemotherapy. *Cell Rep.* **13,** 489–494 (2015).

175. Yan, C. *et al.* Doxorubicin-induced mitophagy contributes to drug resistance in cancer stem cells from HCT8 human colorectal cancer cells. *Cancer Lett.* **388,** 34–42 (2017).

176. Zheng, X., Cui, D., Xu, S., Brabant, G. & Derwahl, M. Doxorubicin fails to eradicate cancer stem cells derived from anaplastic thyroid carcinoma cells: characterization of resistant cells. *Int. J. Oncol.* **37,** 307–315 (2010).

177. Mitra, A., Mishra, L. & Li, S. EMT, CTCs and CSCs in tumor relapse and drug-resistance. *Oncotarget* **6,** (2015).

178. Wong, D. J. *et al.* Module Map of Stem Cell Genes Guides Creation of Epithelial Cancer Stem Cells. *Cell Stem Cell* **2,** 333–344 (2008).

179. Li, C. *et al.* c-Met Is a Marker of Pancreatic Cancer Stem Cells and Therapeutic Target. *Gastroenterology* **141,** 2218–2227.e5 (2011).

180. Batlle, E. & Clevers, H. Cancer stem cells revisited. *Nat. Med.* **23,** 1124–1134 (2017).

181. Sancho, P. *et al.* MYC/PGC-1α Balance Determines the Metabolic Phenotype and Plasticity of Pancreatic Cancer Stem Cells. *Cell Metab.* **22,** 590–605 (2015).

182. Viale, A. *et al.* Oncogene ablation-resistant pancreatic cancer cells depend on mitochondrial function. *Nature* **514,** 628–632 (2014).

183. Vlashi, E. *et al.* Metabolic state of glioma stem cells and nontumorigenic cells. *Proc. Natl. Acad. Sci.* **108,** 16062–16067 (2011).

184. Feng, W. *et al.* Targeting Unique Metabolic Properties of Breast Tumor Initiating Cells: Metabolic Targeting of Tumor Initiating Cells. *STEM CELLS* **32,** 1734–1745 (2014).

185. Liu, P.-P. *et al.* Metabolic regulation of cancer cell side population by glucose through activation of the Akt pathway. *Cell Death Differ.* **21,** 124–135 (2014).

186. Gui, D. Y. *et al.* Environment Dictates Dependence on Mitochondrial Complex I for NAD+ and Aspartate Production and Determines Cancer Cell Sensitivity to Metformin. *Cell Metab.* **24,** 716–727 (2016).

187. Wheaton, W. W. *et al.* Metformin inhibits mitochondrial complex I of cancer cells to reduce tumorigenesis. *eLife* **3,** (2014).

188. Prieto-Vila, M., Takahashi, R., Usuba, W., Kohama, I. & Ochiya, T. Drug Resistance Driven by Cancer Stem Cells and Their Niche. *Int. J. Mol. Sci.* **18,** 2574 (2017).

189. Vidal, S. J., Rodriguez-Bravo, V., Galsky, M., Cordon-Cardo, C. & Domingo-Domenech, J. Targeting cancer stem cells to suppress acquired chemotherapy resistance. *Oncogene* **33,** 4451–4463 (2014).

190. Zhou, X., Wang, G. & Sun, Y. A Reliable Parameter to Standardize the Scoring of Stem Cell Spheres. *PLOS ONE* **10,** e0127348 (2015).

191. Boumahdi, S. *et al.* SOX2 controls tumour initiation and cancer stem-cell functions in squamous-cell carcinoma. *Nature* **511,** 246–250 (2014).

192. Lu, Y. *et al.* Knockdown of Oct4 and Nanog expression inhibits the stemness of pancreatic cancer cells. *Cancer Lett.* **340,** 113–123 (2013).

193. Kreso, A. *et al.* Self-renewal as a therapeutic target in human colorectal cancer. *Nat. Med.* **20,** 29–36 (2014).

194. Campos, B. *et al.* Differentiation Therapy Exerts Antitumor Effects on Stem-like Glioma Cells. *Clin. Cancer Res.* **16,** 2715–2728 (2010).

195. Piccirillo, S. G. M. *et al.* Bone morphogenetic proteins inhibit the tumorigenic potential of human brain tumour-initiating cells. *Nature* **444,** 761–765 (2006).

196. Sung, M. W. & Waxman, S. Combination of cytotoxic-differentiation therapy with 5-fluorouracil and phenylbutyrate in patients with advanced colorectal cancer. *Anticancer Res.* **27,** 995–1001 (2007).

197. Waxman, S., Huang, Y., Scher, B. M. & Scher, M. Enhancement of differentiation and cytotoxicity of leukemia cells by combinations of fluorinated pyrimidines and differentiation inducers: development of DNA double-strand breaks. *Biomed. Pharmacother. Biomedecine Pharmacother.* **46,** 183–192 (1992).

198. Kimmelman, A. C. & White, E. Autophagy and Tumor Metabolism. *Cell Metab.* **25,** 1037–1043 (2017).

199. Lock, R. *et al.* Autophagy facilitates glycolysis during Ras-mediated oncogenic transformation. *Mol. Biol. Cell* **22,** 165–178 (2011).

200. Kondo, Y., Kanzawa, T., Sawaya, R. & Kondo, S. The role of autophagy in cancer development and response to therapy. *Nat. Rev. Cancer* **5,** 726–734 (2005).

201. Shaid, S., Brandts, C. H., Serve, H. & Dikic, I. Ubiquitination and selective autophagy. *Cell Death Differ.* **20,** 21–30 (2013).

202. Pérez-Mancera, P. A., Young, A. R. J. & Narita, M. Inside and out: the activities of senescence in cancer. *Nat. Rev. Cancer* **14,** 547–558 (2014).

203. García-Prat, L. *et al.* Autophagy maintains stemness by preventing senescence. *Nature* **529,** 37–42 (2016).

204. Gordon, R. R. & Nelson, P. S. Cellular senescence and cancer chemotherapy resistance. *Drug Resist. Updat.* **15,** 123–131 (2012).

205. Childs, B. G., Baker, D. J., Kirkland, J. L., Campisi, J. & van Deursen, J. M. Senescence and apoptosis: dueling or complementary cell fates? *EMBO Rep.* **15,** 1139–1153 (2014).

206. Ewald, J. A., Desotelle, J. A., Wilding, G. & Jarrard, D. F. Therapy-Induced Senescence in Cancer. *JNCI J. Natl. Cancer Inst.* **102,** 1536–1546 (2010).

207. Xue, W. *et al.* Senescence and tumour clearance is triggered by p53 restoration in murine liver carcinomas. *Nature* **445,** 656–660 (2007).

208. Barber, M. F. *et al.* SIRT7 links H3K18 deacetylation to maintenance of oncogenic transformation. *Nature* **487,** 114–118 (2012).

209. Seligson, D. B. *et al.* Global Levels of Histone Modifications Predict Prognosis in Different Cancers. *Am. J. Pathol.* **174,** 1619–1628 (2009).

210. Bravo, R. *et al.* Endoplasmic Reticulum and the Unfolded Protein Response. in *International Review of Cell and Molecular Biology* **301,** 215–290 (Elsevier, 2013).

211. Zhang, T. & Kraus, W. L. SIRT1-dependent regulation of chromatin and transcription: Linking NAD+ metabolism and signaling to the control of cellular functions. *Biochim. Biophys. Acta BBA - Proteins Proteomics* **1804,** 1666–1675 (2010).

212. Tissue expression of NAMPT - Staining in bone marrow. *The Human Protein Atlas* Available at: https://www.proteinatlas.org/ENSG00000105835-NAMPT/tissue/bone+marrow. (Accessed: 2nd May 2018)

213. Tissue expression of NAPRT - Staining in bone marrow. *The Human Protein Atlas* Available at: https://www.proteinatlas.org/ENSG00000147813-NAPRT/tissue/bone+marrow. (Accessed: 2nd May 2018)

214. Brower, V. Cancer Stem Cell Hypothesis Evolves With Emerging Research. *J. Natl. Cancer Inst.* **108,** djw139 (2016).

215. Beier, D. *et al.* CD133+ and CD133- Glioblastoma-Derived Cancer Stem Cells Show Differential Growth Characteristics and Molecular Profiles. *Cancer Res.* **67,** 4010–4015 (2007).

216. Wang, J. *et al.* CD133 negative glioma cells form tumors in nude rats and give rise to CD133 positive cells. *Int. J. Cancer* **122,** 761–768 (2008).

217. Kelly, P. N., Dakic, A., Adams, J. M., Nutt, S. L. & Strasser, A. Tumor Growth Need Not Be Driven by Rare Cancer Stem Cells. *Science* **317,** 337–337 (2007).

218. Quintana, E. *et al.* Efficient tumour formation by single human melanoma cells. *Nature* **456,** 593–598 (2008).

219. Baker, M. Cancer stem cells, becoming common. *Nat. Rep. Stem Cells* (2008). doi:10.1038/stemcells.2008.153

220. Chaffer, C. L. *et al.* Normal and neoplastic nonstem cells can spontaneously convert to a stem-like state. *Proc. Natl. Acad. Sci.* **108,** 7950–7955 (2011).

221. Roesch, A. *et al.* A Temporarily Distinct Subpopulation of Slow-Cycling Melanoma Cells Is Required for Continuous Tumor Growth. *Cell* **141,** 583–594 (2010).

APPENDIX A Copyright Permission

April 18, 2018

Mary Ann Liebert, Inc.
140 Huguenot Street, 3rd Floor
New Rochelle, NY 10801-5215

I am preparing my Master's thesis for submission to the Faculty of Graduate Studies at Dalhousie University, Halifax, Nova Scotia, Canada. I am seeking your permission to include a manuscript version of the following paper(s) as a chapter in the thesis:

Regulation of Cancer and Cancer-Related Genes via NAD+. Sharif Tanveer, Martell Emma, Dai Cathleen, Ghassemi-Rad Mohammad Saleh, Kennedy Barry E., Lee Patrick W.K., and Gujar Shashi. Antioxidants & Redox Signaling, online ahead of print, 2018.

Canadian graduate theses are reproduced by the Library and Archives of Canada (formerly National Library of Canada) through a non-exclusive, world-wide license to reproduce, loan, distribute, or sell theses. I am also seeking your permission for the material described above to be reproduced and distributed by the LAC(NLC). Further details about the LAC(NLC) thesis program are available on the LAC(NLC) website (www.nlc-bnc.ca).

Full publication details and a copy of this permission letter will be included in the thesis.

Yours sincerely,

Cathleen Dai

Permission is granted for:

a) the inclusion of the material described above in your thesis.

b) for the material described above to be included in the copy of your thesis that is sent to the Library and Archives of Canada (formerly National Library of Canada) for reproduction and distribution.

Name: Karen Ballen Title: Manager, Reprints + Permissions

Signature: Date: 4/18/18